uOttawa

L'Université canadienne
Canada's university

FACULTÉ DES ÉTUDES SUPÉRIEURES ET POSTOCTORALES

uOttawa

L'Université canadienne
Canada's university

FACULTY OF GRADUATE AND POSDOCTORAL STUDIES

Harminder Phull

AUTEUR DE LA THÈSE / AUTHOR OF THESIS

M.Sc. (Chemistry)

GRADE / DEGREE

Department of Chemistry

FACULTÉ, ÉCOLE, DÉPARTEMENT / FACULTY, SCHOOL, DEPARTMENT

A Preparatory Study for Co2 Activation and Revisitation of a Crystallographic Pitfall

TITRE DE LA THÈSE / TITLE OF THESIS

Sandro Gambarotta

DIRECTEUR (DIRECTRICE) DE LA THÈSE / THESIS SUPERVISOR

CO-DIRECTEUR (CO-DIRECTRICE) DE LA THÈSE / THESIS CO-SUPERVISOR

Tom Baker

Sean Barry

Gary W. Slater

Le Doyen de la Faculté des études superieures et postdoctorales / Dean of the Faculty of Graduate and Postdoctoral Studies

A PREPARATORY STUDY FOR CO_2 ACTIVATION AND REVISITATION OFA CRYSTALLOGRAPHIC PITFALL

A thesis submitted to the
School of Graduate Studies and Research

In partial fulfilment of the requirements
for the degree of
Masters of Science

In the Ottawa-Carleton Chemistry Institute
Department of Chemistry
University of Ottawa
Ottawa, Ontario
Canada

April 2010

Candidate

Harminder Phull

Supervisor

Dr. Sandro Gambarotta

Your file Votre référence
ISBN: 978-0-494-73825-2
Our file Notre référence
ISBN: 978-0-494-73825-2

To *PAS*
For everything.

ABSTRACT

Ruthenium β-diketiminate complexes were studied in attempts to observe small molecule activation. [η^5-*p*-cymene(^{i}PrArNCMe)$_2$C]Ru[(^{i}PrArNCMe)$_2$CH] was prepared by the reaction of [$RuCl_2$(*p*-cymene)]$_2$ with 2 equivalents of [(^{i}PrArNCMe)$_2$CH]K in hexanes. The resulting complex was characterized by X-ray crystallography and ^{1}H NMR. Attempts to reduce the complex *in-situ* using potassium, sodium metal and sodium hydride afford [(^{i}PrArNCMe)$_2$CH]Ru[η^5-1-methyl-4-(propan-2-ylidene)cyclohexa-2,5-dien-1-yl]. The resulting complex was characterized by X-ray crystallography and ^{1}H NMR. The formation of [η^5-*p*-cymene(^{i}PrArNCMe)$_2$C]Ru[(^{i}PrArNCMe)$_2$CH] and [(^{i}PrArNCMe)$_2$CH]Ru[η^5-1-methyl-4-(propan-2-ylidene)cyclohexa-2,5-dien-1-yl] is attributed to nucleophilic attack and dehydrogenation of the π-bound *p*-cymene ring respectively.

While exploring small molecule activation on ruthenium systems a publication detailing the formation of an unprecedented Mg/Al-containing cluster [{R_2Al(μ-NSiMe$_3$)(μ-OSiMe$_3$)Mg(THF)$_2$(μ-**O_2C**)}$_3$]·2 THF (R = Me (**A**), Et (**B**)) detailed the first end-on CO_2 coordination to a d^0 main group metal. This claim prompted a re-investigation of the complex and through detailed X-ray, DFT and NMR analysis the cluster is appropriated re-assigned as [{Me_2Al(μ-OSiMe$_3$)$_2$Mg(THF)$_2$(μ-**OCN**)}]·1.5 THF.

PUBLICATIONS

Fixation of CO_2 by Magnesium Cations: A Reinterpretation

H. Phull, D. Alberti, I. Korobkov, S. Gambarotta and P.H.M. Budzelaar
Angewandte Chemie International Edition **2006**, 45, 5331-5334 (HOT Papers section)

ACKNOWLEDGEMENTS

I would like to start off by thanking my supervisor Dr. Gambarotta without whom, this work would not have been possible. His constant guidance and support throughout this process was appreciated beyond words.

I am also indebted to Dr. Glenn Facey who helped tremendously with all the NMR work during this project. As well, this work could not have been completed without Dr. Peter H.M. Budzelaar who worked on all the theoretical calculations for this project.

To Dr. Jennifer Scott, Dr. Patrick Crewdson, Dr. Davide Alberti, Dr. Ilia Korobkov, Terri Clarke and Indu Pihillagawa Gedara, my co-workers, thank you for your constant assistance, understanding, support and entertainment.

Lastly, but not least, I would like to thank my family who have sacrificed so much so that I could have.

TABLE OF CONTENTS

ABSTRACT iii

PUBLICATIONS iv

ACKNOWLEDGEMENTS v

TABLE OF CONTENTS vi

LIST OF ABBREVIATIONS viii

Chapter One **1**

Introductory Notes 1

The chemistry of ruthenium β-diketiminates 2

Notes on ruthenium 9

Activations, fixations and insertions of CO_2 17

References 28

Chapter Two **32**

Preparation and characterization of ruthenium(II) cymene β-diketiminate complexes 32

Notes on β-diketiminate complexes 33

Results and discussion 49

Experimental section 65

References 71

Chapter Three **76**

Re-visitation and clarification of the real nature of an alleged trimeric magnesium-CO_2 complex 76

Notes on magnesium-CO_2 clusters 77

Results and discussion 88

Experimental section 101

References 105

Concluding Remarks 107

LIST OF ABBREVIATIONS

δ	chemical shift (NMR)
η^6	eta-6-coordination
Ar	aryl group
ArO	aryl-oxide
Asp	aspartic acid
bpy	bis-pyridine
Cy	cyclohexyl
d	doublet
DFT	density functional calculation
DMSO	dimethyl sulfoxide
Et	ethyl
Et_2O	diethyl ether
Glu	glutamine
H_2IMes	1,3-dimesityl-4,5-dihydroimidazol-2-ylidene
HMPA	hexamethylphosphoramide
Im	imidazole
^{i}Pr	*iso*-propyl
IR	infrared spectroscopy
K	Kelvin
Lys	lysine
m	multiplet

MAO	methylaluminoxane
nacnac	β-diketimine ligand
NAMI-A	new anti-tumour metastasis inhibitor - A
NHC	*n*-heterocyclic carbene
NMR	nuclear magnetic resonance
OTf	trifluoromethanesulfonate
p-cymeme	4-isopropyltoluene
PEG	poly-ethylene-glycol
ppm	parts per million
PTrip	$(2,4,6\text{-}^{i}Pr_3C_6H_2)P$
py	pyridine
R	generalized alkyl
RCM	ring closing metathesis
s	singlet
sept	septet
^{t}Bu	tert-butyl
THF	tetrahydrofuran
TMSCl	trimethylsilyl chloride
TMSOTf	trimethylsilyl trifluoromethanesulfonate
tos	tosylate
TTPPTS	*meta*-trisulfonated triphenyl phosphine

CHAPTER ONE

INTRODUCTORY NOTES

THE CHEMISTRY OF RUTHENIUM β-DIKETIMINATES

The improvement of catalytic cycles in all areas of chemistry relies partially on the identification of possible reaction intermediates. The identity of these short-lived intermediates is fundamental to the understanding and improvement of respective catalytic processes. Key steps within many of these processes often involve coordinatively unsaturated metal centres that interact with a given substrate and activate or transform that substrate. By definition, these short-lived intermediates are just that, short-lived, and are often too reactive and unstable to be observed or extensively characterized. In order to trap these intermediates to better understand the mechanisms behind these reactions, a ligand that can impart high thermodynamic and kinetic stability by strong electron donation and steric constraints is often required. One class of ligand that fulfils these requirements are the β-diketimines (**1**).[1]

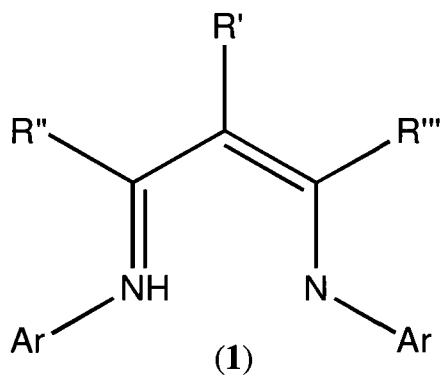

(**1**)

Figure 1: Generalized representation of a β-diketimine ligand

It is only recently that the β-diketimines, also referred to as *nacnac*, have received a steady increase of attention.[1] Major developments within this field occurred in the

1990s when it was recognized that β-diketiminates could in fact play an important role as spectator ligands, much like the formidable cyclopentadienyls, by virtue of their strong metal-ligand bonds and their exceptional and tuneable steric and electronic properties.[2] These properties of the *nacnac* ligand, along with its diversity of bonding modes (***Figure 2***) allow to stabilize transition metal complexes in unusually low oxidation states.[2] In addition, the steric flexibility allows the preparation of complexes where empty coordination sites are sterically protected. In turn, this has enabled activation of small molecules and allowed some of these derivatives to function as catalysts for processes such as olefin metathesis/polymerization and even co-polymerization of epoxides and carbon dioxide.[3]

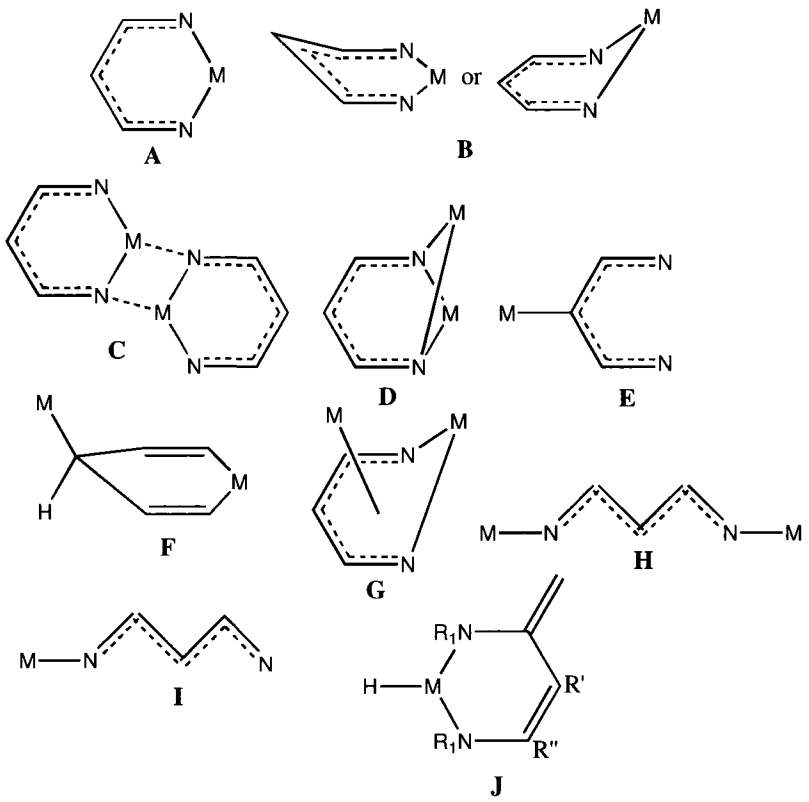

Figure 2: Possible bonding modes for β-diketiminate metal complexes

Some of the most interesting results in the chemistry of this ligand system have been achieved using iron metal. Ruthenium though, has been conspicuously ignored and has remained absent from the literature in spite of the similarity between these two metals.[2]

Iron, which is present in the active sites of nitrogenase enzymes, plays an important role in the activation of dinitrogen and subsequent dinitrogen reduction catalysis. One of the first iron complexes that bound dinitrogen and allowed stepwise reduction, was a low-coordinate Fe complex (**2**) supported by the *nacnac* ligand published by Holland *et. al.* (***Figure 3***).[4]

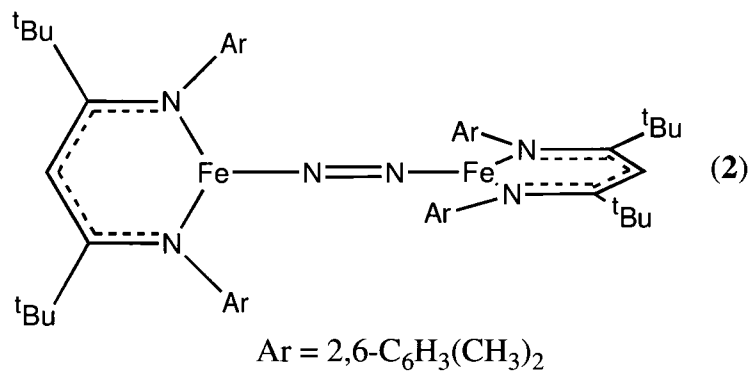

Figure 3: Example of three coordinate dinitrogen complex $L^{tBu}FeNNFeL^{tBu}$ stabilized by the *nacnac* ligand

The electronic and steric stability imparted on the $L^{tBu}FeNNFeL^{tBu}$ complex by the *nacnac* ligand allows it to behave as an *in-situ* source of iron(I). This makes the system capable of reacting with neutral ligands such as C_6H_6 and PR_3, or reductively coupling ketones and aldehydes to diiron(II) pinacolate complexes.[5] with the strong stabilization introduced by the *nacnac* ligand, the $L^{tBu}FeNNFeL^{tBu}$ system indeed exhibits iron(I) behaviour as it also reduces carbon dioxide to carbon monoxide (***Scheme 1***).[5]

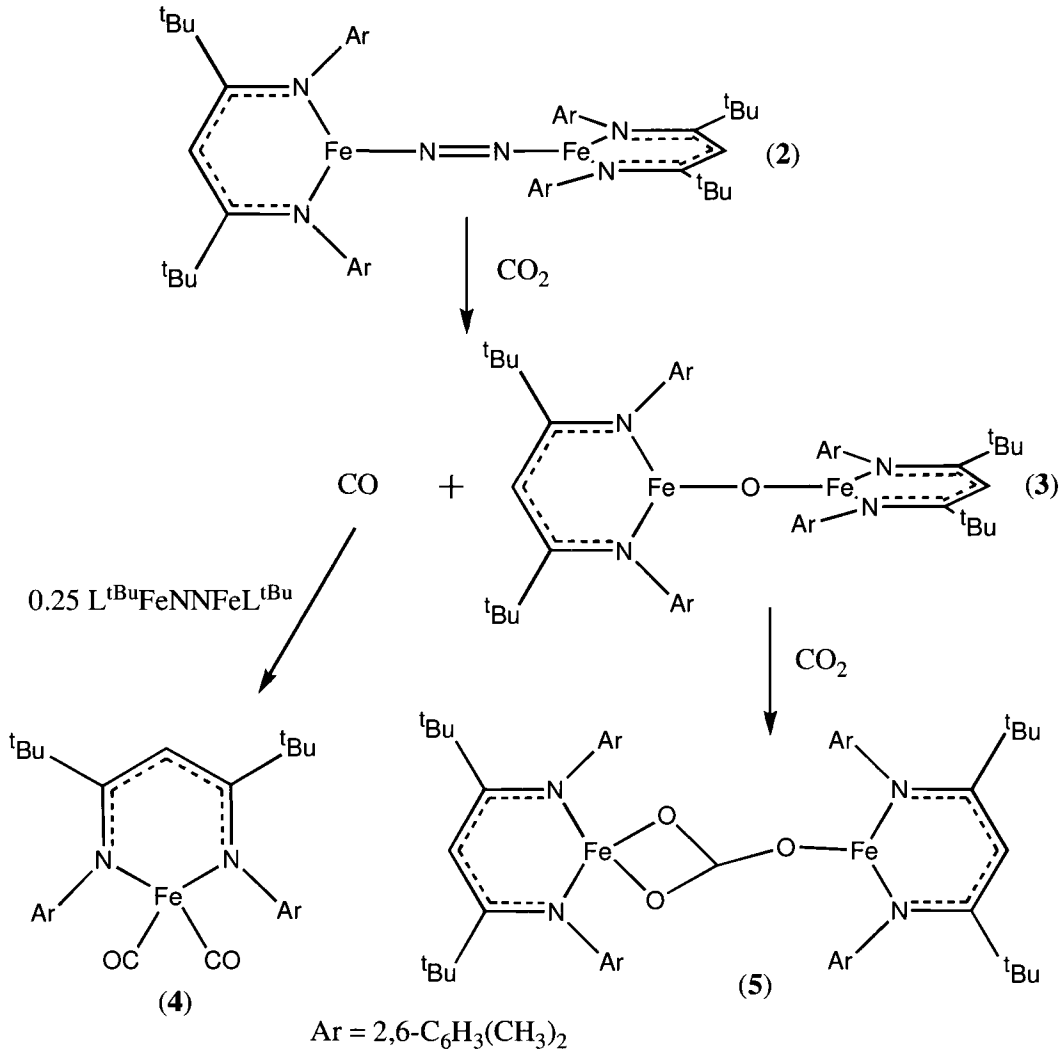

Scheme 1: Reaction pathway of $L^{tBu}FeNNFeL^{tBu}$ with CO_2

The ligands ability to stabilize unique iron complexes, often in low oxidation and coordination states has been well established along with the ability of the *nacnac* ligand backbone to be directly involved in the reactivity of the metal centre.[4,6,14a] More specifically, the central, or α-carbon, has the ability to act as a nucleophile. A recent publication by Holland *et. al.*, demonstrated the involvement of the ligand backbone in the reaction of a cationic three-coordinate iron(II) complex with ethyl diazoacetate (***Scheme 2***).[7]

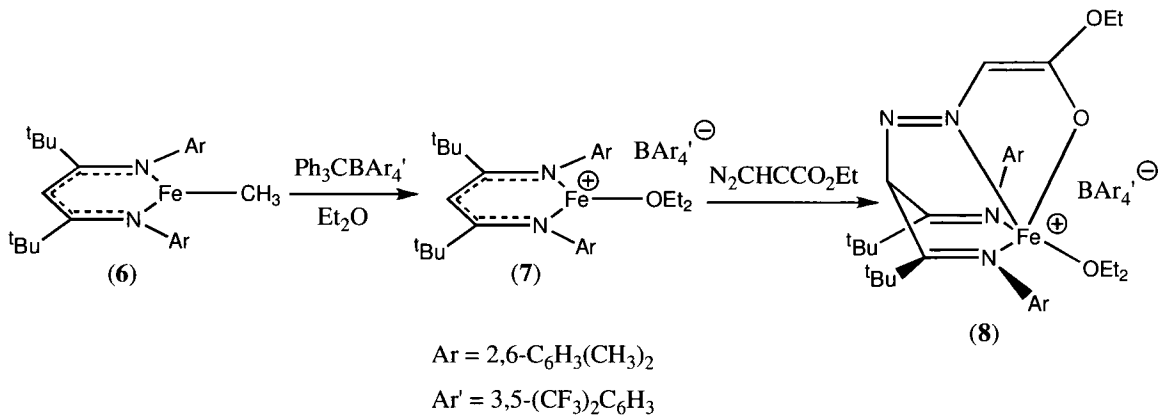

Scheme 2: Synthesis of a cationic high-spin iron(II) complex with *nacnac* ligand participation.

Considering the interesting reactivity surrounding Fe-*nacnac* complexes it is again rather surprising that corresponding ruthenium based complexes have not been reported in the literature when this project started. Ruthenium based complexes with anionic amidinates,[8] neutral diazabutadienes[9a-c] have been known for over twenty years. Furthermore, tetraazacyclotetradecine species,[10] acetylacetone[11] and chelating compounds, such as the unusual η^3-(C,N,N') bonded ruthenium disphosphiminomethanide,[12] have also been recently reported but amongst the myriad of these publications ruthenium-*nacnac* remains notably absent. Only recently, in 2007, Dyson *et. al.*[1] reported the first ruthenium-*nacnac* complex which arose from the reaction of the highly stable $[(\eta^6\text{-}C_6H_6)RuCl_2]_2$ (**10**) with Li[(ArNCMe)$_2$CH] (**9**) (Ar = 2,6-$(CH_3)C_6H_3$) in dichloromethane which results in the formation of (η^6-C_6H_6)RuCl((ArNCMe)$_2$CH) (**11**) (***Scheme 3***).

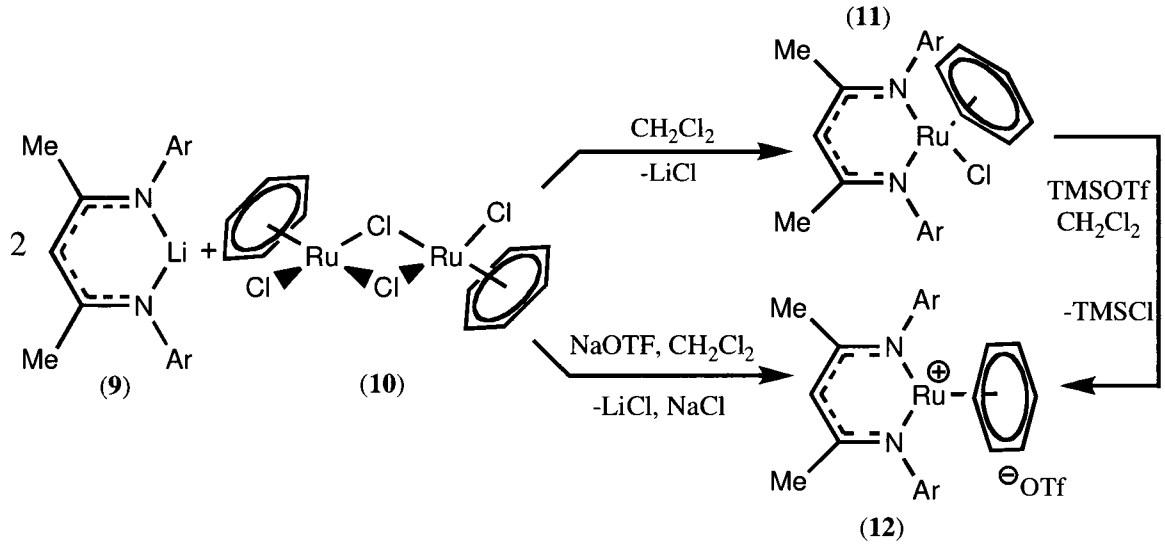

***Scheme 3**:* Synthesis of (η^6-C_6H_6)RuCl((ArNCMe)$_2$CH) and [(η^6-C_6H_6)Ru((ArNCMe)$_2$CH)]OTf

Further, by simply removing the chloride substituent of the ruthenium-*nacnac* complex, using Me_3SiOTf, [(η^6-C_6H_6)Ru((ArNCMe)$_2$CH)]OTf (**12**) forms and further exposure of this complex to either ethylene (**13**), acetylene (**14**) or hydrogen gas (**15**) affords the activation of each respective molecule. Specifically, ethylene and acetylene both insert between the ruthenium and the central α-carbon of the *nacnac* ligand. The activation of hydrogen results in a single hydrogen molecule being delivered to the ruthenium centre and the other to the α-carbon of the *nacnac* ligand. In the process of these activations, the chelating β-diketiminate transforms into a β-diimine ligand (***Scheme 4***).

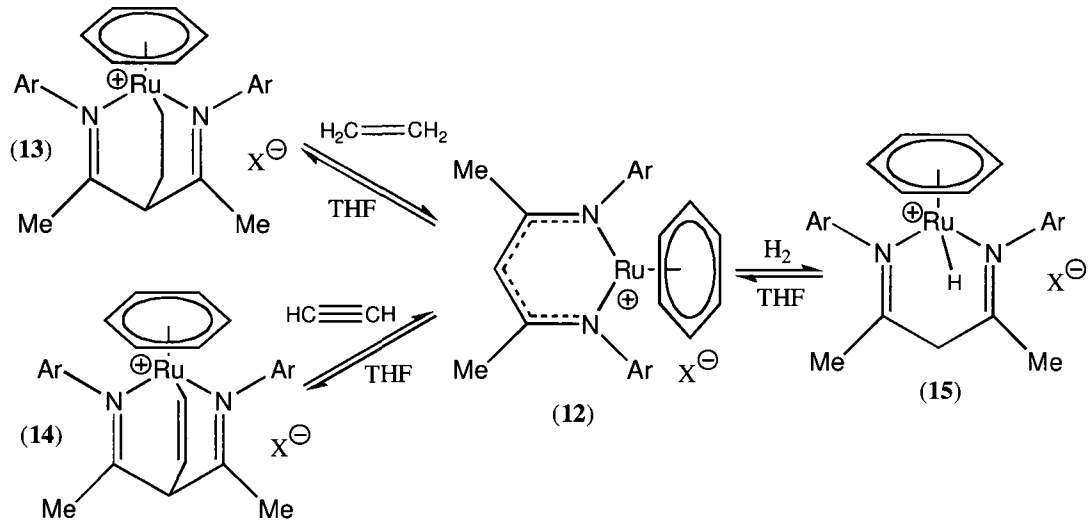

Scheme 4: Small molecule activation by $[(\eta^6\text{-}C_6H_6)Ru((ArNCMe)_2CH)]X$ (X = OTf^-)

What is remarkable about this system is that all the cycloaddition reactions are in fact reversible, with acetylene being released at room temperature over a period of one day and ethylene being released only at elevated temperatures (>50°C). The reaction between H_2 and the ruthenium-*nacnac* system, at 100 bar of pressure, results in the formation of a highly reactive solid that readily releases H_2 at room temperature. The lifetime of this unstable ruthenium species can be extended by lowering the temperature of the complex below -25°C. Nonetheless, it represents a rare example of reversible heterolytic cleavage of dihydrogen by a nucleophilic carbon centre, whereas in the majority of previously reported cases, dihydrogen cleavage is facilitated by electronegative elements such as N, O, S and Cl.[1] There have been a number of other β-diketiminate complexes featuring Rh, Ir and Pt[13a-c] which form terminal hydrides as well as Fe and Cr[14a,b] species containing bridging hydrides have been reported. However, none involve the interaction and reversible transformation of the β-diketiminate ligand system as uniquely observed in the ruthenium derivatives shown above. The key to these compounds reactivity is the

formation of a vacant coordination site at the ruthenium centre, that allows for the activation of these small molecules resulting in thermally reversible cycloaddition with ligand participation.

Dyson's work is the only report exploring ruthenium-*nacnac* complexes, yet quite clearly demonstrates the potential for a wealth of interesting reactivity. Given the well-known nature of the *nacnac* ligand for stabilization and the ability of the ligand backbone to participate in the reaction, further exploration of this system with varying ligand substitution patterns can only add to the sparse field of ruthenium β-diketiminate chemistry. Its exceptional properties and abilities are a natural complement to the no less exceptional and abundantly exciting abilities of ruthenium.

NOTES ON RUTHENIUM

This rare transition metal really has unique and unparalleled chemical behaviour. Its versatility and usage is in diverse areas such as catalysis, microelectronics, solar cells and even in the treatment of cancer.[15] Over the last four decades there have been thousands of inorganic drugs screened for their medicinal activity in a wide range of diseases, but only a handful have actually made it into clinical usage.[16] One of the most attractive aspects of organometallic complexes in medicine, specifically cancer treatment, is their promise in overcoming several types of drug resistance and allowing improved specificity and reduced side effects.[16]

Rapidly dividing cancer cells, and those infected by parasites, have a much higher iron requirement than healthy cells, and in order to satisfy this need these cells increase the expression of transferrin-receptors. Transferrin is a natural transport protein which binds iron(III) in the blood and delivers it to cells according to the number of transferrin-receptors expressed on the cell surface. Drugs that can take advantage of transferrin-mediated transport and delivery have been shown to accumulate in those diseased cells and this is where the unique metal ruthenium comes into play. Ruthenium(III) has been shown to mimic iron binding to this transport protein and thus, organo-ruthenium drugs that retain this capability could potentially exploit this iron delivery system to gain entry into diseased cells. Once inside these cells, ruthenium(III) is reduced to ruthenium(II), a form which is generally more toxic for biological systems. This mechanism of transport and activation has been suggested as an explanation for the mode of action and low toxicity of the ruthenium salt, $ImH[Ru(Im)(Me_2SO)Cl_4]$ (Im = Imidazole) called NAMI-A (**16**) (***Figure 4***).[16]

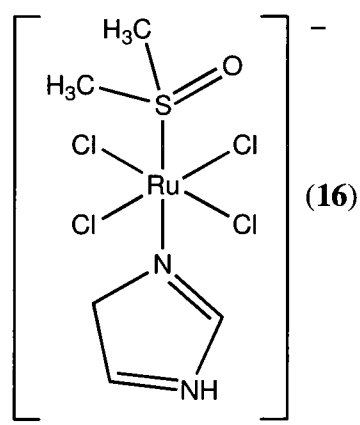

(**16**)

NAMI-A

Figure 4: The chemical structure of NAMI-A

Further studies have shown that there are numerous ruthenium(II)-arene complexes (***Figure 5***) that demonstrate anticancer/antimetastasis activity (**17-22**) as well as remarkably low toxicity, despite the fact that these complexes enter the physiological environment in the more biologically active ruthenium(II) form.[16]

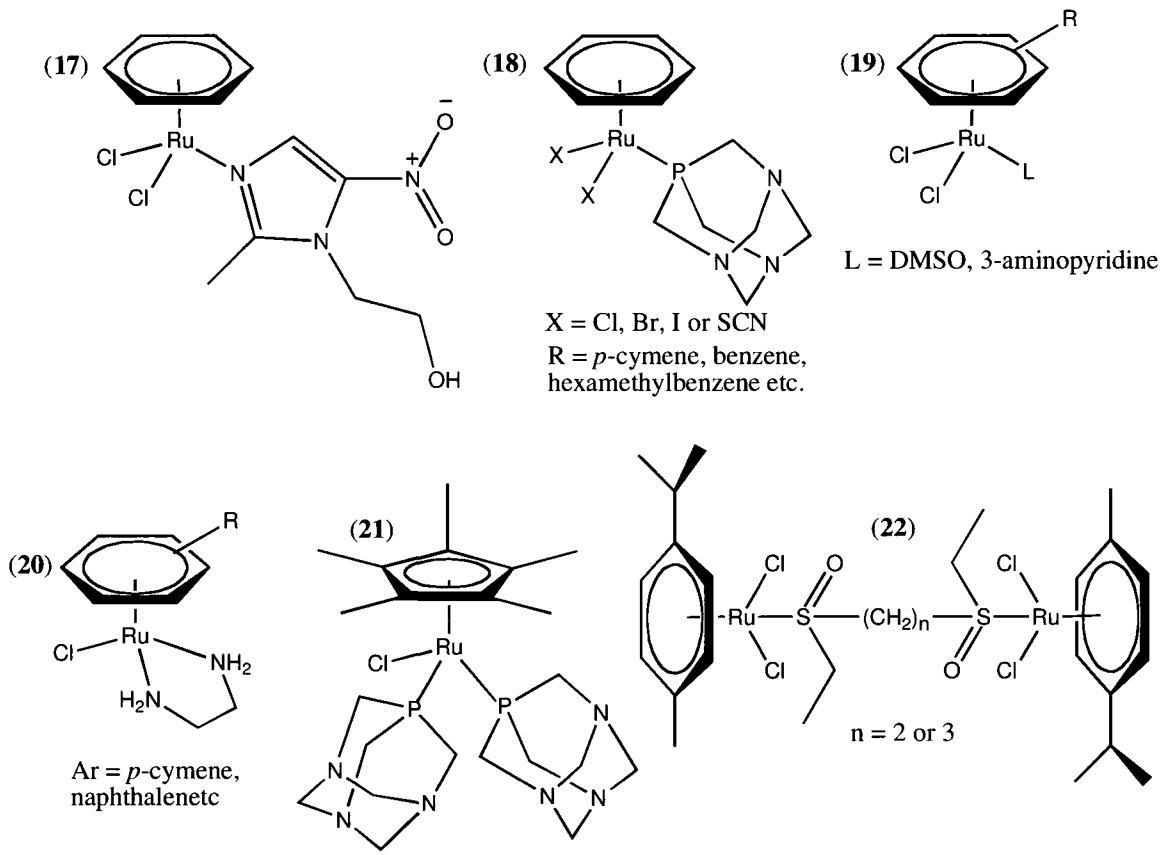

Figure 5: Selected Ruthenium(II)-arene anticancer complexes

Ruthenium is not only the centre of attention in important discoveries such as cancer fighting drugs, but it also plays a remarkable role in the ongoing quest for viable hydrogen fuel cell technology. Hydrogen itself represents an important alternative energy feed for both environmental and economic reasons and when this gas is combined with

fuel-cell technology, highly efficient energy conversions can be realized.[17] Using hydrogen as opposed to fossil fuels is advantageous but is limited mainly due to storage and delivery problems. Consequently, there is a great deal of research being undertaken to develop new materials such as metal hydrides and carbon nanostructures that have the ability to store hydrogen efficiently, but so far there have not been any satisfactory options discovered. Hydrogen storage is one challenging issue but an equally important issue is the source of hydrogen in these fuel systems. Formic acid has come to the forefront as a potential source of hydrogen and has a significant advantage over other substrates since only gaseous products are formed (H_2/CO_2). This effectively prevents the accumulation of by-products, which would seriously impede future mobile applications of this technology.[17] Recently, Dyson *et. al.* reported a robust homogeneous ruthenium based catalyst which is completely selective for the formation of hydrogen gas from formic acid in a solution of water. A hydrophilic catalyst generated from a simple reaction of *meta*-trisulfonated triphenylphosphine (TPPTS) with either $[Ru(H_2O)_6]^{2+}$ or $RuCl_3$ generates H_2/CO_2 pressures between 1 and 220bar with no inhibition of catalytic activity observed up to pressures of 750bar. All the formic acid is consumed and remarkably $[Ru(H_2O)_6](tos)_2$ is stable up to 170°C and remains active after one year in solution. A continuous system was developed in which formic acid was added under pressure into a reactor containing 12 mL of catalyst solution and gases were released at a constant pressure from the reactor. The purity of hydrogen obtained in this manner makes this catalytic system suitable for use with all types of fuel cells. In addition, since a constant pressure of hydrogen is produced, it can be used directly in combustion or fuel-cell powered electric engines. This ruthenium-based system essentially overcomes any

previous limitations to the application of formic acid as a hydrogen-storage material and formation of any side products, making this system an excellent candidate for real-world application.[17]

The ability of ruthenium to interact with hydrogen is well known and has been studied in-depth.[18] Bis(dihydrogen) complexes are rare and the majority of these exist on ruthenium centres supported by bulky phosphines. In an early discovery by Chaurdet *et. al.* a ruthenium bis(dihydrogen) system displays a fascinating and reversible reactivity with hydrogen and dinitrogen (***Scheme 5***).[19]

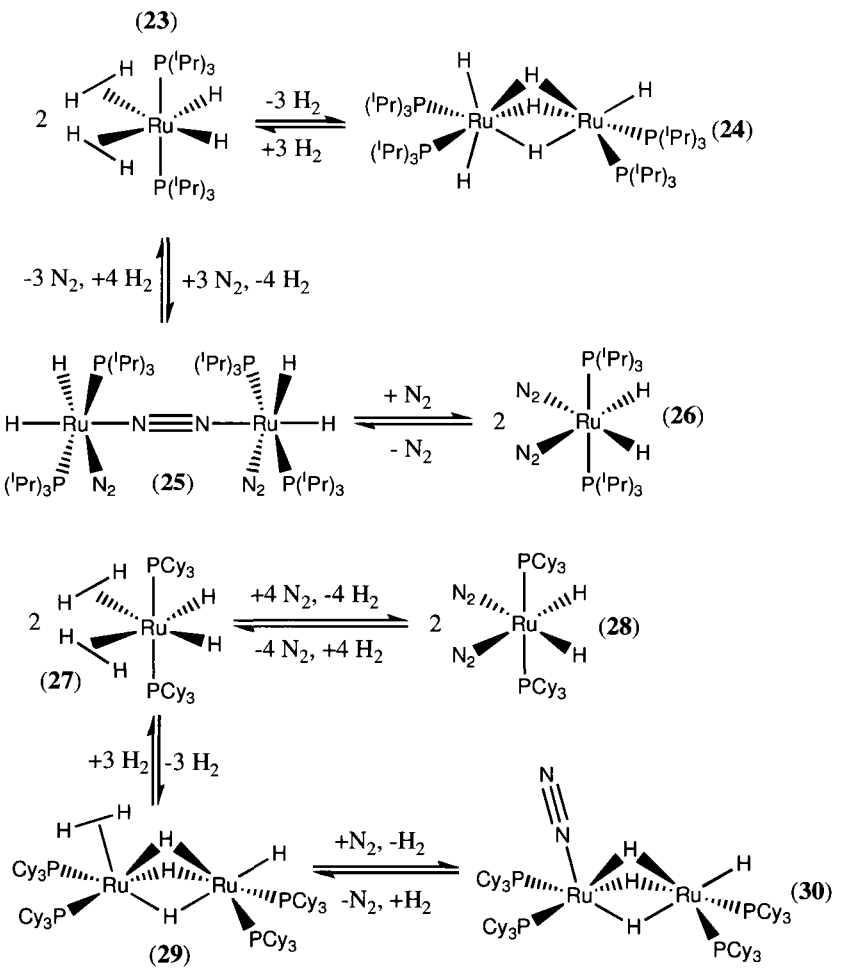

Scheme 5: Bis(hydrogen) $RuH_2(\eta^2\text{-}H_2)_2(PR_3)_2$ (R = ^{i}Pr, Cy) reversible reactivity

Ruthenium not only activates molecules such as hydrogen and dinitrogen, but also has the ability to easily add other small molecules, such as CO, even in the presence of coordinative saturation. Caulton *et. al.* observed that by using a bisphosphinimino methanide ligand system, which shows remarkably variable bonding, and a ruthenium centre, which dissociates one imine nitrogen arm of the ligand, a CO molecule readily reacts with an $18e^-$ ruthenium centre affording $(C_5Me_5)Ru(CO)[\eta^2\text{-}HC(PPh_2NPh)_2]$ (***Scheme 6***).[20]

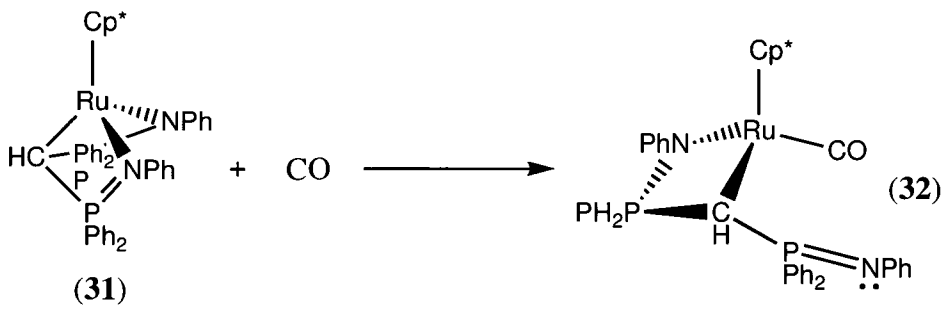

Scheme 6: Addition of CO to an 18-electron ruthenium(II) centre

A particularly desirable property of ruthenium consistent throughout its chemistry is its inherent stability and ability to catalyze reactions in a wide range of solvents. Where other complexes may decompose or show a reduced reactivity, ruthenium excels. An example of this is the ability of an aqua complex $[(\eta^6\text{-}C_6Me_6)Ru^{II}(bpy)(OH_2)](SO_4)$ to react and form a hydride with $NaBH_4$ in water at pH 7 at 25°C. Addition of CF_3SO_3Na to the hydride solution results in the formation of $[(\eta^6\text{-}C_6Me_6)Ru^{II}(bpy)H](CF_3SO_3)$ (**33**) (***Figure 6***).[21]

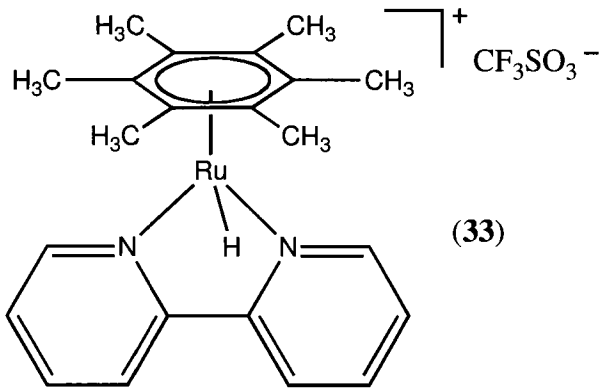

(**33**)

Figure 6: Structural representation of $[(\eta^6\text{-}C_6Me_6)Ru^{II}(bpy)H](SO_4)$

This hydride complex $[(\eta^6\text{-}C_6Me_6)Ru^{II}(bpy)H](SO_4)$ reduces CO_2 dissolved in H_2O at pH 4.0 at 25°C to form formate ion. This is of course an extremely attractive reaction since it activates CO_2 in aqueous medium.[21]

Not only does ruthenium play an important role in the activation of a wide range of small molecules but also has a well-established history in the field of olefin metathesis.[22] In particular, recent developments of ruthenium olefin metathesis catalysts show high activity and a wide range of functional group tolerance, which has expanded the current scope of olefin metathesis. However, performing metathesis reactions in aqueous media is still a challenge and is critical for some biological applications. Recently Grubbs *et. al.* developed a water soluble metathesis catalyst (**34**) which uses PEG (polyethylenglycol) on the backbone of a saturated 1,3-dimesityl-4,5-dihydroimidazol-2-ylidene (H_2IMes) to enhance its solubility in water as well as organic solvents (***Figure 7***).[23]

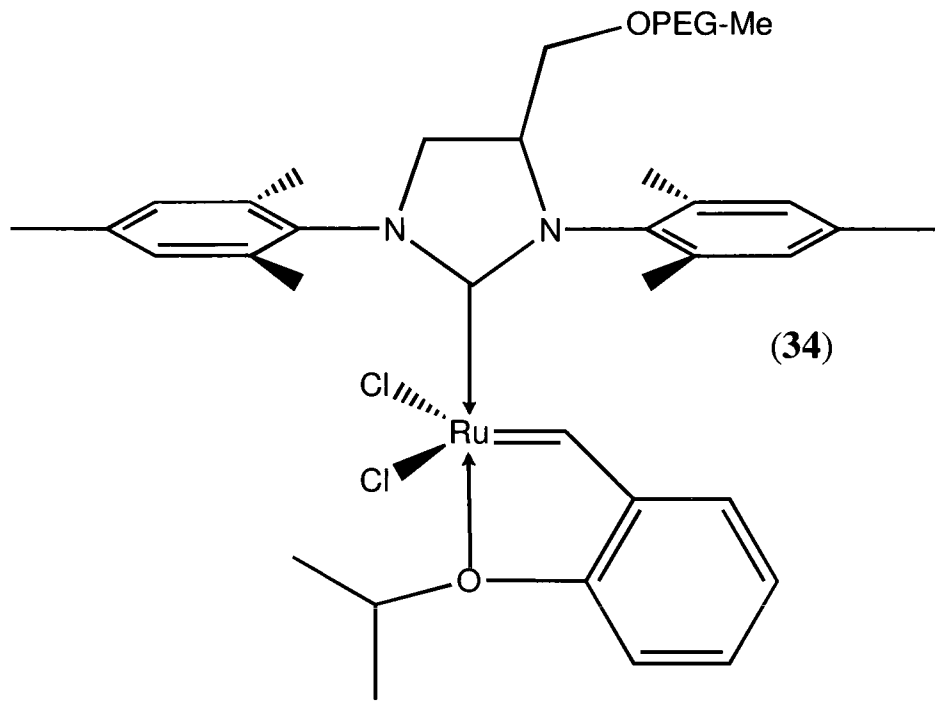

(34)

Figure 7: Water-soluble olefin metathesis catalyst bearing a pendant PEG

The catalyst shows unprecedented RCM activity with water soluble α,ω-dienes in water yielding the corresponding five and six-membered products in good to excellent yields (>95% to <5%).[23]

The wide range of reactivity displayed by ruthenium across solvents and ligands is enormous and only a handful of examples have been herein discussed, nonetheless, based on its history this metal centre provides an established record of interesting and novel reactivity and should prove intriguing when combined with a β-diketimine ligand. Chapter two of this thesis is an account of my attempts to generate Ru-β-diketiminate complexes for further reactivity studies targeting reversible activation of small molecules. Unfortunately, while this work was in progress, the appearance in the literature of the Dyson *et. al.*[1] report removed some novelty of my findings.

ACTIVATIONS, FIXATIONS AND INSERTIONS OF CO_2

Carbon dioxide plays a pivotal role in synthetic biological chemistry as a one-carbon building block.[24] This is in sharp contrast with the great thermodynamic stability of this molecule which makes its activation a challenging task. Nature disregards the large bond enthalpy of the C=O bond (532kJ/mol) and is capable of utilizing first-row late transition metals to fixate and reduce CO_2 to CO by using acetyl coenzyme A synthase/CO dehydrogenase.[24] The fundamental challenge and motivation for this chemistry is based greatly on the discrepancy between the high complexity of the system employed by nature to convert CO_2 into organic matter and the difficulties encountered by chemists in converting CO_2 via efficient catalytic reactions into non-trivial products.[25] By employing enzymatic systems, in which metal centres are instrumental, nature is able to convert CO_2 under mild conditions. The most abundant enzyme of the entire biosphere is probably the *rubisco* enzyme (**36**) (***Figure 8***), which involves a magnesium(II) centre, utilized in the Calvin cycle to catalyze the first major step of carbon dioxide fixation.[24]

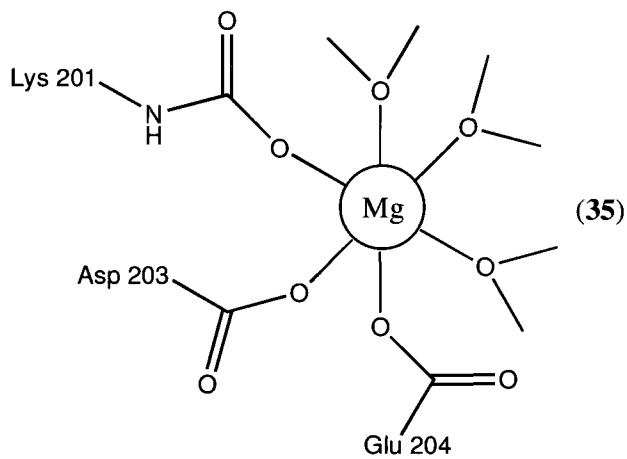

(**35**)

Figure 8: Structure of an active metal containing *rubisco* unit without substrate

The central magnesium ion does not only induce a certain spatial orientation of the reacting compound but it also causes entatic states due to its positive charge. The carbamato/carboxylato groups in the active centres of many of biological enzymes have varying modes of coordination to metal ions (Mg, Mn, Ni, Zn) indicating that they may display a rich co-ordination chemistry (***Figure 9***).[24]

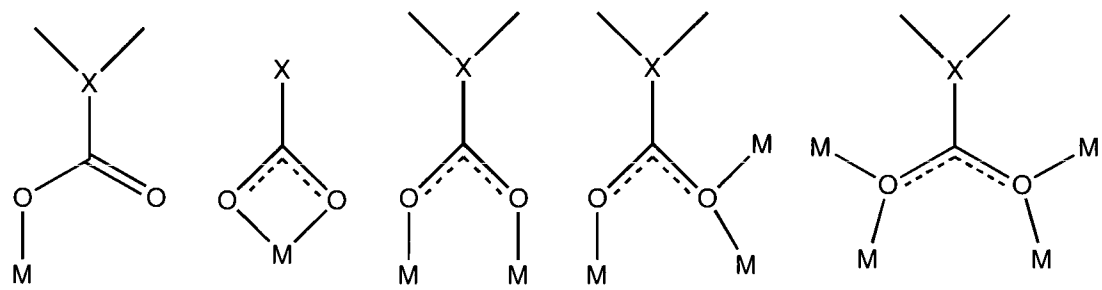

Figure 9: Possible bonding types of carboxylate (X = C) and carbamato (X = N) ligands.

Be it in biological or synthetic systems, the Lewis basic oxygen atom, or the electrophilic central carbon of carbon dioxide will usually bond to a metal centre generally leading to activation and further transformation.[25] In attempts to better understand biological processes and generate models for surface-bound intermediates in catalytic conversion processes, the insertion of carbon dioxide into Mg-C, Mg-N and interaction with heterogeneous Mg-O has been studied.[24,25,26a-d,27] Carbon dioxide ligated magnesium compounds often yield linear trimeric and cage structures with various bonds between the carboxylato or carbamato ligands and magnesium atoms.[25] A few CO_2 insertion/activation reactions involve main group elements such as aluminium and magnesium. In 1995 Chang *et. al.* synthesized and characterized several mixed aluminium-magnesium complexes and studied their reactions with CO_2.[27a,b]

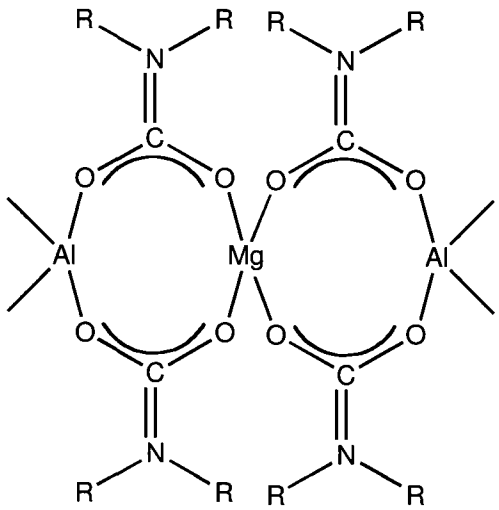

Figure 10: Generalized structure of a selected mixed Al-Mg carbamato complex presented by Chang *et. al.*

The reactivity of CO_2 with metal has received a great deal of attention under growing concern about climate change and the compelling need for reduced CO_2 emissions.[28] The hope is that studying CO_2 chemistry will allow for the reversible utilization of CO_2 as an alternative source of carbon, alleviate global climate change and extend the present limited carbon sources. Laboratory-scale photosynthetic modelling studies are obviously the starting point for these goals. However, these possible beneficial outcomes are still far from being realized due to the great kinetic inertness of CO_2. The holy grail of CO_2 activation is to develop a method to force the molecule into selective transformations under relatively mild conditions. All methods of activation and fixation, be they biological, electrochemical, thermal, all rely on the activation of CO_2 by coordination of the molecule to a transition metal centre as shown below (***Figure 11***).[28]

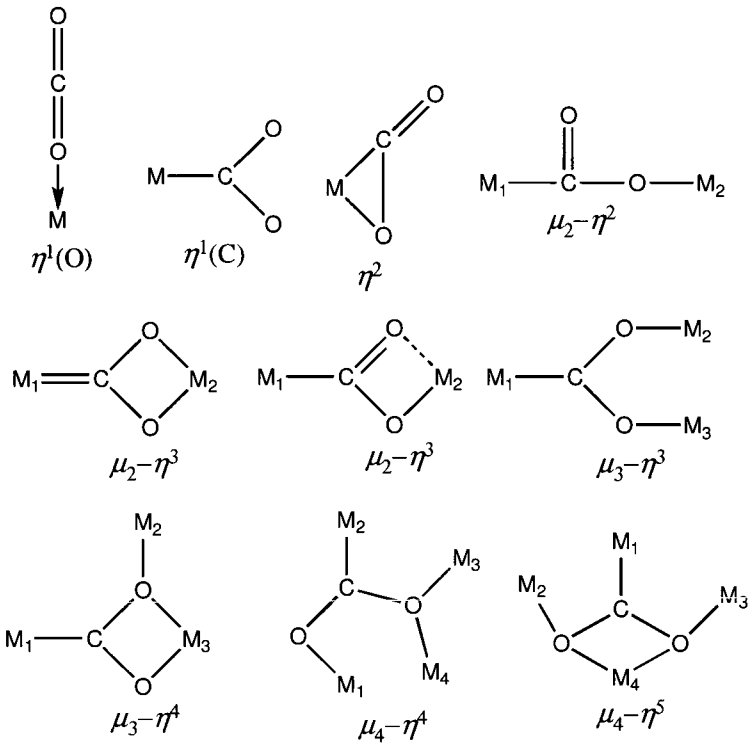

Figure 11: Structural types of metal-CO_2 complexes.

Some of the very first examples of CO_2 coordination to a transition metal centre were reported by Herskovitz and Aresta on rhodium (**37**) and nickel (**38**) metal centres respectively. As shown below (***Figure 12***), they exhibited the very first structurally defined example of η^1(C) and η^2 bonding modes.[29]

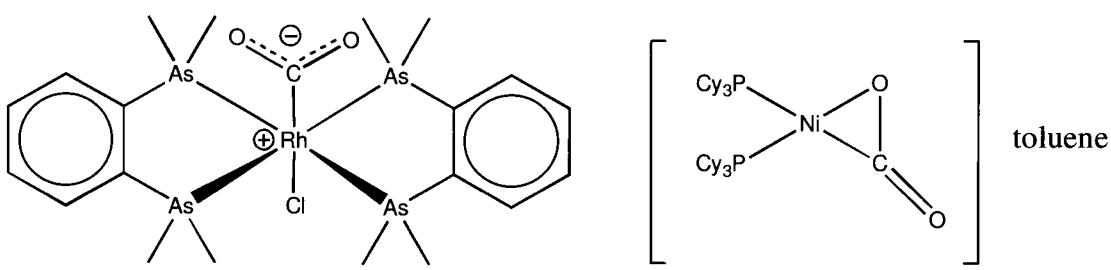

η^1 (C) *Herskovitz Complex*
(**37**)

η^2 *Aresta Complex*
(**38**)

Figure 12: Structurally defined example of η^1(C) and η^2 bonding modes

Following the publications of these groundbreaking complexes a myriad of results were published detailing the unique and novel reactivity of carbon dioxide with various metal centres.[28,29,30a-j] Since the time of these discoveries, the importance and sense of urgency surrounding the chemistry of carbon dioxide has intensified greatly. With this renewed purpose and vast knowledge of the chemical reactivity of carbon dioxide, current experimental publications may be interesting and novel from an academic standpoint but remain far from the ultimate target of discovering catalytic and useful methods of transforming carbon dioxide.

Catalytic co-polymerization of carbon dioxide, most often with epoxides, is the best example of catalytic incorporation of CO_2. It has received much current interest, again due to the obvious environmental implications.[31] The catalytic cycle may be triggered by a variety of complexes based on metals such as zinc, aluminium, chromium, cadmium, magnesium and cobalt.[32] A recent and interesting example of the progress made in this field is provided by a lanthanide hydride complex (**39**) that shows a strong inclination towards carbon dioxide fixation and copolymerization with cyclohexene oxide without necessity for the use of a co-catalyst (***Scheme 7***).[32]

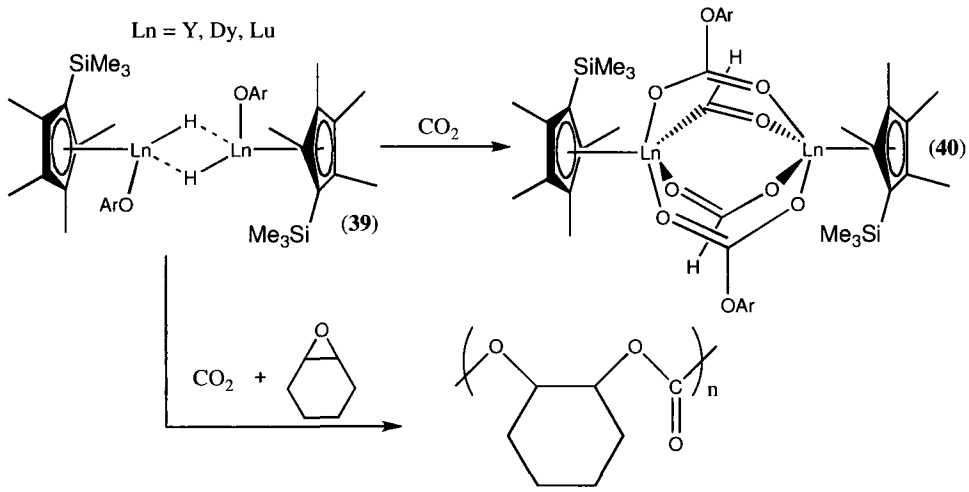

Scheme 7: Reactions of *mono*(cyclopentadienyl)-ligated rare earth-metal hydride/arloxido complexes

Besides copolymerization with epoxides, the deoxygenation of carbon dioxide resulting in carbon monoxide formation is another typical outcome of carbon dioxide reactivity. A recent publication by Sadighi *et. al.* reports the deoxygenation of carbon dioxide across Ni^0 centres (***Figure 13***).[33]

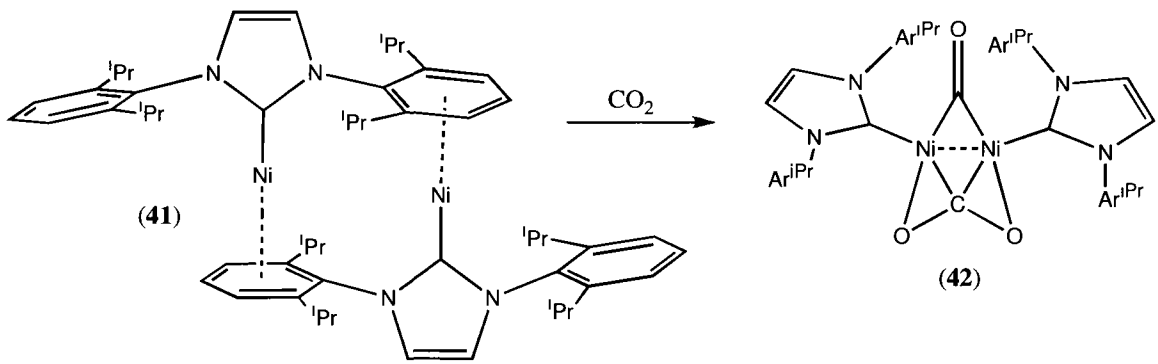

Figure 13: Deoxygenation of CO_2 by a Ni^0 complex resulting in the formation of $[(IPr)Ni]_2(\mu\text{-}CO)(\mu\text{-}\eta^2,\eta^2\text{–}CO_2)$ (**42**) (IPr = 1,3-bis(2,6-diisopropylphenyl)imidazol-2-ylidene)

These reactions along with disproportionations, hydrogenations and insertions[30a-k] of carbon dioxide are the typical disappointing outcomes of this chemistry. Nonetheless, their merit is to demonstrate that significant efforts have been devoted towards exploring technologies for carbon dioxide transformation wherein metal catalysts play a key role.

The majority of the transformations described above imply a two-electron attack on the electrophilic carbon atom of the CO_2. A much more challenging, and atypical, transformation is the one electron attack, which, by imparting a radical type of behaviour to the CO_2 carbon atom, may prelude to coupling and formation of oxalates. Incidentally, catalytically transforming CO_2 gas into a solid oxalate or oxalic acid would be a possible solution to the CO_2 related environmental problem. A recent publication by Lu *et. al.* exhibits this coupling in a structurally unique Fe core (***Scheme 8***).[30l] This system readily reacts with CO_2 at ambient temperatures to mediate the reductive cleavage of the carbon dioxide, which results in the major bimetallic cleavage product, Fe(μ-O)(μ-CO)Fe (**44**), and the minor Fe(μ-η^2:η^2-oxalato)Fe (**45**) oxalate product. This iron(I) system is unique as it is able to mediate both the reductive cleavage and coupling of CO_2.[30l-k]

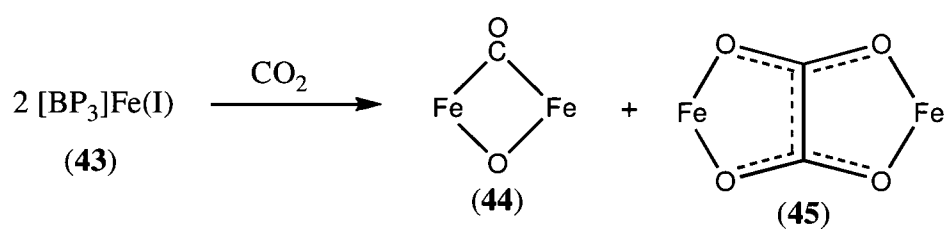

$[BP_3]Fe(I)$ = "$[PhB(CH_2P(CH_2Cy)_2)_3]Fe$"

Scheme 8: Structurally unique Fe(μ-O)(μ-CO)Fe core along with Fe(μ-η^2:η^2-oxalato)Fe

One particular branch of CO_2 chemistry, specifically the hydrosilylation of CO_2, has recently broken free of the dependence on metal catalysts. Much like the Ni^0 system, *n*-heterocyclic carbenes effectively convert CO_2 to methanol under mild conditions using air as a feedstock (***Figure 14***).[34]

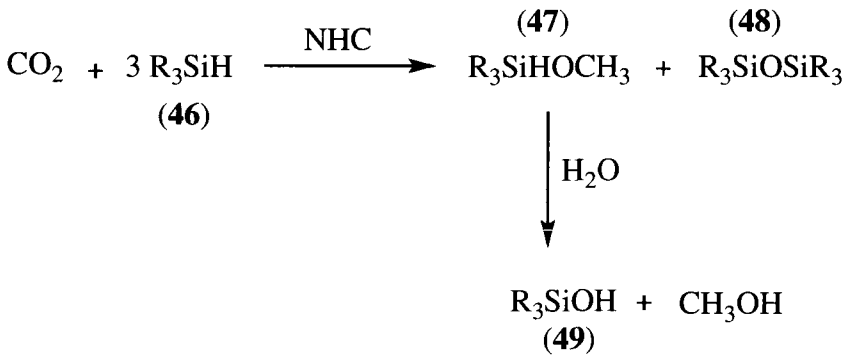

Figure 14: Overall stoichiometric reaction resulting in conversion of CO_2 to methanol

As demonstrated above, there have been some recent interesting developments that have contributed greatly to the field of CO_2 chemistry. However, these results are still far from being engineered into a commercial process that would directly impact the environment. Regardless of the wealth of information generated by the recent advances and previous studies, the linear μ(O,O')-CO_2 coordination mode of carbon dioxide remained unknown for a very long time. This was until the discovery reported in *Science* by Meyer *et. al.* which described the linear coordination of CO_2 (CO_2 angle of 178.0°) to an electron rich and sterically crowded U(III) centre (**50**) (***Figure 15***).[35] More recently, Gao *et. al.* published results detailing an inorganic polyoxoanion in water that exhibits a relatively linear μ(O,O')-CO_2 bonding mode (CO_2 angle of 158.7°) between Mo and Co metal centres.[36]

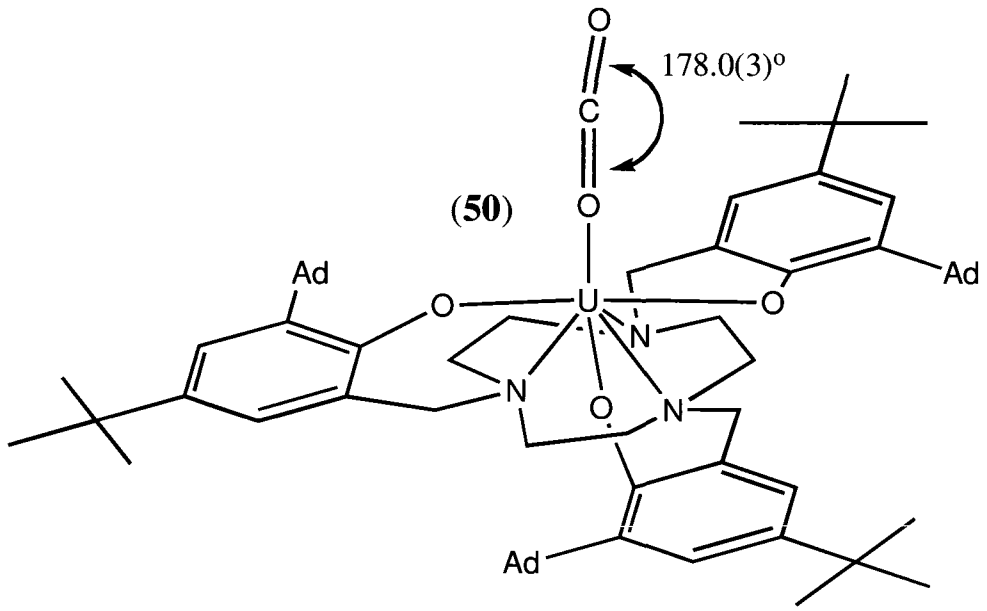

Figure 15: Uranium-CO_2 complex featuring a linearly bound CO_2

These two examples are unique amongst the myriad of metal-promoted CO_2 chemistry but the coordination of the CO_2 molecule in both cases occurs at or across transition metal centres. This bonding mode has never been observed on any other group of elements except the transition metals mentioned above, thus when a report by Chang *et. al.* claimed the linear bonding mode of CO_2 on a main group metal, magnesium, a detailed re-investigation of this groundbreaking report was deemed necessary.[36]

The publication describes the reaction of $Mg[N(SiMe_3)_2]_2$ with one equivalent of AlR_3 (R = Me, Et) in THF at room temperature under an atmosphere of carbon dioxide. The reaction mixture was subsequently cooled and yielded a trimeric complex where the metal centres were linked by linear CO_2 units (**51**) (***Figure 16***). Carbon dioxide presumably reacted with $Mg[N(SiMe_3)_2]_2$ resulting in an oxo-transfer product $Mg[N(SiMe_3)_2](OSiMe_3)$. This species formed a bridged Al-Mg intermediate with AlR_3

(R = Me, Et). In turn, this intermediate subsequently loses a ligand from the magnesium centre and is attacked by a second molecule of carbon dioxide with the oxygen atom as a weak electron donor.[37] The overall process resulted in the formation of a trinuclear magnesium μ(O,O')-CO_2 cluster.

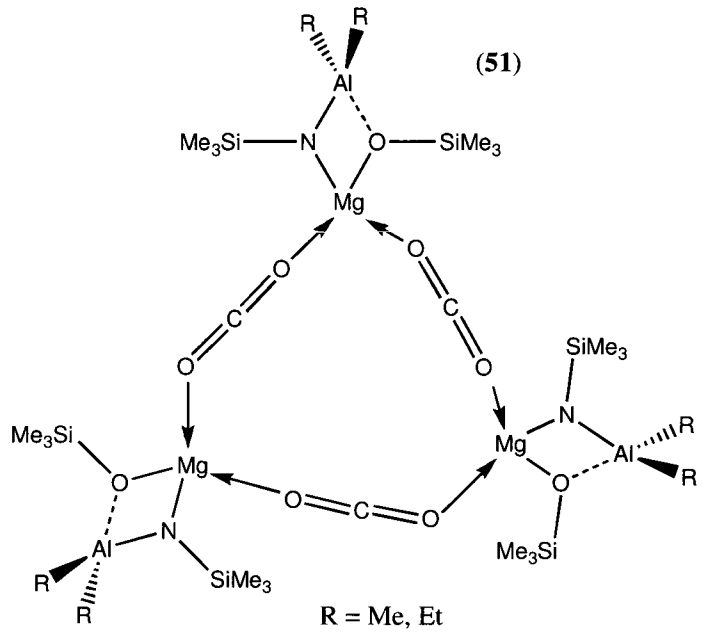

Figure 16: Schematic representation of {[$R_2Al(\mu$-$NSiMe_3)(\mu$-$OSiMe_3)Mg(thf)_2(\mu$-$O_2C)$]} (THF molecules were omitted for clarity)

The bonding mode in the structure is remarkable but begs to be questioned when one considers that direct CO_2 coordination has never been observed in d^0 or main group systems. The trimeric magnesium cluster appears to be a breakthrough representing the first case of irreversible CO_2 coordination to a non-transition metal centre in an unprecedented end on fashion. The experiment conducted by Chang *et. al.* was revisited

in chapter three and conclusively reinterpreted as the fixation of isoelectronic NCO^- anions instead of bridging CO_2 molecules.

The chemistry of small molecule activation has always been of interest to chemists and the two main publications discussed by Dyson *et. al.* for ruthenium and Chang *et. al.* for magnesium-CO_2 are examples of just how interesting and unpredictable this chemistry can be. Further exploration of these systems allows for an opportunity to add to the respective fields of ruthenium and main-group chemistry while pushing forward in the quest to discover new chemical systems that may have practical applications. In this thesis we aimed at exploring the chemistry of ruthenium supported by a β-diketiminate ligand system in hopes of achieving small molecule activation and discovering new bonding modes as well as interesting transformations that would add to the sparse field of ruthenium β-diketiminate chemistry. Accompanying this exploration is an investigation into another rare and very new bonding mode of CO_2 within a magnesium cluster and its implications on interactions with main group metal centres. Unfortunately, time constraints did not allow for a more in-depth investigation into these areas but chapter two goes on to report two new ruthenium β-diketiminate complexes that are hypothesized to have originated from an unprecedented nucleophilic mode of action displayed by the free β-diketiminate ligand. Further, chapter three details the true nature of an apparently unprecedented CO_2 interaction with a particular magnesium cluster and its implications on future interpretations of these interactions.

REFERENCES

1. A.D. Phillips, G. Laurenczy, R. Scopelliti, P.J. Dyson, *Organometallics* **2007**, 26, 1120
2. L. Bourget-Merle, M.F. Lappert, J.R. Severn, *Chem. Rev.* **2002,** 102, 3031
3. a) M. Cheng, E.B. Lobkovsky, G.W. Coates, *J. Am. Chem. Soc.* **1998**, 120, 11018; b) Z.J. Tonzetich, A.J. Jiang, R.R. Schrock, P. Müller, *Organometallics* **2006**, 25, 4725; c) S.D. Allen, D.R. Moore, E.B. Lobkovsky, G.W. Coates, *J. Am. Chem. Soc.* **2002**, 124, 48; d) P.G. Hayes, W.E. Piers, R. McDonald, *J. Am. Chem. Soc.* **2002**, 124, 2132; e) G.W. Coates, *Chem. Rev.* **2000**, 100, 1223; f) G.B. Nikiforov, H.W. Roesky, T. Schulz, D. Stalke, M. Witt, *Inorg. Chem.* **2008**, 47, 6435
4. J.M. Smith, R.J. Lachicotte, K.A. Pittard, T.R. Cundari, G. Lukat-Rodgers, K.R. Rodgers, P.L. Holland, *J. Am. Chem. Soc.* **2001**, 123, 9222
5. A.R. Sadique, W.W. Brennessel, P.L. Holland, *Inorg. Chem.* **2008**, 47, 784
6. a) A.R. Sadique, E.A. Gregory, W.W. Brennessel, P.L. Holland, *J. Am. Chem. Soc.* **2007**, 129, 8112; b) P.L. Holland, *Acc. Chem. Res.* **2008**, 41, 905; c) Y. Yu, W.W. Brennessel, P.L. Holland, *Organometallics* **2007**, 26, 3217
7. E.A. Gregory, R.J. Lachicotte, P.L. Holland, *Organometallics* **2005**, 24, 1803
8. H. Nagashima, H. Kondo, T. Hayashida, Y. Yamaguchi, M. Gondo, S. Masuda, K. Miyazaki, K. Matsubara, K. Kirchner, *Coord. Chem. Rev.* **2003**, 245, 177
9. a) P.J. Bailey, L.A. Mitchell, S. Parson, *J. Chem. Soc. Dalton Trans.* **1996**, 13, 2839; b) D. Zuccaccia, S. Sabatini, C. Bellachioma, G. Cardaci, E. Clot, A.

Macchioni, *Inorg. Chem.* **2003**, 42, 5465; c) H. tom Dieck, W. Kollvitz, I. Kleinwaechter, *Organometallics* **1986**, 5, 1449

10. A. Klose, E. Solari, J. Hesschenbrouk, C. Floriani, N. Re, S. Geremia, L. Randaccio, *Organometallics* **1999**, 18, 360
11. R. Fernandez, M. Melchart, A. Habtemariam, S. Parsons, P.J. Sadler, *Chem. Eur. J.* **2004**, 10, 5173
12. C. Bibal, M. Pink, Y.D. Smurnyy, J. Tomaszewski, K.G. Caulton, *J. Am. Chem. Soc.* **2004**, 126, 2313
13. a) P.H.M. Budzelaar, R. de Gelder, A.W. Gal, *Organometallics* **1998**, 17, 4121; b) W.H. Bernskoetter, E. Lobkovsky, P.J. Chirik, *J. Chem. Commun.* **2004**, 7, 764; c) U. Fekl, W. Kaminsky, K.I. Goldberg, *J. Am. Chem. Soc.* **2003**, 125, 15286
14. a) J.M. Smith, R.J. Lachicotte, P.L. Holland, *J. Am. Chem. Soc.* **2003** 125, 15752; b) L.A. MacAdams, G.P. Buffone, C.D. Incarvito, J.A. Golen, A.L. Rheingold, K.H. Theopold, *Chem. Commun.* **2003**, 10, 1164
15. M.J. Clarke, *Coord. Chem. Rev.* **2003**, 236, 209
16. C.S. Allardyce, P.J. Dyson, *Topics in Organometallic Chemistry: Bioorganometallic Chemistry* Springer **2006**, Vol. 17
17. C. Fellay, P.J. Dyson, G. Laurenczy, *Angew. Chem. Int. Ed.* **2008**, 47, 3966
18. P.G. Jessop, F. Joó, C.-C. Tai, *Coord. Chem. Rev.* **2004**, 248, 2425
19. G. Alcaraz, M. Grellier, S. Sabo-Etienne, *Acc. Chem. Res.* **2009**, 42, 1640
20. C. Bibal, Y.D. Smurnyy, M. Pink, K.G. Caulton, *J. Am. Chem. Soc.* **2005**, 127, 8944

21. H. Hayashi, S. Ogo, T. Abura, S. Fukuzumi, *J. Am. Chem. Soc.* **2003**, 125, 14266

22. B. Alcaide, P. Almendros, A. Luna, *Chem. Rev.* **2009**, 109, 8, 3817

23. S.H. Hong, R.H. Grubbs, *J. Am. Chem. Soc.* **2006**, 128, 3508

24. D. Walther, M. Ruben, S. Rau, *Coord. Chem. Rev.* **1999**, 182, 67

25. K.C. Yang, C.C. Chang, C.S. Yeh, G.H. Lee, Y. Wang, *Organometallics* **2002**, 21, 1296

26. a) R. Zevenhoven, S. Eloneva, S. Teir, *Catalysis Today* **2006**, 115, 73; b) C.C. Chang, M.S. Ameerunisha, *Coord. Chem. Rev.* **1999**, 189, 199 c) K.C. Yang, C.C. Chang, C.S. Yeh, G.H. Lee, S.M.Peng, *Organometallics* **2001**, 20, 126 d) K. Yamaguchi, K. Ebitani, T. Yoshida, H. Yoshida, K. Kaneda, *J. Am. Chem. Soc.* **1999**, 121, 4526

27. C.C. Chang, B. Srinivas, M.L. Wu, W.H. Chiang, M.Y. Chiang, C.S. Hsiung, *Organometallics* **1995**, 14, 5150; b) D.A. Dickie, M.V. Parkes, R.A.Kemp, *Angew. Chem. Int. Ed.* **2008**, 47, 9955

28. X.Yin, J.R. Moss, *Coord. Chem. Rev.* **1999**, 181, 27

29. D.H. Gibson, *Chem. Rev.* **1996**, 96, 2063

30. a) A. Behr, *Angew. Chem. Int. Ed. Engl.* **1988**, 27, 661; b) D.B. Dell'Amico, F. Calderazzo, L. Labella, F. Marchetti, G. Pampaloni, *Chem. Rev.* **2003**, 103, 3857; c) P. Braunstein, D. Matt, D. Nobel, *Chem. Rev.* **1988**, 88, 747; d) P.G. Jessop, T. Ikariya, R. Noyori, *Chem. Rev.* **1995**, 95, 259; e) W. Leitner, *Coord. Chem. Rev.* **1996**, 153, 257; f) D.J. Darensbourg, *Chem. Rev.* **2007**, 107, 2388; g) T. Sakakura, J.C. Choi, H. Yasuda, *Chem. Rev.* **2007**, 107, 2365; h) K. Tanaka, D. Ooyama, *Coord. Chem. Rev.* **2002**, 226, 211; i) C.C. Lu, C.T. Saouma, M.W. Day, J.C.

Peters, *J. Am. Chem. Soc.* **2007**, 129, 4; j) W.J. Evans, D.K. Drummond, *J. Am. Chem. Soc.* **1988**, 110, 2772; k) W.J. Evans, C.A. Seibel, J.W. Ziller, *Inorg. Chem.* **1998**, 37, 770

31. a) D.F. Darensbourg, R.M. Mackiewicz, A.L. Phelps, D.R. Billodeaux, *Acc. Chem. Res.* **2004**, 37, 836; b) P.T. Anastas, M.M. Kirchhoff, *Acc. Chem. Res.* **2002**, 35, 686
32. D. Cui, M. Nishiura, O. Tardif, Z. Hou, *Organometallics* **2008**, 27, 2428
33. C.H. Lee, D.S. Laitar, P. Mueller, J.P. Sadighi, *J. Am. Chem. Soc.* **2007**, 129, 13802
34. S.N. Riduan, Y. Zhang, J.Y. Ying, *Angew. Chem. Int. Ed.* **2009**, 48, 1
35. I. Castro-Rodriguez, H. Nakai, L.N. Zakharov, A.L. Rheingold, K. Meyer, *Science* **2004**, 305, 1757
36. G. Gao, F. Li, L. Xu, X. Liu, Y. Yang, *J. Am. Chem. Soc.* **2008**, 130, 10838
37. C.C. Chang, M.C. Liao, T.H. Chang, S.M. Peng, G.H. Lee, *Angew. Chem. Int. Ed.* **2005**, 44, 7418

CHAPTER TWO

PREPARATION AND CHARACTERIZATION OF RUTHENIUM (II) CYMENE β-DIKETIMINATE COMPLEXES

NOTES ON β-DIKETIMINATE COMPLEXES

The birth of β-diketonate coordination chemistry took place in the mid 1960s with the appearance in the literature of a large series of synthetic, structural, magnetic, and spectroscopic studies on homoleptic M (II) (M = Co, Ni, Cu) derivatives.[1.2a] A major development took place in the mid 1990s with their modification into the β-diketiminates, or *nacnac*. These ligands may act as useful spectator ligands by virtue of their strong metal-ligand bonds and ability to be tuned to meet various steric demands (***Figure 1***). These features account for the rapid increase of popularity experienced by these supporting molecules.[2]

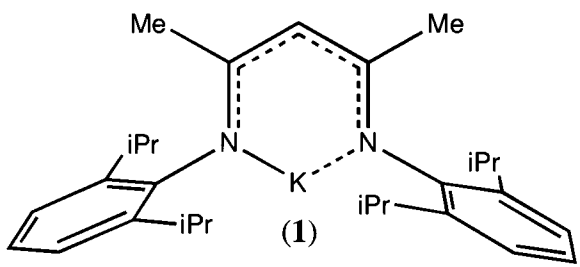

Figure 1: Structure of the potassium *nacnac* ligand utilized in current study

This class of ligand has been used for a wide range of applications such as catalyst design for polymerization across group 3-6 metal systems, one of the first being a zirconium based system that, upon activation with MAO, polymerizes ethylene and propylene.[2a,3] Various other β-diketiminate polymerization catalysts in combination with Ti, Cr, Co, Ni and Pd have received considerable attention.[1,2a,3] One of the key features of the *nacnac* ligand system that makes this ligand so versatile is its ability to stabilize transition metals

in unusual oxidation states and coordination numbers which is an excellent starting point for possibly activating small molecules such as H_2, N_2, O_2.[2a,4a-q] Interesting and unusual results quite often surround the chemistry of *nacnac*. Even though the *nacnac* ligand is considered to be quite robust, it can be transformed and involved in reactions depending on the coordinating metal. Some of these reactions include metathesis, C-H abstraction[4] of aryl groups attached to the nitrogen. Other transformations include deprotonation of methyl groups attached to the NCCCN framework and involvement of the β-carbon of the *nacnac* backbone, which is susceptible to electrophilic attack.[5] This last type of transformation is particularly interesting and often results in a coordinated diimine type ligand (***Figure 2***).[6] As shown below, even a simple lithiated *nacnac* ligand coordinating an adamantone reveals its nucleophilic nature through the β-carbon of the backbone, resulting in a dinuclear diimine formation.[7]

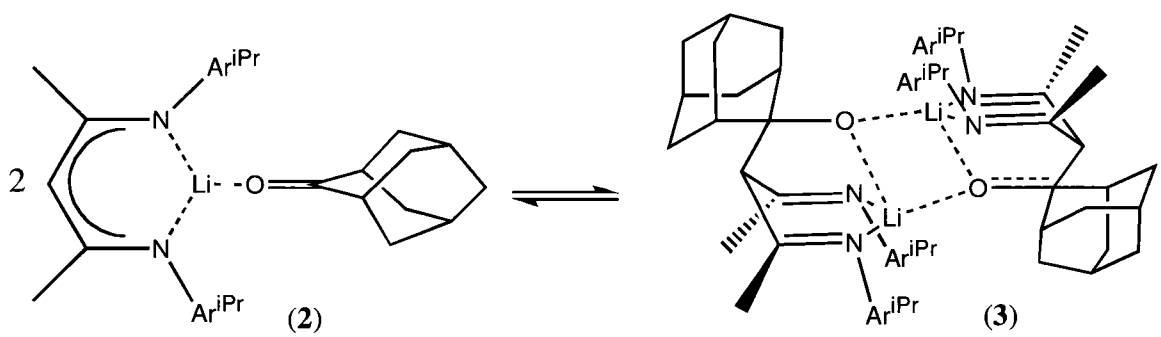

Figure 2: Adamantone as an electrophile in a lithiated *nacnac* complex resulting in diimine formation

Cationic aluminium alkyls are and always have been of interest for catalytic applications such as olefin polymerization. Fairly recently Jordan *et. al.* described several classes of aluminium dialkyl compounds {L-X}AlR_2 that incorporate bidentate,

monoanionic nitrogen based L-X$^-$ ligands including amidinates (**I**) guanidinates (**II**), and aminotroponiminates (**III**). The reactions of these aluminium alkyl species with various cationic activators result in the formation of the corresponding cationic aluminium alkyls. Complexes such as type **VI**, which coordinate weak solvent or counterion, are of particular interest for catalytic applications such as olefin polymerization. (***Figure 2***).[8]

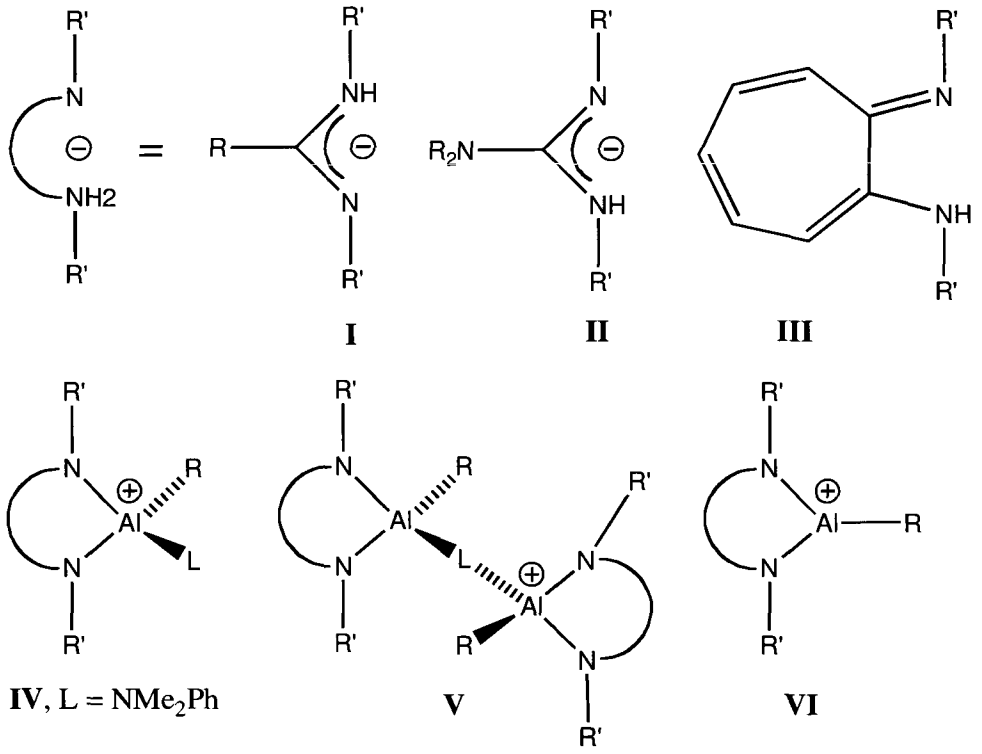

Figure 2: Common ligand systems used to synthesize aluminium dialkyls (**I-III**) and general cationic aluminium alkyls (**IV-VI**) incorporating bidentate nitrogen based ligands

In order to disfavour the formation of species as **IV** and **V**, Jordan *et. al.* synthesized a crowded Al-*nacnac* system in hopes that the increased steric demand of the ligand and the consequent tension in the six-membered chelate ring would result in the formation of a type **VI** complex (***Scheme 1***).

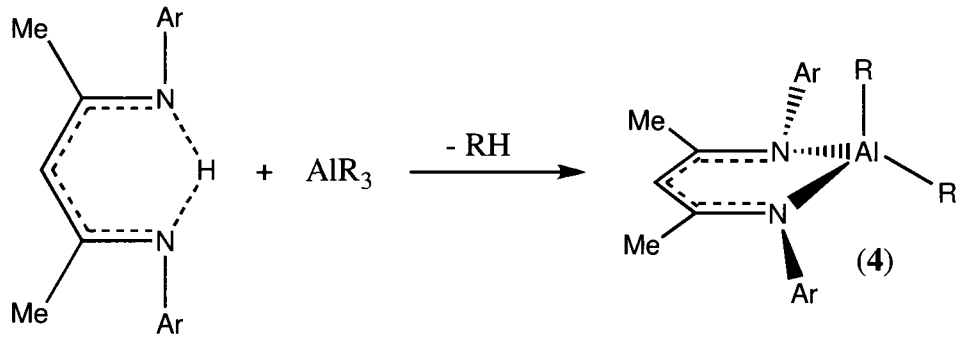

Ar = 2,6-$^{i}Pr_2$-C_6H_3 R = Me, Et, ^{i}Bu

Scheme 1: Synthesis of {L-X}AlR_2 complexes

The resulting aluminium β-diketiminate complex (**4**) is, unsurprisingly, not an active catalyst but nonetheless displays an interesting behaviour when exposed to cationic activators. Treatment of the system with one equivalent of $[PH_3C][B(C_6F_5)_4]$ and futher exposure to ethylene was anticipated to generate a catalytically active type **VI** cationic aluminium species. The reaction resulted, instead, in the 1,4 cycloaddition of ethylene to $[HC(CMeNAr)_2]AlEt^+$ (**6**) which underwent cycloreversion and ethylene loss upon reaction with one equivalent of $[HNMe_2Ph][B(C_6F_5)_4]$ (***Scheme 2***).[8]

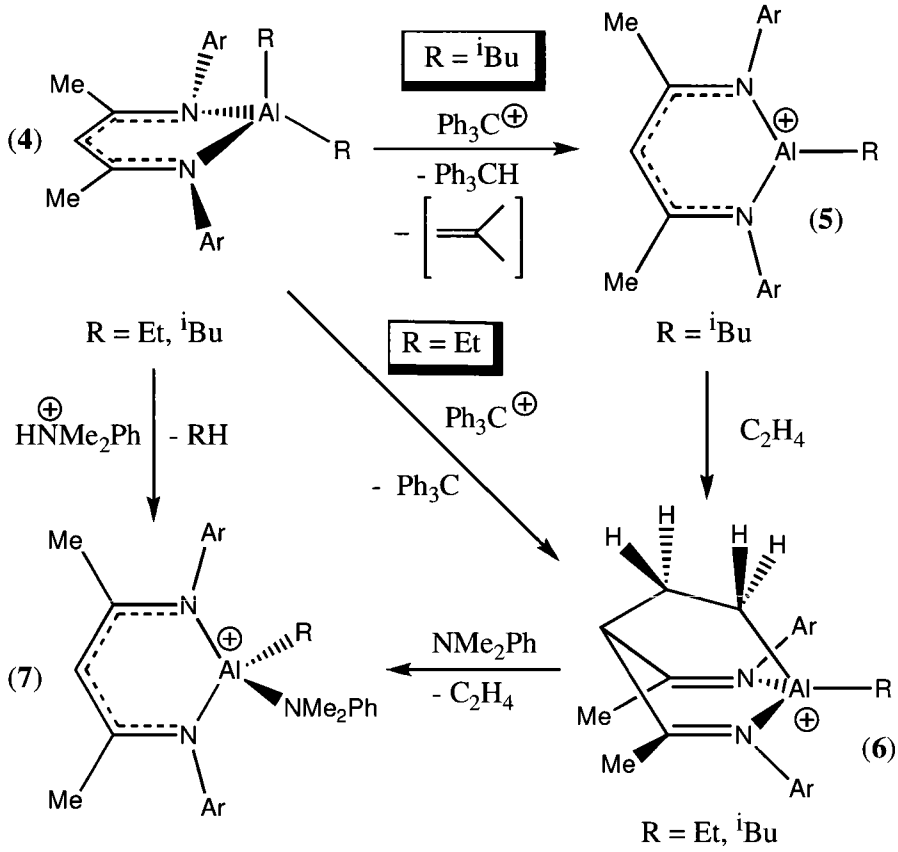

Scheme 2: Reaction summary of {L-X}AlR_2 complexes

This surprising discovery was made with a cationic *main group nacnac* complex which reacted with an *unactivated* olefin (ethylene) to afford *reversible* cycloaddition.[8] Besides the uniqueness of this behaviour, this provides an excellent illustration of the potential nucleophilic character of the β-carbon of the *nacnac* backbone and the ligands ability to participate in the reaction.

The majority of *nacnac* type ligands are commonly prepared by the reaction of acetylacetone and various anilines, affording stable ligand backbones allowing the characterization and synthesis of a wide variety of metal complexes.[9] Yet, little attention has been given to possible *nacnac* ligand degradation reactions that may take place in the

process of preparing and isolating various organometallic complexes. In 2002, Yokota *et. al.* published a work detailing copper(II) and zinc(II) complexes supported by the *nacnac* ligand which easily undergo an oxidative degradation to afford a ketone diimine species (**8**) (***Scheme 3***).[9]

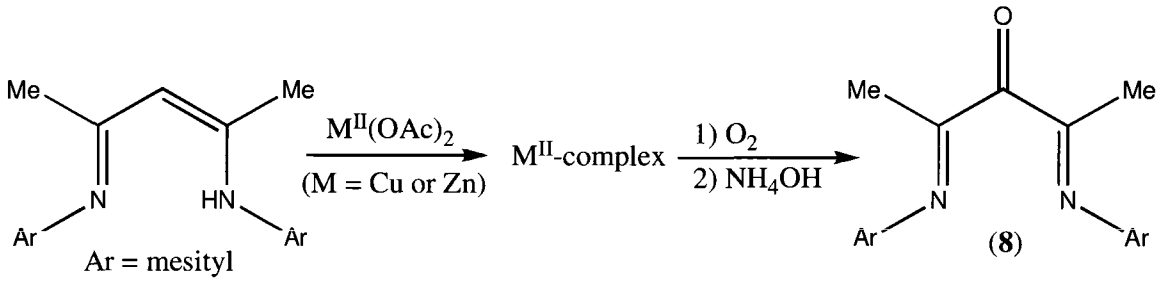

Scheme 3: General representation of *nacnac* ligand oxidative addition

Treatment of the zinc(II) and copper(II) complexes in methanol at 50°C under aerobic conditions results in the oxidative degradation of the ligand backbone. The origin of the oxygen was confirmed when the reactions were carried out in anaerobic conditions using $^{18}O_2$, which resulted in the corresponding ^{18}O-labelled product. Although mechanistic details surrounding the formation of ketone diimine were not completely disclosed in the study, a speculative reaction pathway based on one-electron transfer reduction of O_2 to a superoxide ion was used to account for the mechanism (***Scheme 4***).[9] Fukuzumi *et. al.* demonstrated that electron transfer reduction of O_2 to a superoxide ion is significantly enhanced by redox-inactive Lewis acids and thus, the drive of the reaction has been ascribed to the coordinative interaction between the Lewis acid and $O_2^{\cdot -}$.[10]

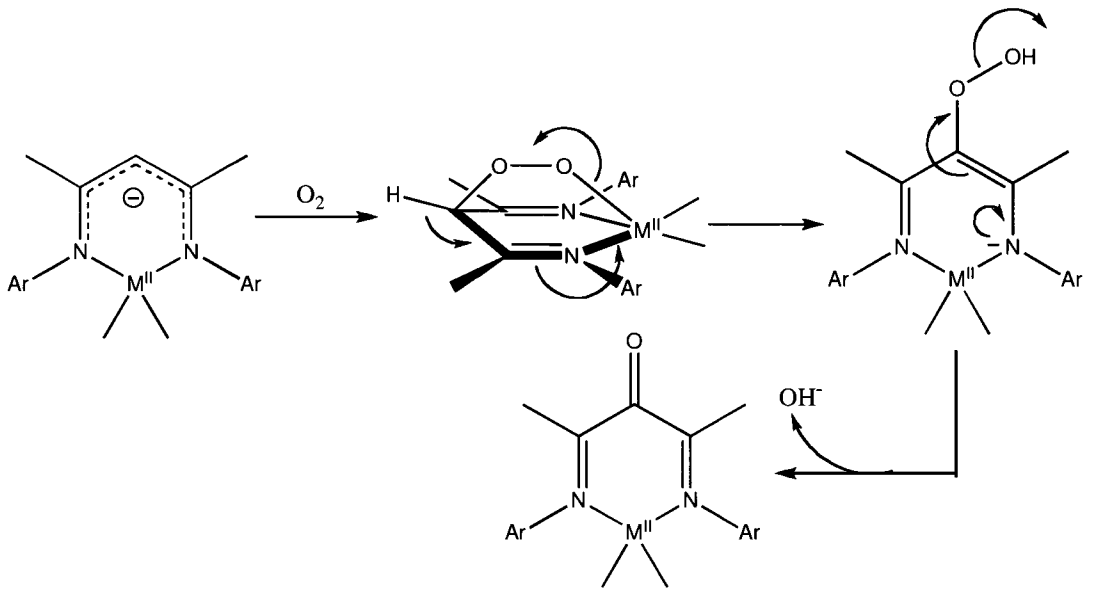

Scheme 4: Proposed mechanism for ketone-diimine formation

Although the mechanism of the ketone-diimine formation is nothing more than speculation, the involvement of the β-carbon in the transformation is hypothesized as being an integral step of the activation and conversion of the O_2 molecule. It is also worthy to note that during a previous study of the reactivity of a macrocyclic cobalt(II) complex,[11] using a tetraaza macrocyclic dianionic ligand, a similar degradation product, a ketone-diimine, was observed (**9**). This time a peroxo species was isolated as an intermediate (***Figure 3***).

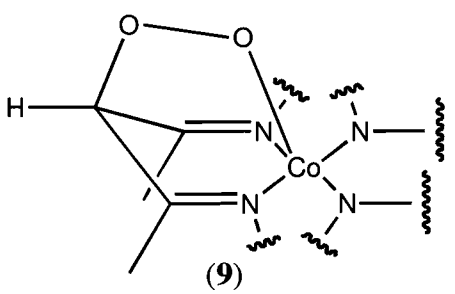

(**9**)

Figure 3: Macrocyclic peroxo cobalt-diimine type intermediate

The versatility and ability of the ligand to stabilize coordinatively unsaturated species, which are notoriously difficult to characterize owing to their inherent reactivity, is well known. This fact was further substantiated in a publication by Fekl *et. al.* while studying the coordination sphere of Pt(IV) alkyl species.[12] These particular platinum species have been consistently proposed as key intermediates in reductive/oxidative addition reactions that form or break C—C, C—H, C—O, and C—I bonds through Pt(IV)/Pt(II) complexes. These species have never been unambiguously characterized. Attempts to generate them experimentally have led to the observation that weakly coordinating anions or solvent molecules bind to the metal making examination of the coordinately unsaturated compound impossible. This changed when a reaction of platinum(IV) triflate with a potassium-*nacnac* ligand afforded the very first example of an isolable five coordinate (L)$PtMe_3$ species. Five coordinate Pt(IV) alkyl complexes are highly labile and although the (L)$PtMe_3$ (**10**) is stable in pentane or cyclohexane at ambient temperatures when protected form light, exposure to ambient room light results in methyl-migration from the platinum centre to the β-carbon of the *nacnac* ligand backbone (***Scheme 5***).[12]

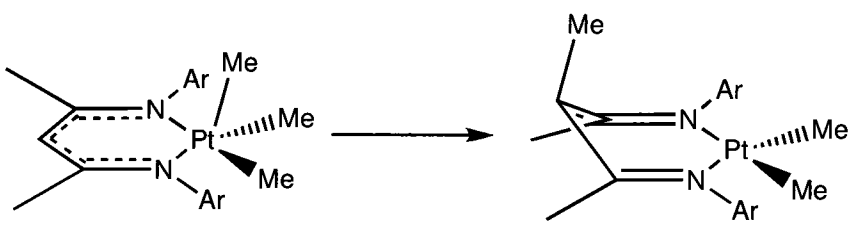

Ar = 2,6-^{i}Pr-C_6H_3

(**10**)

Scheme 5: Methyl migration resulting in Pt(II) centre

The resulting (L-Me)$PtMe_3$ complex is a four-coordinate Pt(II) complex. This confirms the ability of the *nacnac* ligand to support a wide variety of complexes but also demonstrates the importance of the involvement of the β-carbon of the ligand in the reactivity with a variety of substrates.

The involvement of the activated β-carbon is a common theme across various *nacnac* systems and, as previously mentioned, even a tetraaza macrocyclic dianionic ligand system displays similar reactivity. In fact it was one of the first examples documenting the involvement of the β-carbon in the activation of alkenes.[6,11] The macrocyclic ligand derived from the condensation of *o*-phenylenediamine with 2,4-pentandione is a ligand with a high degree of distortions. This leads to strained coordination environments for metal ions as is the case of the respective cobalt complex. The reaction of the free ligand, $C_{22}H_{24}N_4$, with 1 equivalent of $Co(OAc)_2 \bullet 4H_2O$ in a methanol/acetonitrile solution yields a four-coordinate Co(II) complex (**11**), which after oxidation with O_2 yields the six-coordinate species $[CoL(py)_2]^+$ (**12**). Under acidic conditions, complex **12** readily adds one molecule of nitrile (**13**) with a wide variety of substituents, not to mention acetylene and various monosubstituted acetylenes (**14**) (R = -Ph, $-CH_2OH$, $-CH_3$) (***Scheme 6***). The addition of acetylenes across the six-membered chelate is similar to a 1,4-addition type reaction. Although this report was one of the first to demonstrate this type of activation it clearly became a common theme across more modern *nacnac* metal systems.

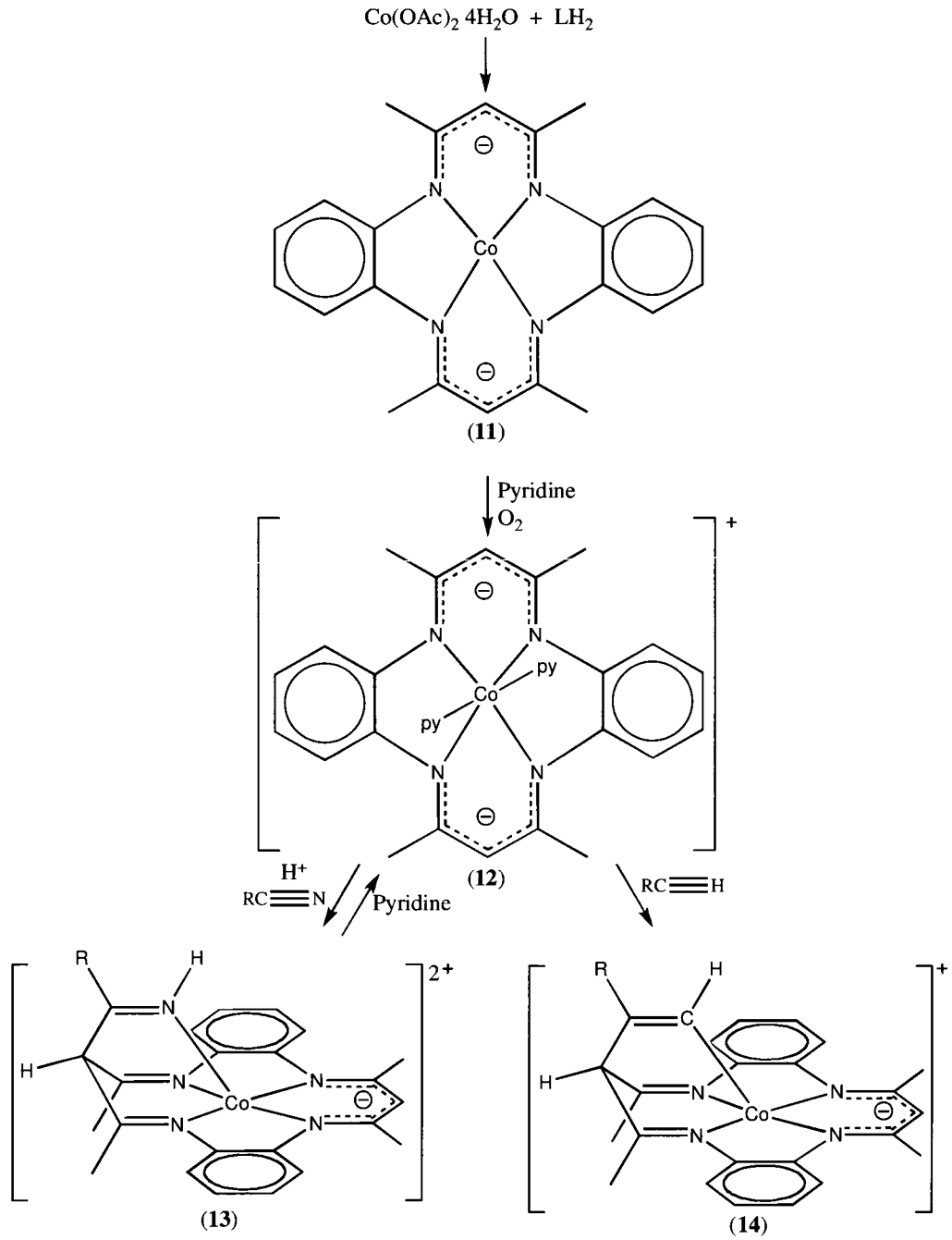

Scheme 6: Selective reaction scheme of $[Co(C_{22}H_{24}N_4)]$

The 1,4 addition type reactions involving the *β*-carbon of the *nacnac* system are not the only ways in which this versatile ligand system can interact and affect the chemistry of transition metal systems. In some instances, metathesis type reactions

involving the C-N branch of the *nacnac* ligand can take place, resulting in the formation of carbene type, or various other substituents, terminally bonded to metal centres. Mindiola *et. al.* studied titanium-*nacnac* systems[13] in search of a terminally bonded and labile phosphine moiety, a phosphinidene. The strategy developed by Mindiola involved the treatment of a nucleophilic four-coordinate titanium alkyldiene (*nacnac*)Ti=CH^{t}Bu(OTf) (**15**) (*nacnac*$^-$ = [Ar]NC(Me)CHC(Me)N[Ar], Ar = 2,6-^{i}Pr$_2$C$_6$H$_3$) with a primary lithium phosphide in a cold ether solution. The resulting complexes **19a** and **19b** were the final products whose intermediates were the first titanium complexes containing a terminal phosphinidene ligand (***Scheme 7***). Upon inspection of the structure of **19b** it is evident that the [PTrip] fragment migrates to the β-carbon of the former *nacnac* ligand via a possible metathesis type reaction. The intermediate complex **17c**, containing the phosphinidene moiety, is extremely reactive and in order to kinetically stabilize the titanium-phosphinidene complex the (*nacnac*)Ti=CH^{t}Bu(OTf) was treated with a bulkier phosphide LiPHMes* (Mes*$^-$ = 2,4,6-^{t}Bu$_3$C$_6$H$_2$) in pentane at -35°C and ultimately characterized by X-ray analysis.[13]

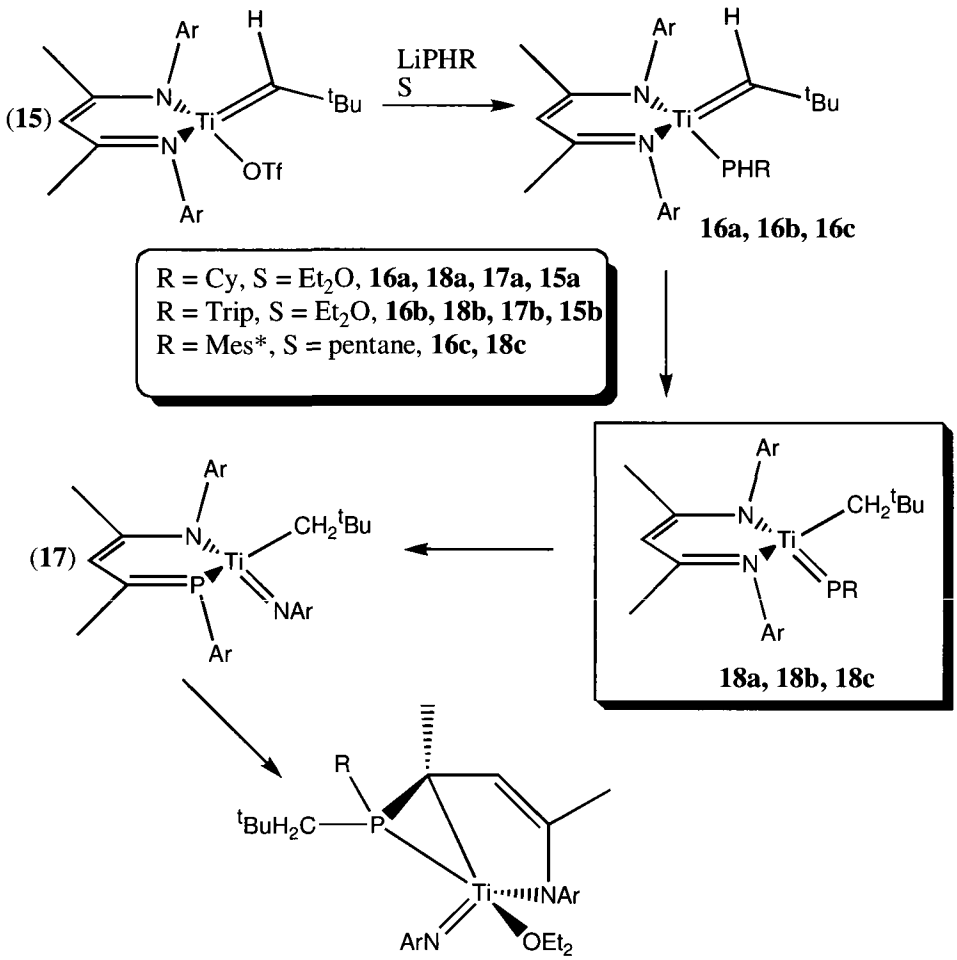

Scheme 7: Reaction scheme outlining proposed intermediates along the pathway to generate complexes **19a** and **19b**

High-oxidation state complexes containing alkylidyne functionalities have always attracted much attention due to their involvement in reactions such as alkyne metathesis.[14] An important note is that although d^0 early-transition metals complexes with these terminal alkylidene functionalities are well known, the majority of these systems contain second and third row transition metals and only a handful of Fischer type carbenes have been reported for vanadium and chromium.[14] Mindiola *et. al.* added to this handful of vanadium systems with a new class of vanadium(V) complexes bearing a

terminal neopentylidyne. These species were prepared and stabilized using a *nacnac* ligand system, which eventually undergoes a cross-metathesis type rearrangement to yield the vanadium product.[16] In a previous publication by Mindiola *et. al.* it was shown that one electron oxidation of (*nacnac*)V($CH_2{}^tBu)_2$ (**21**) (*nacnac*$^-$ = [Ar]NC(CH_3)CHC(CH_3)N[Ar], Ar – 2,6-$(CHMe_2)_2C_6H_3$) with $AgBPh_4$ (**22**) followed, by nucleophilic addition of MgI_2 promoted α-hydrogen abstraction to form the four coordinate neopentylidene complex (*nacnac*)V=CH^tBu(I) (**23**) (***Scheme 8***).[15]

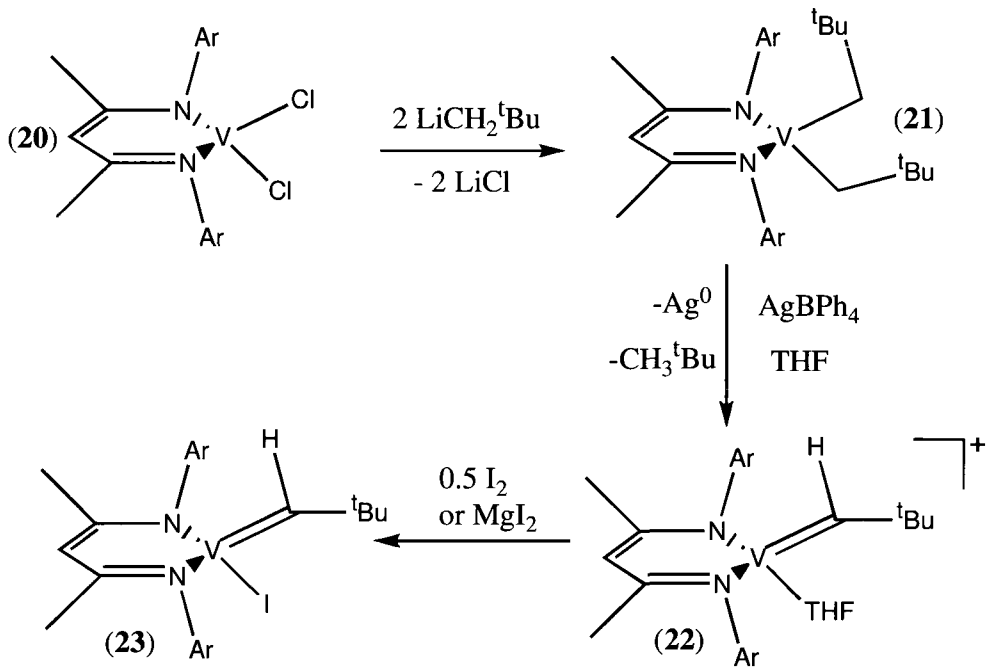

Scheme 8: Synthesis of vanadium(IV)-alkylidene complexes

This observation, along with the fact that vanadium alkylidyne complexes were unknown, prompted Mindiola *et. al.* to alkylate (*nacnac*)V=CH^tBu(I) (**23**) with $LiCH_2SiMe_3$ to form (*nacnac*)V$CH_2{}^tBu(CH_2SiMe_3)$ (**24**). Futher oxidation by one electron yielded the neutral (*nacnac*)V≡C^tBu(OTf) (**25**) which slowly undergoes a cross

metathesis reaction with the ligand backbone to form the vanadium-imido complex (^{t}BuC=C(Me)CHC(Me)N[Ar])V= NAr(OTf) (**26**) (***Scheme 9***).[16]

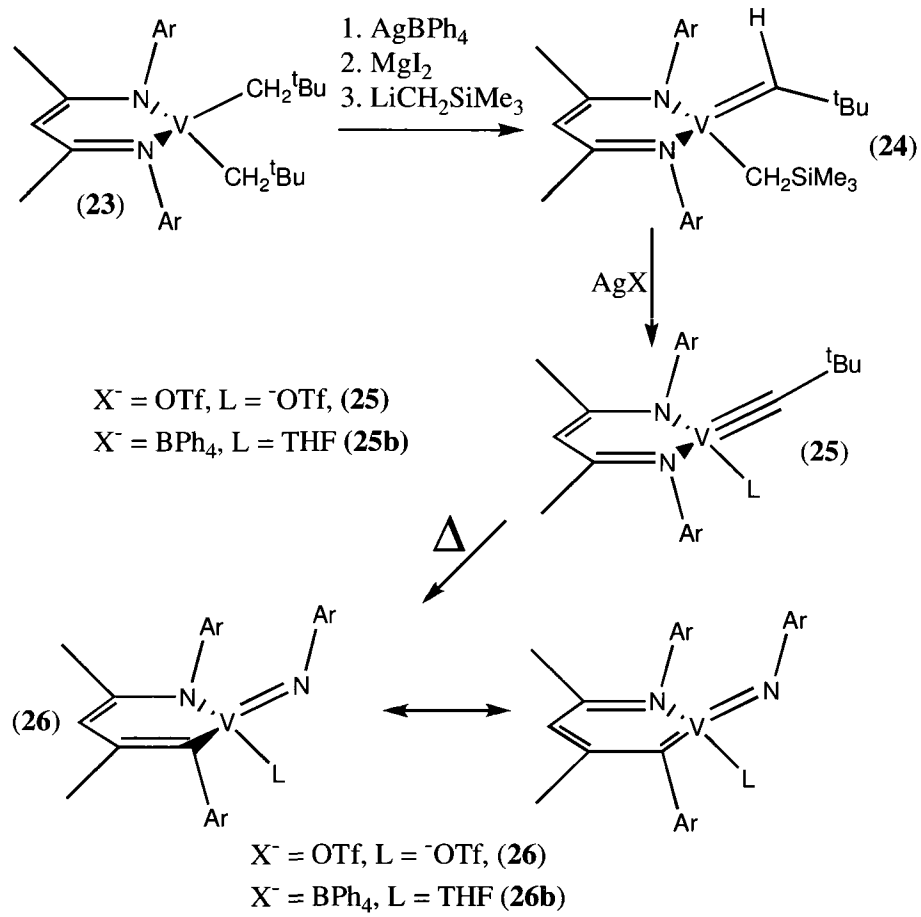

Scheme 9: Synthesis of neutral and cationic four-coordinate vanadium(IV) alkylidyne complexes

The cross metathesis type of interaction with the *nacnac* ligand provides a unique strategy to prepare d^0 metal alkylidynes from vanadium-alkylidynes and is quite contrasting to Schrock's two electron reduction reactions of high-valent alkylidynes to prepare similar Ta≡C linkages. What is more revealing is the *nacnac* ligands ability to

stabilize reactive vanadium-carbon double and triple bonds, and constantly interact with numerous substrates resulting in a wealth of unique and interesting results.

Among the series of characterized *nacnac* complexes, which clearly exhibit a consistently unique reactivity, ruthenium–*nacnac* complexes have been notably absent from the literature. This is surprising when considering that for well over two decades there have been examples of ruthenium complexes bearing smaller diazo-coordinating ligands [i.e., $(R)N(CH)_nN(R)$, n=1 (anionic amidinate),[17] **2** (neutral diazabutadienes)[18]], in addition to tetraazacyclotetradecine species[19] (**28**) and acetylacetone chelating compounds. Not to mention the unusual η^3-(C,N,N')-bonded ruthenium bisphosphiniminomethanide complex that has also been recently reported (**27**) (***Figure 4***).[20]

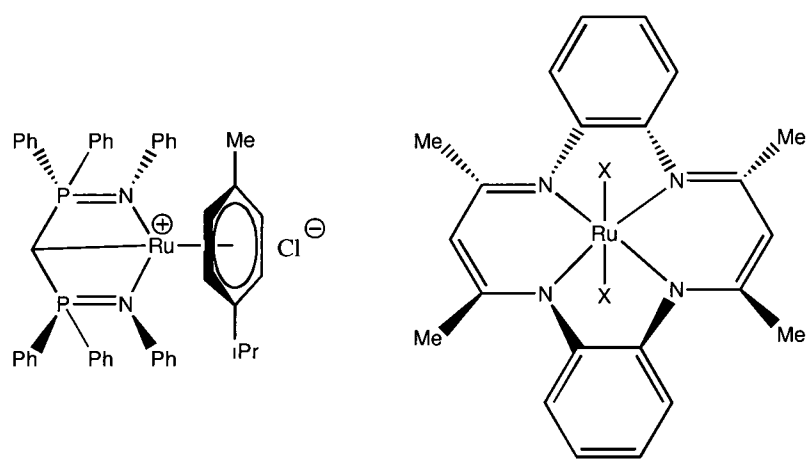

(**27**) (**28**)

Figure 4: Previously reported ruthenium compounds that bear structural resemblance to the *nacnac* ligand system

Yet, despite the similarity of these ligands to the *nacnac* system there has not been a single reported *nacnac* complex until *Dyson et. al.*[21] recently explored the very first

ruthenium-*nacnac* complexes and discovered that these species support the activation of small molecules and perform styrene hydrogenation. Besides the work of Dyson *et. al.*, information about ruthenium-*nacnac* remains extremely scarce. Given the wealth of interesting reactivity discovered with various other *nacnac* complexes we have decided to expand this field of chemistry with the hopes of observing further interesting reactivity possibly related to the activation of small molecules and hydrogenation chemistry. For this purpose, we also felt that attempts to lower the oxidation state of the metal centre could be rewarded with an enhanced tendency of the metal towards oxidative addition, which, of course, would be the starting point for molecular activation. Herein, I report some preliminary and unique observations of this ever-interesting ligand system and remarkably reactive metal.

RESULTS AND DISCUSSION

The *nacnac* ligand selected for this work was the $[(^{i}PrArNCMe)_2CH]^-$ anion. This particular form of the ligand had not been previously used in ruthenium chemistry and the steric constraints provided by the 2,6-*iso*-propyl groups on each respective arene ring was hoped to aid in sterically protecting empty coordination sites on a potential Ru(I). As a ruthenium starting material, we have selected the $[RuCl_2(p\text{-cymene})]_2$ complex, available both commercially or through simple inorganic synthesis, due to the fact it already contains the metal in its formal divalent state.

The reaction of $[RuCl_2(p\text{-cymene})]_2$ with 2 equivalents of $[(^{i}PrArNCMe)_2CH]K$, (1:1, ligand to metal) in hexanes was expected to generate (η^6-*p*-cymene)RuCl($(^{i}PrArNCMe)_2CH$) which would serve as the starting point for further 1-electron reductions to generate Ru(I) (***Figure 5***)

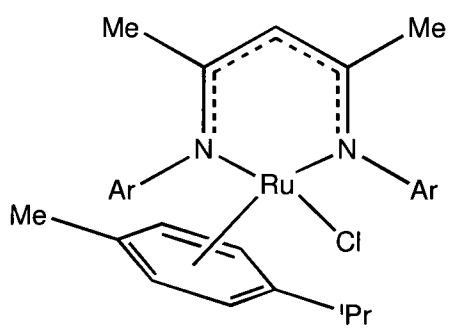

Figure 5: Expected product (η^6-*p*-cymene)RuCl[$(^{i}PrArNCMe)_2CH$]

What resulted from the reaction was largely unexpected and unique. The unprecedented [η^5-*p*-cymene(^{i}PrArNCMe)$_2$C]Ru[(^{i}PrArNCMe)$_2$CH] (**1**) was isolated as a dark red/purple complex in moderate yield. Compound **1** displays a ligand to metal 2:1 stoichiometry ratio. Therefore, the reaction was optimized to generate a higher yield of **1** by appropriately increasing the amount of ligand (***Scheme 10***).

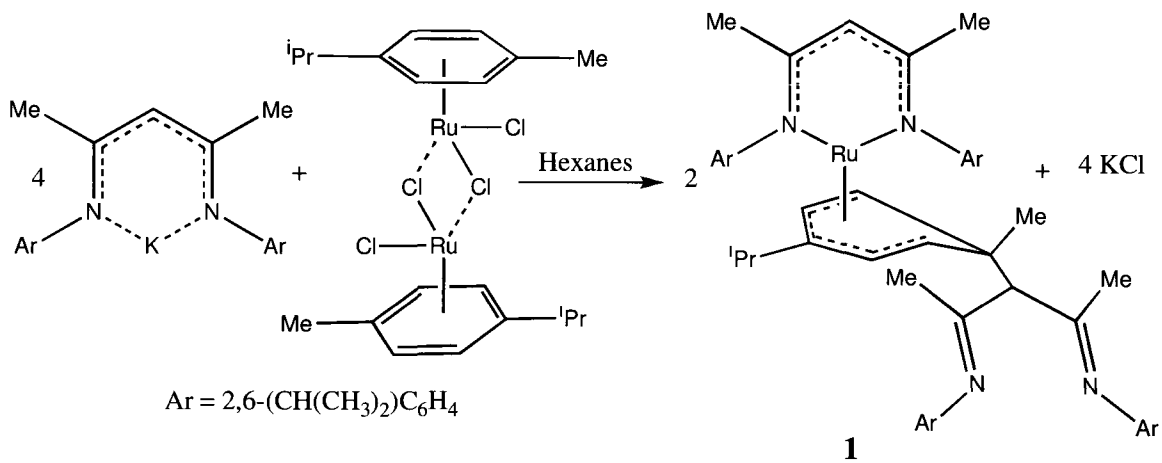

Scheme 10: Synthesis of [η^5-*p*-cymene(^{i}PrArNCMe)$_2$C]Ru[(^{i}PrArNCMe)$_2$CH]

Complex **1** contains a ruthenium (II) d^6, 16-electron unit that displays an activated cymene ring which has been attacked by another [(^{i}PrArNCMe)$_2$CH]K ligand at the least hindered *para*-methyl position via the β-carbon of the ligand backbone. The structure of **1** was revealed by X-ray diffraction (***Figure 6***) and confirmed by ^{1}H-NMR spectroscopy.

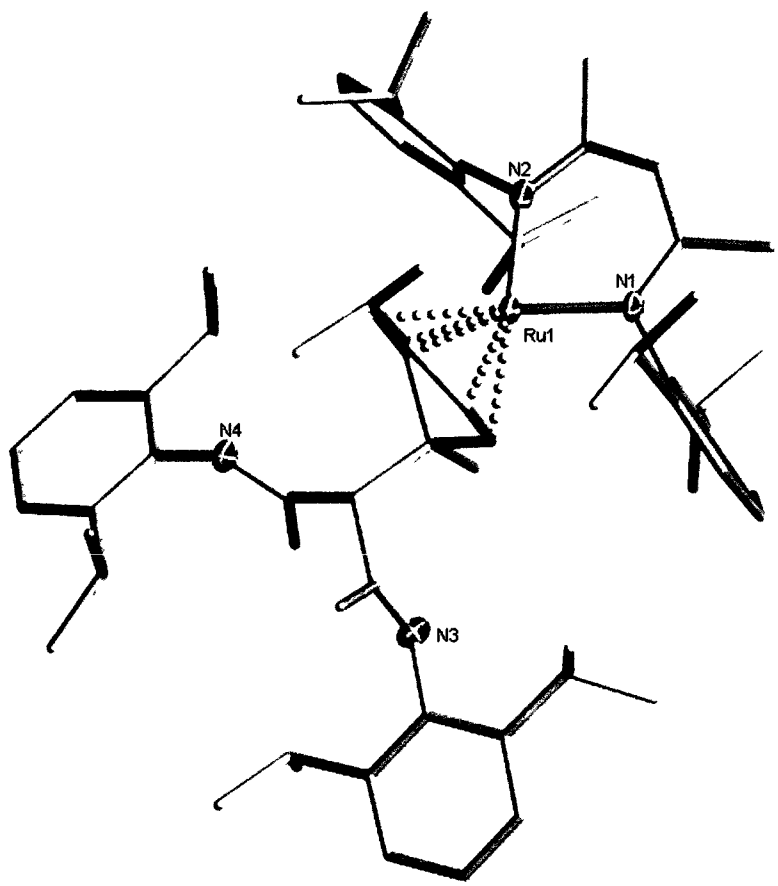

Figure 6: Thermal ellipsoid plot of [η^5-*p*-cymene (^{i}PrArNCMe)$_2$CH]Ru [(^{i}PrArNCMe)$_2$CH] showing selected atom labelling. Thermal ellipsoids are drawn at the 50% probability level.

Complex **1** has the Ru metal center in a distorted square-pyramidal geometry with the cymene ring having lost its aromaticity slipping from the original η^6- to a η^5-type of bonding mode. The Ru(1)-N(2) bond distance of 2.072(6)Å is slightly longer than the neighbouring Ru(1)-N(1) bond length of 2.100(5)Å. The second *nacnac* molecule attached to the cymene ring adopted a configuration reminiscent of a diimine type ligand as indicated by its short N-C bond lengths [N(4)-C(43) = 1.291(8)Å and N(3)-C(41) = 1.256(9)Å respectively]. In contrast, the N-C distances of the *nacnac* residue coordinated

to the metal [N(1)-C(2) = 1.323(9)Å and N(2)-C(4) = 1.349(9)Å] are longer but still indicating the presence of a partial double bond character. Compound **1** shows a very complex ^{1}H NMR in C_6D_6 at room temperature (***Figure 7***) displaying five *iso*-propyl septets and a complex set of corresponding *iso*-propyl methyl doublets in the range 0.95-1.50 ppm. The signals corresponding to the ruthenium bound η^5-cymene protons appear as doublets at 2.53 and 3.39 ppm respectively. This is a rather significant upfield shift when comparing to the ruthenium bound η^6-cymene which appears at 5.23 and 5.41 ppm. This strong upfield shift is consistent with a higher degree of shielding that is caused by the attack of the β-diimine *nacnac* on the cymene ring. The *iso*-propyl group of the cymene ring appears at 2.72ppm, again upfield from the typical 2.84 ppm, while the remaining *iso*-propyl septets are attributed to the two *nacnac* ligands with the β-diimine signal appearing at 4.21 ppm (***Figure 8***). The β-carbon hydrogen of the *nacnac* ligand gives a sharp singlet at 5.06 ppm while, in contrast, the β-carbon of the β-diimine shifts much lower at 2.89 ppm. The opposite is observed in the NC*Me* signals which both result in sharp singlets at 1.49 and 1.64 ppm for the *nacnac* and β-diimine respectively.

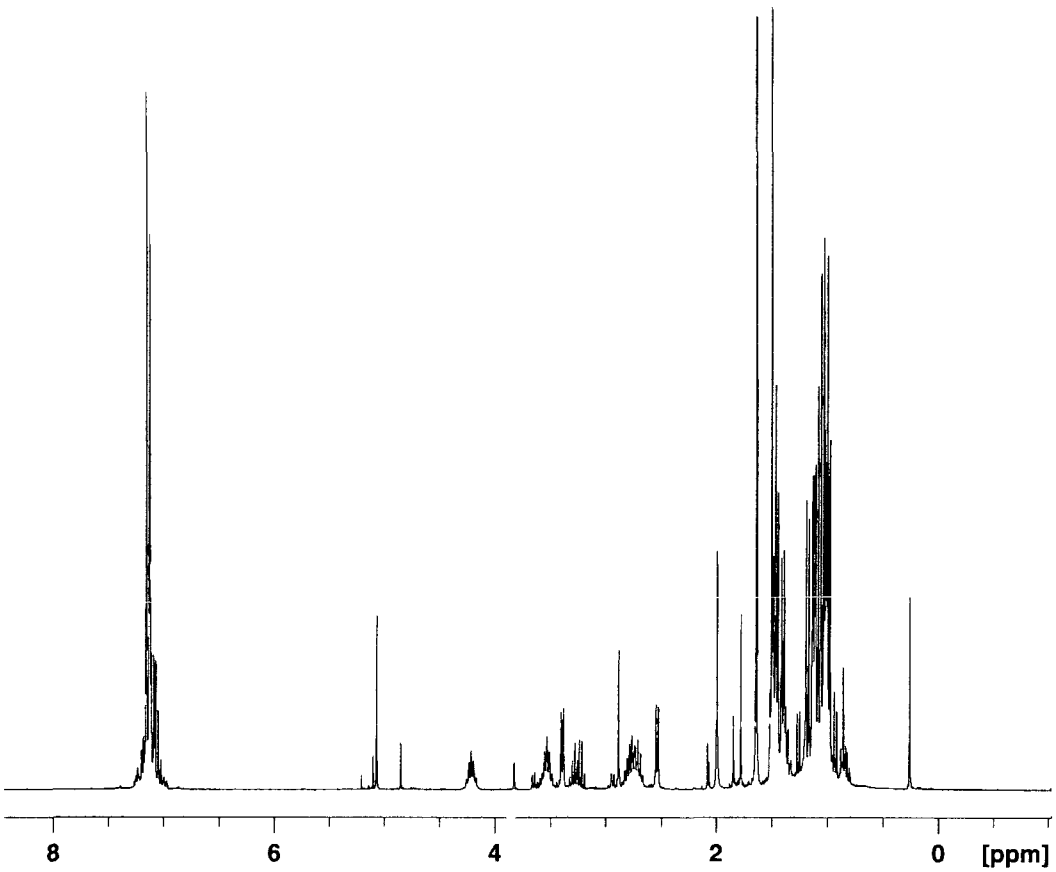

Figure 7: ^{1}H NMR of [η^{5}-*p*-cymene(^{i}PrArNCMe)$_2$C]Ru [(^{i}PrArNCMe)$_2$CH] (**1**)

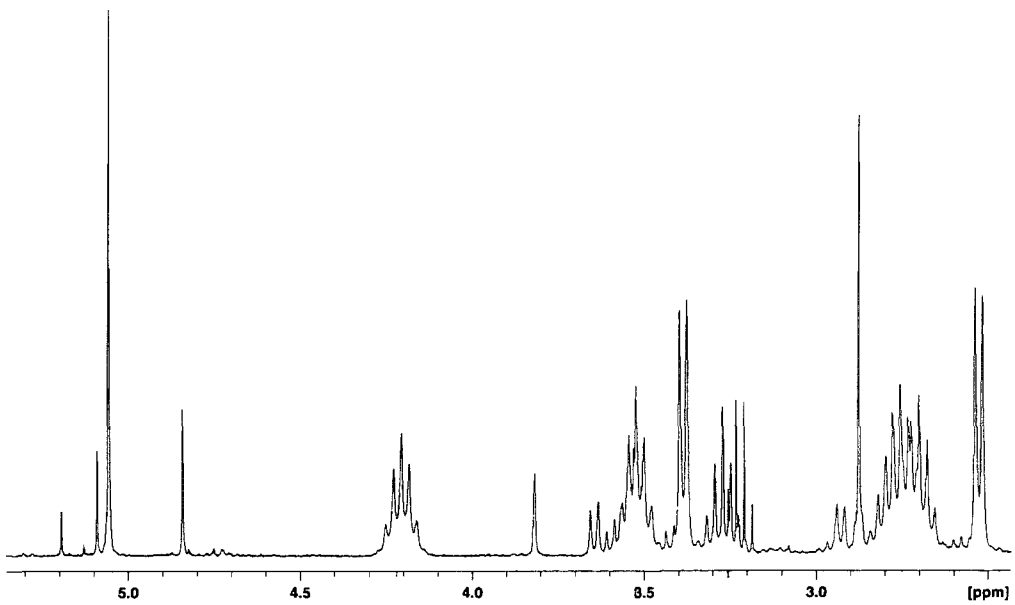

Figure 8: *iso*-propyl signals of complex **1**

Complex **1** is highly soluble, even in hexanes, and is moderately stable upon exposure to air where decomposition starts to be visible in approximately four hours. The formation of this interesting molecule can be hypothesized through the formation of a short lived η^6-*p*-cymene[(^{i}PrArNCMe)$_2$C]RuCl (**A**) compound whose cymene ring is ultimately attacked by a free [(^{i}PrArNCMe)$_2$CH]K ligand. (***Scheme 11***)

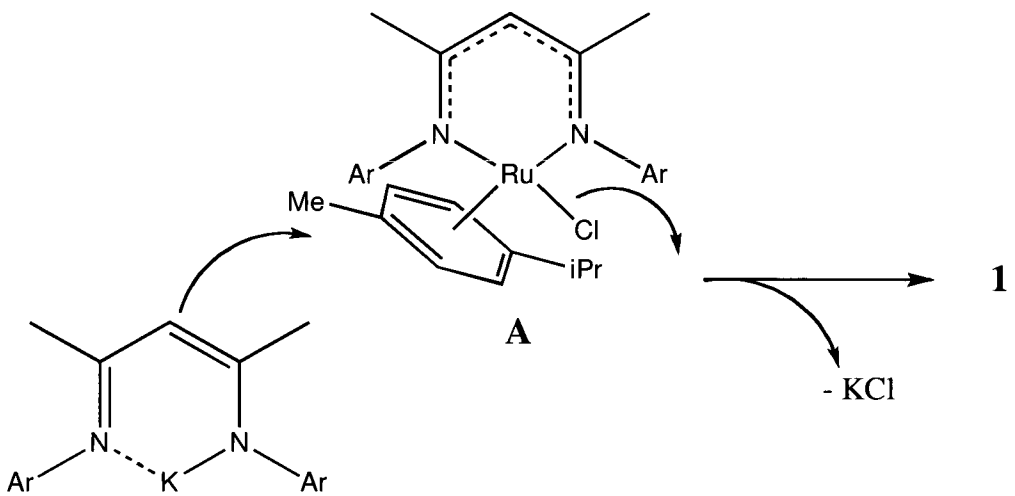

Ar = 2,6-(CH(CH$_3$)$_2$)C$_6$H$_4$

Scheme 11: Theorized formation of complex **1**

The hypothetical complex **A** is similar to the ruthenium (II) *nacnac* complex (η^6-C$_6$H$_6$)RuCl[(ArNCMe)$_2$CH] (Ar = 2,6-dimethlyphenyl) reported by Dyson *et. al.*[21] It is though much more sterically hindered due to the presence of both the cymene of the ruthenium and *iso*-propyl moieties (benzyl and methyl groups in the Dyson case respectively) on the phenyl groups of the *nacnac* ligand. Thus, based on the finding of Dyson it is a fair assumption that **A** is a likely intermediate of the reaction leading up to the formation of complex **1**. The degree of activation of the aromatic ring towards

nucleophilic attack may be correlated to steric bulk, again, drawing this conclusion when comparing to the Dyson complex. Using the same metal centre and ligand, in the Dyson case does not result in any form of nucleophilic attack on the π-bound aromatic ring. By simply increasing the bulk of the ligand and the metal precursor we see a marked increase in vulnerability of the π-bound aromatic ring of ruthenium towards attack. It is entirely plausible that the increased activation of the cymene ring, due to the steric bulk of the complex, is the driving force for the attack of another *nacnac* ligand at the *para*-methyl position. The attack results in the release of a chlorine atom, shift from η^6 to η^5 coordination, loss of aromaticity and distortion of the cymene ring. All of these events release the bulk around the ruthenium coordination sphere while maintaining a stable ruthenium(II) oxidation state. Very recently, Dyson *et. al.,* while exploring the potential toxicity of β-diketiminato-ruthenium complexes, obtained a similar reaction involving an electron deficient π-bound arene to a ruthenium centre.[22] Dyson also proposed a similar reaction pathway (***Scheme 12***).

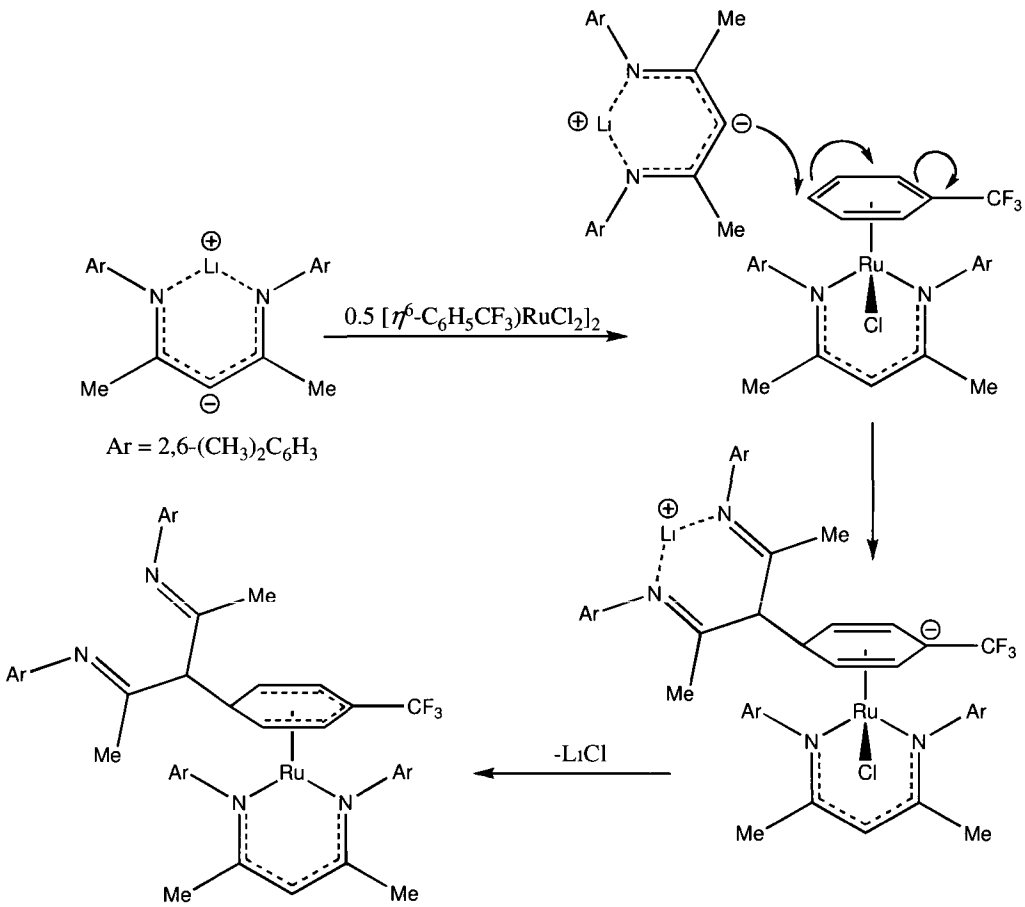

Scheme 12: Proposed mechanism for the formation of $\{\eta^6$-1,4-$CF_3C_6H_5$[2,6-$(CH_3)_2C_6H_3NC(CH_3)]_2CH\}$Ru[2,6-$(CH)C_6H_3NC(CH_3)]_2CH$

In this particular example, the arene ring is activated by the addition of an electron-withdrawing group making it more susceptible to nucleophilic attack. Complex **1** does not contain electron withdrawing groups on the cymene ring, but rather electron-donating alkys, thus strong metal-ligand bonding and enhanced electron transfer to the ruthenium(II) centre from the cymene ring could also still result in a more electrophilic arene. Nucleophilic addition to coordinated ruthenium η^6-arenes has been observed for other types of ruthenium (II) complexes with varying nucleophiles.[23] Work by Bhambri

showed the possibility of attack by CN^- affording the corresponding cyclohexadienyl derivative shown below (***Scheme 13***).[23h]

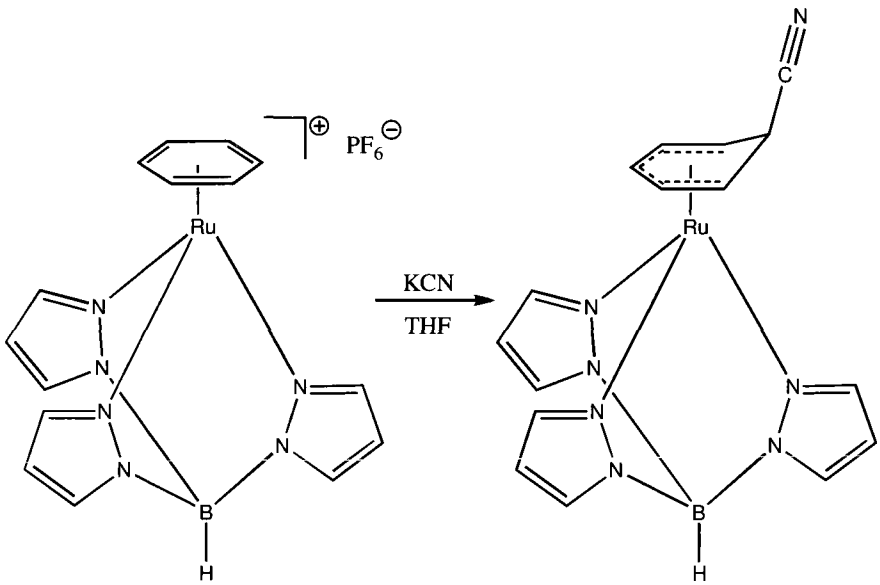

Scheme 13: Synthesis of $[Ru(\eta^5\text{-}C_6H_6CN)(Pz_3BH)]$ via nucleophilic attack on the coordinate arene ring

This particular reaction reiterates the enhanced electrophilic character of the π-bound arene ring, which can be solely attributed in this case to electron transfer from the ring to the ruthenium(II) centre. Considering all this information the susceptibility and activation of the cymene ring to nucleophilic attack can be attributed to a combination of sterics around the ruthenium centre and strong electron transfer to ruthenium by the cymene ring.

Although complex **1** was unexpected given the low nucleophilicity of the nacnac anion , we decided to delve a little deeper into this reaction and continue to explore the interactions of **1** with various reducing agents. The ultimate target was to lower the ruthenium(II) oxidation state,[24] to ruthenium(I) or even ruthenium(0). This was encouraged by the remarkable versatility of the *nacnac* ligand to support low oxidation

states and coordination numbers. Attempts to reduce **1** and generate a low valent state of ruthenium were carried out with several reducing agents including magnesium, potassium, sodium and sodium hydride ultimately affording interesting results. Several reductions were simultaneously attempted in a one-pot preparation, allowing the complex to be formed in solution and then exposed to reducing agents. As shown in ***Scheme 14***, the initial attempt of an *in-situ* reduction with magnesium powder resulted in the expected 2-electron reduction of the ruthenium centre but also led to leaching of the metal centre forming a magnesium complex (**1b**) while depositing black ruthenium(0) in the reaction vessel.

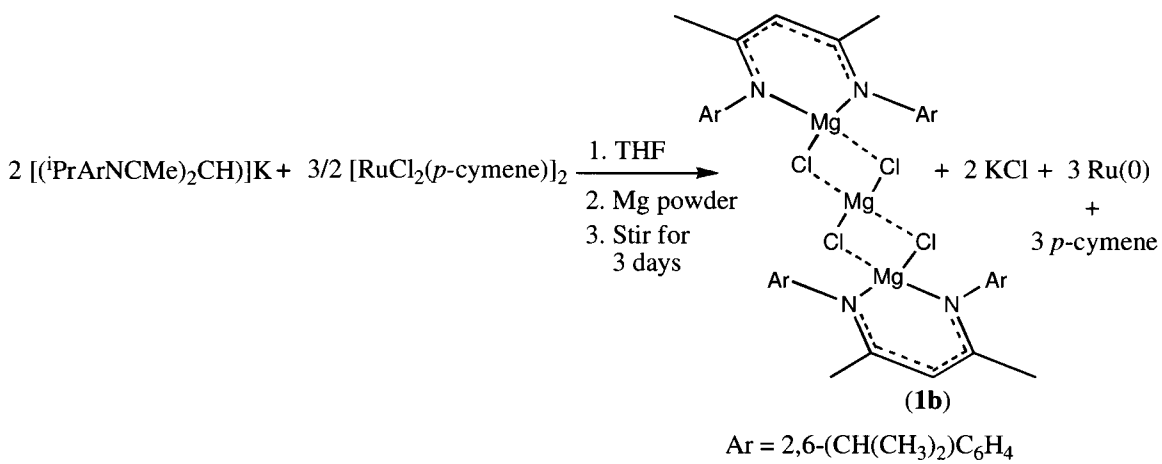

Scheme 14: In-situ reduction attempt of compound **1**

The tri-metallic structure was determined by X-ray diffraction and, based on the resulting structure, it was clear that the reducing magnesium was added too early in the reaction sequence. It was hypothesized that unreacted $[RuCl_2(p\text{-cymene})]_2$ is reduced by magnesium, generating $MgCl_2$ along with Ru(0) while $MgCl_2$ continues to react with free

ligand to form the tri-metallic magnesium product. Further *in-situ* reductions that were attempted with sodium and potassium alkali metals resulted in remarkably different products. As outlined in ***Scheme 15***, both reductions led to the formation of an unsaturated ruthenium-*nacnac* complex [(^{i}PrArNCMe)$_2$CH]Ru[η^5-1-methyl-4-(propan-2-ylidene)cyclohexa-2,5-dien-1-yl] (**2**).

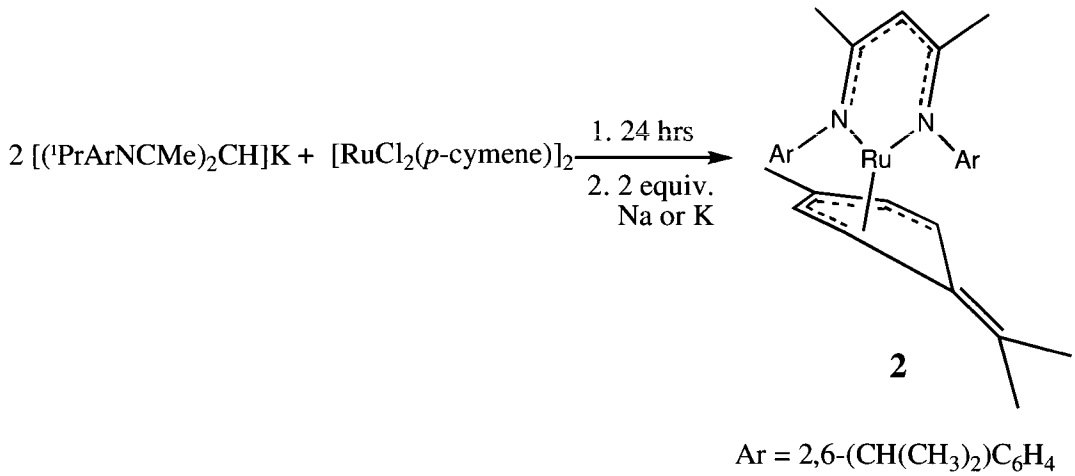

Scheme 15: Synthesis of [(^{i}PrArNCMe)$_2$CH]Ru[η^5-1-methyl-4-(propan-2-ylidene)cyclohexa-2,5-dien-1-yl]

Complex **2** is another ruthenium(II) d^6, 16-electron unit that displays an activated cymene ring that has lost the *ipso*-hydrogen of the *iso*-propyl group in the *para* position. This hydrogen loss results in the formation of a double bond on the ring destroying the aromaticity of the ring system. The structure of **2** was determined by X-ray crystallography (***Figure 9***) and confirmed by ^{1}H-NMR characterization.

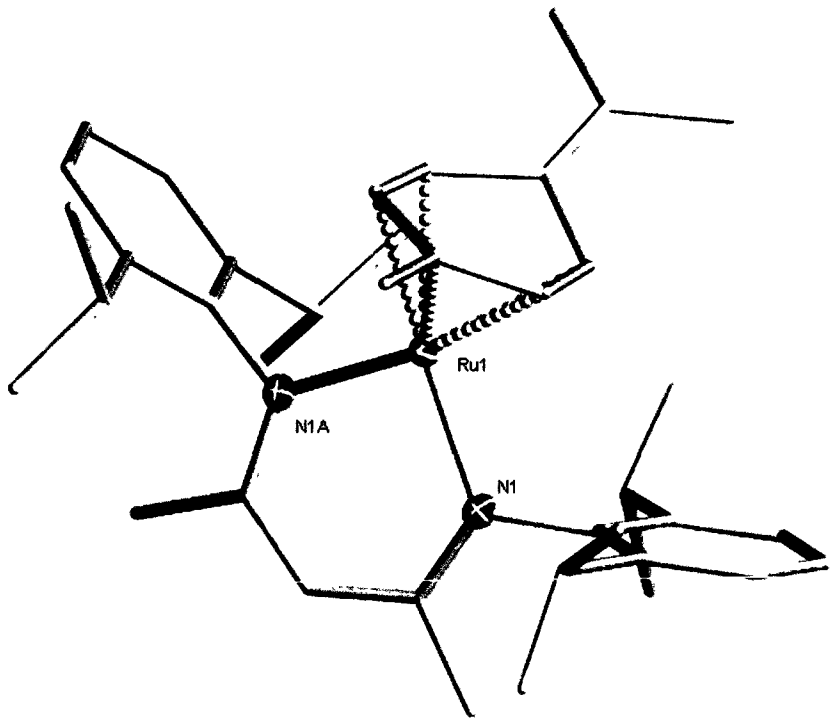

Figure 8: Thermal ellipsoid plot of [(^{i}PrArNCMe)$_2$CH]Ru[η^5-1-methyl-4-(propan-2-ylidene)cyclohexa-2,5-dien-1-yl] (**2**) showing selected atom labelling. Thermal ellipsoids are drawn at the 50% probability level.

Complex **2**, much like **1** exhibits a distorted octahedral geometry and a cymene ring, which has lost its aromaticity. The loss of the *ipso*-hydrogen results in the formation of a double bond on the *iso*-propyl group of the cymene and the contraction of the bond length from 1.512(6)Å in **1** to 1.374(6)Å. The Ru(1)-N(1) and Ru(1)-N(1A) distances are both 2.065(5)Å both slightly shorter in comparison to complex **1** while the *nacnac* ligand itself retains its double bond character within the backbone as demonstrated by the N(1)-C(14) and N(1A)-C(14A) distances of 1.335(3)Å. The ^{1}H NMR of **2** displays a mixture of partially unreacted ligand along with complex **2**. The *nacnac* β-carbon hydrogen shifts at 5.25 ppm while the NC*Me* methyl groups appear at 1.87ppm. The doublets of the Ar-

iso-propyl groups at 1.26 and 1.08 ppm along with the isopropyl septet at 3.60ppm all account for the ligated *nacnac* ligand. The now unsaturated cymene displays a set of doublets at 2.87 and 3.49 ppm, again upfield with respect to the typical cymene hydrogen shifts (5.23 and 5.41ppm). The lack of cymene isopropyl signal and the downfield shift of the CH_3 groups from 1.21ppm to 2.10 ppm are all in agreement with the presence of the [η^5-1-methyl-4-(propan-2-ylidene)cyclohexa-2,5-dien-1-yl] moiety π-bound to the ruthenium centre.

In order to better comprehend the reaction and possibly determine a mechanism, $[RuCl_2(p\text{-cymene})]_2$ was reacted with sodium and potassium in THF overnight followed by an ^{1}H-NMR analysis. The resulting NMR showed formation of a sharp hydride singlet at -10ppm integrating to one hydrogen atom. The cymene signals showed multiple splitting, beyond the typical set of doublets, indicating loss of symmetry within the $[RuCl_2(p\text{-cymene})]_2$ unit. The source of hydride in this reaction can only be assumed to be the solvent or another $[RuCl_2(p\text{-cymene})]_2$ unit that extracts a hydride from a cymene ring. The low yield of this reaction may be an indication of sacrificial cymene ring hydrogen at the expenses of another dimeric ruthenium unit. The poor yield of this reaction along with the realization that a hydride may be a partner product of the reaction mixture prompted the use of a hydride source, namely sodium hydride, in order to attempt to improve the yield of the reaction (***Scheme 16***).

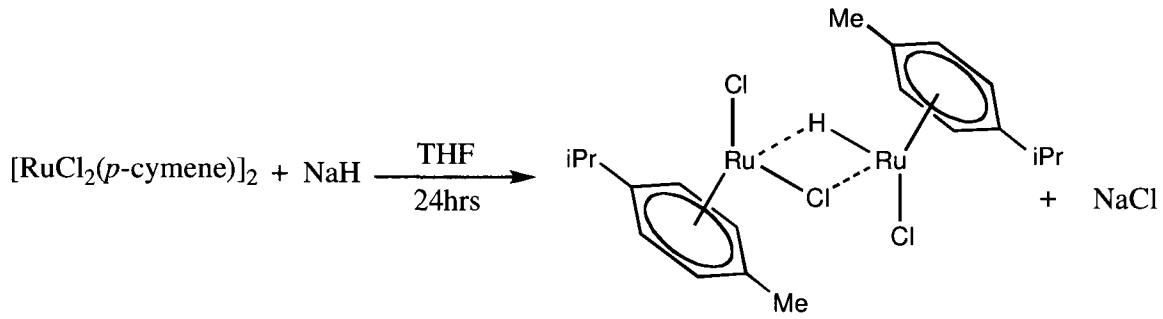

Scheme 16: Synthesis of [Ru(η^6-cymene)Cl]$_2$(μ-Cl)(μ-H)

The mono-hydride ruthenium complex, previously reported,[25] was isolated as deep-red crystals in excellent yield and its structure was determined via X-ray analysis and verified by ^{1}H-NMR. The proton spectrum of the mono-hydride complex matches the spectra of the products obtained from the reactions with metallic sodium and potassium. Reacting the isolated mono-hydride ruthenium complex, from the reaction with sodium hydride, in the presence of [(^{i}PrArNCMe)$_2$CH]K in THF results in a small improvement of the yield of complex **2.** The proposed reaction pathway for the formation of **2** (***Scheme 17***) relies on the well-known ability of ruthenium to perform hydrogenation reactions.[26] The mechanism is again based on the formation of a Dyson-type of the intermediate (**B**) as a hydride instead of a chloride. In this case though, we hypothesized the activation of the π-bound cymene where the hydride the *ipso*-hydrogen of the *iso*-propyl group. The consequent release of elemental hydrogen transformed the aromatic ring into the dienyl-ylidene anion and gave rise to **2.**

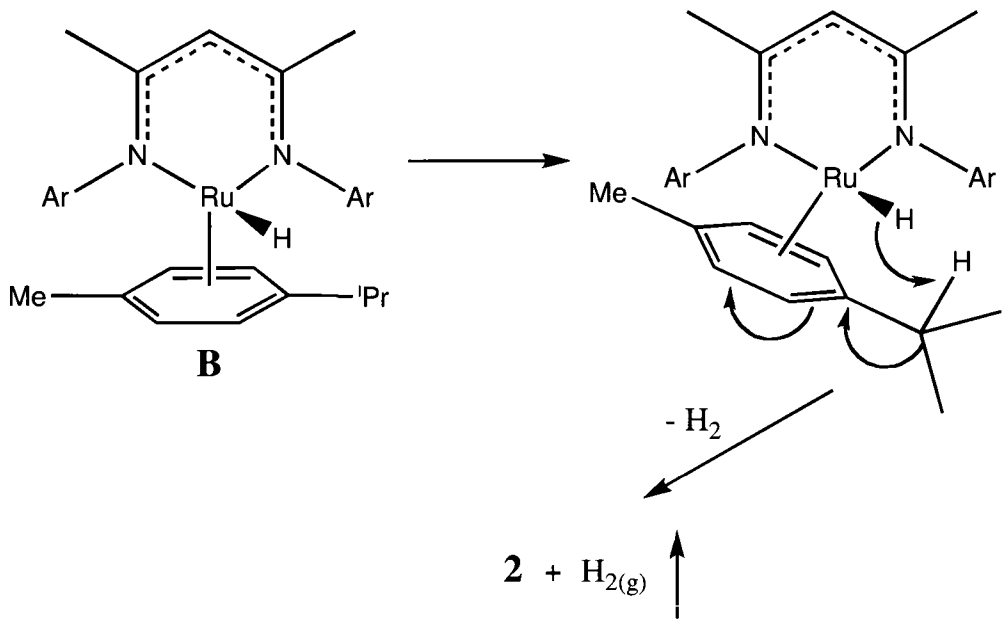

Scheme 17: Proposed mechanism for the formation of [('PrArNCMe)$_2$CH]Ru[η^5-1-methyl-4-(propan-2-ylidene)cyclohexa-2,5-dien-1-yl]

Based on the behaviour of this ruthenium-*nacnac* ligand system and the subsequent formation of complexes **1** and **2** it is evident that the cymene ligand is non-innocent and prone to involvement in each respective reaction. The degree of activation of the cymene ring, based on these initial observations, seems to be the direct result of the steric bulk of the π-bound arene (cymene in this case) in combination with the bulk of the *nacnac* arenes (2,6-diisopropylphenyl in this case) as well as the strong metal-ligand bonding between the *p*-cymene and ruthenium(II) metal centre. The activation and attack at the cymene ring by nucleophiles ultimately relieves the strain around the co-ordination sphere while maintaining the robust ruthenium (II) oxidation state. The initial attempt to generate a ruthenium-*nacnac* system with the ability to activate small molecules was confirmed by Dyson[21] who utilized a less sterically hindered ligand and precursor thus avoiding nucleophilic attack at the coordinated arene ring. The Dyson type of complex is

probably involved in our reaction but only as a possible intermediate that leads to formation of **1** and **2**. The initial attempts to create a low-valent ruthenium(I)-*nacnac* system were unsuccessful, however, these results provide a potentially original and unprecedented mode of action of the *nacnac* ligand. In many reports where the *nacnac* system has been employed, including the publication by Dyson *et. al.*, the *ligand* β-carbon is often involved in the reactions as a nucleophile. It is always the β-carbon *within* the ligand backbone that is involved in the chemistry of these metal-ligand systems attacking electrophiles and various other substrates, which ultimately lead to unusual molecules where a molecular bridge is established between the ruthenium centre and the β-carbon. Presented here are results which account for the only other known ruthenium-*nacnac* complexes that not only confirm the nucleophilicty of the *nacnac* ligand but present a mode of action unseen among ruthenium-*nacnac* systems as well as any combination of transition metal and *nacnac*. The ligand system does more than just bridge substrates between the β-carbon and metal centre. In its entirety, it acts a nucleophile and participates in a sequence of nucleophilic attacks, which result in compounds **1**, and promotes the de-hydrogenation of the π-bound *p*-cymene during the formation of **2**.

EXPERIMENTAL SECTION

All operations were performed either under a nitrogen atmosphere using standard Schlenk techniques or in a purified nitrogen-filled dry-box. The ligand [(^{i}PrArNCMe)$_2$CH]K was prepared following standard procedures. The [RuCl$_2$(p-cymene)]$_2$ (anhydrous) was purchased from Strem Chemicals and used as received. Metallic Na and K were purchased from Aldrich and washed with hexane under nitrogen to remove the oil. Powdered Mg (reagent grade, 20-230 mesh) was also purchased from Aldrich and used as received. NMR spectra were recorded with a Varian AMX-500 MHz and a Bruker Avance 500 MHz spectrometer by using NMR tubes that were prepared inside a drybox. Data for X-ray crystal structure determinations were obtained with a Bruker diffractometer equipped with a Smart CCD area detector.

Preparation of [(^{i}PrArNCMe)$_2$CH]K

A mixture of [(^{i}PrArNCMe)CH(^{i}PrArNHCMe)] (1.00g, 2.39mmol) and 1.5 equivalents of KH (0.144g, 3.59mmol) is dissolved in THF (35mL) and allowed to stir 24 hours. The resulting yellow solution is brought to dryness under vacuum and extracted into hexanes (35ml) while gently heating at the same time to ensure maximum solution. The hexane solution is then centrifuged to remove un-reacted ligand and particulate matter. The resulting solution is by vacuumed leaving behind a pale yellow powder which is heated under vacuum to remove any remaining THF leaving behind [(^{i}PrArNCMe)$_2$CH]K (0.980g, 2.14mmol, 89%) as a yellow powder. ^{1}H NMR (500 MHz C_6D_6, 23°C): δ = 1.17 (d, 3H, C*Me*), 1.22 (d, 3H, C*Me*), 3.32 (sept, 4H, C*H*Me$_2$), 1.68 (s, 24H, CH*Me*$_2$) 4.89 (s, 1H, C*H*), 7.16-7.210 (m, 6H, Ar*H*); ^{13}C NMR (125.72 MHz C_6D_6, 23°C): δ = 20.79 (s, C*Me*), 23.45 (s, CH*Me*$_2$), 24.55 (s, CH*Me*$_2$), 28.61 (s, *C*HMe$_2$), 94.25 (s, *C*H), 123.56, 125.84, 141.22, 142.74 (s, *C*$_6$H$_3$), 161.48 (*C*Me).

Preparation of [η^5-cymene(^{i}PrArNCMe)$_2$C]Ru[(^{i}PrArNCMe)$_2$CH] (1)

A solution of [(^{i}PrArNCMe)$_2$CH]K (0.300 g, 0.65 mmol) in hexanes (15 mL) was added dropwise to a suspension of [RuCl$_2$(cymene)]$_2$ (0.100 g, 0.16 mmol) in the same solvent (10 mL). Addition of the ligand resulted in the slow formation of a dark purple coloured solution. The reaction was allowed to stir for 48 hours. The resulting deep red-purple solution was evaporated under vacuum and re-extracted into a small amount of hexanes (15mL) and centrifuged to remove KCl and

particulate matter. The solution was allowed to stand at -35°C for five days upon which deep-red crystals of **1** were deposited (0.132 g, 0.124 mmol, 40%). ^{1}H NMR (500 MHz C_6D_6, 23°C): δ = 1.03 (d, 3H, η^5-*p-cymene*[(^{i}PrArNCMe)$_2$CH]), 1.07 (d, 6H, CH*Me*$_2$), 1.13 (d, 6H, CH*Me*$_2$), 1.14 (d, 6H, CH*Me*$_2$), 1.18 (d, 6H, CH*Me*$_2$), 1.40 (d, 6H, CH*Me*$_2$), 1.45 (d, 12H, CH*Me*$_2$), 1.48 (d, 3H, η^5-*cymene*[(^{i}PrArNCMe)$_2$CH]), 1.49 (s, 6H, C*Me*), 1.64 (s, 6H, C*Me*), 1.99 (s, 3H, η^5-*cymene*[(^{i}PrArNCMe)$_2$CH]), 2.53 (d, 2H, η^5-*cymene*[(^{i}PrArNCMe)$_2$CH]), 3.28 (sept, 2H, C*H*Me$_2$), 3.39 (d, 2H, η^5-*cymene*[(^{i}PrArNCMe)$_2$CH]), 3.53 (sept, 2H, C*H*Me$_2$), 4.21 (sept, 1H, η^5-*cymene*[(^{i}PrArNCMe)$_2$CH]), 5.06 (s, 1H, C*H*), 6.91-7.32 (m, 12H, Ar*H*); **η^5-*cymene*[(^{i}PrArNCMe)$_2$CH]:** δ = 2.72 (sept, 2H, C*H*Me$_2$), 2.77 (sept, 2H, C*H*Me$_2$), 2.88 (s, 1H, CH); ^{13}C NMR (125.72 MHz C_6D_6, 23°C): δ = 22.2 (s, η^5-*cymene*[(^{i}PrArNCMe)$_2$CH]), 22.42 (s, C*Me*), 22.87 (s, η^5-*cymene*[(^{i}PrArNCMe)$_2$CH]), 23.43 (s, CH*Me*$_2$), 23.66 (s, CH*Me*$_2$), 25.11 (s, CH*Me*$_2$), 25.58 (s, η^5-*cymene*[(^{i}PrArNCMe)$_2$CH]), 26.29 (s, CH*Me*$_2$), 27.59 (s, *C*HMe$_2$), 28.58 (s, *C*HMe$_2$), 30.04 (s, η^5-*cymene*[(^{i}PrArNCMe)$_2$CH]), 44.39 (s, η^5-*cymene*[(^{i}PrArNCMe)$_2$CH]), 50.10 (s, η^5-*cymene*[(^{i}PrArNCMe)$_2$CH]), 73.01 (s, η^5-*cymene*[(^{i}PrArNCMe)$_2$CH]), 97.49 (s, *C*H), 124.77 (s, Ar *p-C*H), 128.52 (s, Ar *m-C*H), 136.32 (s, Ar *o-C*), 143.24 (s, η^5-*cymene*[(^{i}PrArNCMe)$_2$CH]), 152.43 (s, Ar *i-C*), 160.92 (s, *C*Me); **η^5-*cymene*[(^{i}PrArNCMe)$_2$CH]:** δ = 23.22 (s, CH*Me*$_2$), 25.24 (s, C*Me*), 26.28 (s, CH*Me*$_2$), 28.07 (s, *C*HMe$_2$), 28.23 (s, *C*HMe$_2$), 29.02 (CH*Me*$_2$), 123.17 (s, Ar *p-C*H), 126.08 (s, Ar *m-C*H), 135.98 (s, Ar *o-C*), 147.12 (s, Ar *i-C*), 168.61 (s, *C*Me).

Preparation of {Mg[(^{i}PrArNCMe)$_2$CH](μ-MgCl$_2$) {Mg[(^{i}PrArNCMe)$_2$CH]}} (1b)

A yellow solution of K[(^{i}PrArNCMe)$_2$CH (0.149 g, 0.32 mmol) in THF (15 mL) was added dropwise to a suspension of [RuCl$_2$(p-cymene)]$_2$ (0.100 g, 0.16 mmol) in THF (10 mL) resulting in an immediate reaction and colour change of the solution to dark purple/red. The reaction mixture was stirred for three hours after the further addition of metallic Mg (0.009 g, 0.37 mmol. After three days of stirring. The magnesium metal was completely consumed. The insoluble solid was extracted with hexanes and filtered to remove any particulate matter. The hexane solution was slowly evaporated over a period of 5 days, which resulted in pale-colored crystals depositing at the bottom and along the vial walls in relatively low yield (0.122 g, 0.12 mol, 36%).

Preparations of [(^{i}PrArNCMe)$_2$CH]Ru[η^5-1-methyl-4-(propan-2-ylidene)cyclohexa-2,5-dien-1-yl] (2)

a) A solution of [(^{i}PrArNCMe)$_2$CH]K (0.149 g, 0.33 mmol) in THF (15 mL) was added dropwise to a suspension of [RuCl$_2$(cymene)]$_2$ (0.100 g, 0.16 mmol) in THF (10 mL). The solution was stirred 5 hours, resulting in a dark purple/red solution with no visible remaining starting material. To this solution metallic Na (0.008 g, 0.35 mmol) was added and stirring was continued for 24 hours. The resulting dark brown/red solution was evaporated in vacuo, repeatedly extracted with hexanes and centrifuged to remove any particulate matter. Slow evaporation over three days resulted in dark crystalline needles of **2 i**n low yield (0.04 g, 0.05 mmol, 36%). b) Identical procedure was followed as described in a) with the

exception of the addition of metallic K (0.013 g, 0.33 mmol) instead of metallic sodium to also generate **2** in a low yield (0.032 g, 0.04 mmol, 29%). c) A suspension of $[RuCl_2(cymene)]_2$ (0.100 g, 0.16 mmol) and NaH (0.078 g, 0.33 mmol) in THF (15mL) was allowed to stir four days to ensure completion and formation of the previously reported ruthenium mono-hydride. The resulting deep red solution was evaporated under vacuum and re-extracted into fresh THF (15 mL) followed by centrifugation to remove NaCl and particulate matter. A solution of $[(^{i}PrArNCMe)_2CH]K$ (0.149 g, 0.36 mmol) in THF (10 mL) was added dropwise to the mono-hydride solution and allowed to stir for 48 hours. The resulting deep red-purple solution was evaporated under vacuum and re-extracted into Et_2O (15 mL) and cooled to -35°C for 5 days after which deep red crystals of **2** (0.055 g, 0.078 mmol, 50%) were deposited. ^1H NMR (500 MHz C_6D_6, 23°C): δ = 1.08 (d, 12H, CHMe_2), 1.26 (d, 12H, CHMe_2), 1.87 (s, 6H, CMe), 2.10 (s, 6H, Me(C_6H_4)C(Me)$_2$), 3.60 (sept, 4H, CHMe$_2$), 2.87, 3.49 (d, 2H, η^5-Me(C_6H_4)C(Me)$_2$), 5.25 (s, 1H, CH), 7.05-7.21 (m, 6H, ArH); ^{13}C NMR (125.72 MHz C_6D_6, 23°C): δ = 19.37 (s, η^5-Me(C_6H_4)C(Me)$_2$), 21.41 (s, η^5-Me(C_6H_4)C(Me)$_2$), 23.07 (s, CHMe_2), 23.45 (s, CMe), 25.74 (s, CHMe_2), 27.70 (s, CHMe$_2$), 53.83 (s, η^5-Me(C_6H_4)C(Me)$_2$), 65.87 (s, η^5-Me(C_6H_4)C(Me)$_2$), 98.21 (s, CH), 121.23 (s, Ar *p*-CH), 125.76 (s, Ar *m*-CH), 137.62 (s, η^5-Me(C_6H_4)C(Me)$_2$) 139.47 (s, Ar o-C), 143.75 η^5-Me(C_6H_4)C(Me)$_2$) 151.36 (s, η^5-Me(C_6H_4)C(Me)$_2$), 159.98 (s, Ar *i*-C), 160.23 (s, CMe).

Table 1. Crystal Data and Structure Analysis Results

	1	**2**
Formula	$C_{68}H_{96}N_4Ru$	$C_{21.50}H_{32.50}N_{0.50}Ru_{0.50}$
M_w	1070.56	363.52
Crystal system	Monoclinic	Monoclinic
Space group	P2/c	P2(1)/m
a (Å)	12.764(6)	10.681(5)
b (Å)	23.442(11)	16.936(8)
c (Å)	20.808(10)	11.632(6)
α (deg)	90	90
β (deg)	93.634	111.637
γ(deg)	90	90
V (Å^3)	6213(5)	1955.8(16)
Z	4	4
Radiation (Kα, Å)	0.71073	0.71073
T (K)	200	201
D_{calcd} (g cm^{-3})	1.144	1.235
μ_{calcd} (mm^{-1})	0.294	0.434
F_{000}	2304	778
R, $R_w{}^{2\,a}$	0.0708, 0.1019	0.0286, 0.0785
GoF	1.089	1.027

REFERENCES

1. a) S.G. McGeachin, *Can. J. Chem.* **1968**, 46, 1903; b) L.C. Dorman, *Tetrahedron Lett.* **1966**, 4, 459; c) J.E. Parks, R.H. Holm, *Inorg. Chem.* **1968**, 7, 1408
2. a) L. Bourget-Merle, M.F. Lappert, J.R. Severn, *Chem. Rev.* **2002,** 102, 3031; b) W.E. Piers, D.J.H. Emsile, *Coord. Chem. Rev.* **2002**, 233, 131
3. a) D.S. Richeson, J.F. Mitchell, K.H. Theopold, *Organometallics* **1989**, 8, 2570; b) W.-K. Kim, L.M. Liable-Sands, I.A. Guzei, A.L. Rheingold, K.H. Theopold, *Organometallics* **1998**, 17, 4541; c) L.A. MacAdams, W.-K. Kim, L.M. Liable-Sands, I.A. Guzei, A.L. Rheingold, K.H. Theopold, *Organometallics* **2002**, 21, 952; d) K.H. Theopold, L.A. MacAdams, C. Puttnual, G.P. Buffone, A.L. Rheingold, *Poly. Mater. Sci. Eng.* **2002**, 86, 310; e) S. Zhang, W.E. Piers, X. Gao, M. Parvez, *J. Am. Chem. Soc.* **2000**, 122, 5499 f) P.G. Hayes, W.E. Piers. L.W. M. Lee, L.K. Knight, M. Parvez, M.R.J. Elsegood, W. Clegg, *Organometallics* **2001**, 20, 2533; g) P.G. Hayes, W.E. Piers, M. Parvez, *J. Am. Chem. Soc.* **2003**, 125, 5622; h) M. Rahim, N.J. Taylor, S. Xin, S. Collins, *Organometallics* **2000**, 19, 2161; i) S.B. Cortright, J.N. Johnston, *Angew. Chem. Int. Ed.* **2002**, 41, 345; j) V.C. Gibson, C. Newton, C. Redshaw, G. Sloan, A.J.P. White, D.J. Williams, P.J. Maddox, *Chem. Commun.* **1998**, 1651; k) J.C. Dohetry, K.H.D. Ballem, B.O. Patrick, K.M. Smith, *Organometallics* **2004**, 23, 1487; l) M. Rahim, N.J. Taylor, S. Xin, S. Collins, *Organometallics* **1998**, 17, 1315; m) B.-J. Deelman, P.B. Hitchcock, M.F. Lappert, W.-P. Leung, H.-K. Lee, T.C.W. Mak, *Organometallics* **1999**, 18, 1444; n) P.H.M. Budzelaar, A.B. van Oort, A.G. Orpen, *Eur. J. Inorg.*

Chem. **1998**, 10, 1485; o) L. Giannini, E. Solari, S.D. Angelis, T.R. Ward, C. Floriani, A. Chiesi-Villa, C. Rizzoli, *J. Am. Chem. Soc.* **1995**, 117, 5801; p) A. Martin, R. Uhrhammer, T.G. Gardener, R.F. Jordan, R.D. Rogers, *Organometallics* **1998**, 17, 382

4. a) J.M. Smith, R.J. Lachicotte, K.A. Pittard, T.R. Cundari, G. Lukat-Rodgers, K.R. Rodgers, P.L. Holland, *J. Am. Chem. Soc.* **2001**, 123, 9222; b) A.R. Sadique, W.W. Brennessel, P.L. Holland, *Inorg. Chem.* **2008**, 47, 784; c) E.A. Gregory, R.J. Lachciotte, P.L. Holland, *Organometallics* **2005**, 24, 1803; d) P.H.M. Budzelaar, R. de Gelder, A.W. Gal, *Organometallics* **1998**, 17, 4121; e) L.A. MacAdams, G.P. Buffone, C.D. Incarvito, J.A. Golen, A.L. Rheingold, K.H. Theopold, *Chem. Commun.* **2003**, 10, 1164; f) X. Dai, P. Kapoor, T.H. Warren, *J. Am. Chem. Soc.* **2004**, 126, 4978; g) J.D. Masuda, D.W. Stephen, *Can. J. Chem.* **2005**, 83, 324; h) G. Bai, P. Wei, D.W. Stephen, *Organometallics* **2006**, 25, 2649; i) A. Hadzovic, D. Song, *Organometallics* **2008**, 27, 1290; j) J.M. Smith, A.R. Sadique, T.R. Cundari, K.R. Rodgers, G. Lukat-Rodgers, R.J. Lachicotte, C.J. Flaschenriem, J. Vela, P.L. Holland, *J. Am. Chem. Soc.* **2006**, 128, 756; k) J. Chai, H. Zhu, A.C. Stückl, H.W. Roesky, J. Magull, A. Bencini, A. Caneschi, D. Gatteschi, *J. Am. Chem. Soc.* **2005**, 127, 9201; l) J.M. Smith, R.J. Lachicotte, P.L. Holland, *Organometallics* **2002**, 21, 4808; m) A.R. Sadique, E.A. Gregory, W.W. Brennessel, P.L. Holland, *J. Am. Chem. Soc.* **2007**, 129, 8112; n) G. Bai, P. Wei, A. Das, D.W. Stephen, *Organometallics* **2006**, 22, 5870; o) Y. Yu, A.R. Sadique, J.M. Smith, T.R. Dugan, R.E. Cowley, W.W. Bresnnessel, C.J. Flaschenriem, E. Bill, T.R. Cundari, P.L. Holland, *J. Am. Chem. Soc.* **2008**, 130 6624; p) P.L.

Holland, *Acc. Chem. Res.* **2008**, 41, 905; q) Y. Yu, W.W. Brennessel, P.L. Holland, *Organometallics* **2007**, 26, 3217

5. F. Basuli, U.J. Kilgore, D. Brown, J.C. Huffman, D.J. Mindiola, *Organometallics* **2004**, 23, 6166
6. a) F.A. Cotton, J. Czuchajowska, *J. Am. Chem. Soc.* **1991**, 3427; b) D.P. Riley, J.A. Stone, D.H. Busch, *J. Am. Chem. Soc.* **1977**, 99, 767
7. D.T. Carey, E.K. Cope-Eatough, E. Vilaplana-Mafe, F.S. Mair, R.G. Pritchard, J.E. Warren, R.J. Woods, *Dalton Trans.* **2003**, 6, 1083
8. C.E. Radzewich, M.P. Coles, R.F. Jordan, *J. Am. Chem. Soc.* **1998**, 120, 9384
9. S. Yokota, Y. Tachi, S. Itoh, *Inorg. Chem.* **2002**, 41, 1342
10. S. Fukuzumi, K. Ohkubo, *Eur. J. Chem.* **2000**, 6, 4532
11. J.W. Faller, A.M. Rosan, *J. Am. Chem. Soc.* **1976**, 98(11), 3389
12. U. Fekl, W. Kaminsky, K.I. Goldberg, *J. Am. Chem. Soc.* **2001**, 123, 6423
13. F. Basuli, J. Tomaszewski, J.C. Huffman, D.J. Mindiola, *J. Am. Chem. Soc.* **2003**, 125, 10170
14. a) J.D. Protasiewicz, S.J. Lippard. *J. Am. Chem. Soc.* **1991**, 113, 6564; b) R.R. Schrock, *Chem. Rev.* **2002**, 102, 145; c) Schrock R.R., *Acc. Chem. Res.* **1986**, 19, 342; d) P.F. Engel, M. Pfeffer, *Chem. Rev.* **1995**, 95, 2281
15. F. Basuli, U.J. Kilgore, X. Hu, K. Meyer, M. Pink, J.C. Huffman, D.J. Mindiola, *Angew. Chem. Int. Ed.* **2004**, 43, 3156
16. F. Basuli, B.C. Bailey, D. Brown, J. Tomaszewski, J.C. Huffman, M.-H. Baik, D.J. Mindiola, *J. Am. Chem. Soc.* **2004**, 126, 10506

17. H. Nagashima, H. Kondo, T. Hayashida, Y. Yamaguchi, M. Gondo, S. Masuda, K. Miyazaki, K. Matsubara, K. Kirchener, *Coord. Chem. Rev.* **2003**, 245, 177

18. a) P.J. Bailey, L.A. Mitchell, S.J. Parsons, *J. Chem. Soc. Dalton Trans.* **1996**, 13, 2839; b) D. Zuccaccia, S. Sabatini, G. Bellachioma, G. Cardaci, E. Clot, A. Macchioni, *Inorg. Chem.* **2003**, 42, 5465; c) H. tom Dieck, W. Kollvitz, I. Kleinwaechter, *Organometallics* **1986**, 5, 1449

19. A. Klose, E. Solari, J. Hesschenbrouck, C. Floriani, N. Re, S. Geremia, L. Randaccio, *Organometallics* **1999**, 18, 360

20. Y.D. Smurnyy, C. Bibal, M. Pink, K.G. Caulton, *Organometallics* **2005**, 24, 3849

21. A.D. Phillips, G. Laurenczy, R. Scopelliti, P.J. Dyson, *Organometallics* **2007**, 26, 1120

22. A.D. Phillips, A. Zava, R. Scopelitti, A.A. Nazarov, P.J. Dyson, *Organometallics* **2010,** 29, 417

23. a) S.C. Huckett, R.J. Angelici, *Organometallics* **1988**, 7, 1941; b) S.-M. Yang, M.C.-W. Chan, S.-M. Peng, C.-M. Che, *Organometallics* **1988**, 17, 151; c) D.R. Robertson, T.A. Stephenson, *J. Organometallic Chem.* **1977**, 142, C31; d) M.R.J. Elsegood, J.W. Steed, D.A. Tocher, *J. Chem. Soc.* **1992**, 1797; e) C.C. Neto, D.A. Sweigart, *J. Chem. Soc. Chem. Comm.* **1990**, 1703; f) J.W. Steed, D.A. Tocher, *J. Chem. Soc. Dalton Trans.* **1993**, 3187; g) D.R. Robertson, I.W. Robertson, T.A. Stephenson, *J. Organometallic Chem.* **1980**, 202, 309; h) S. Bhambri, D.A. Tocher, *J. Organometallic Chem.* **1996**, 507, 291

24. a) M.A. Bennett, *Coord. Chem. Rev.* **1997**, 166, 225; b) B. Therrien, *Acc. Chem. Res.* **2009**, 253, 493; c) C. Gemel, K. Folting, K.G. Caulton, *Inorg. Chem.* **2000**,

39, 1593; d) M.J. Ingleson, M. Pink, J.C. Huffman, H. Fan, K.G. Caulton, *Organometallics* **2006**, 25, 1112; e) M. Käβ, A. Friedrich, M. Drees, S. Schneider, *Angew. Chem. Int. Ed.* **2009**, 48, 905

25. M. Cokoja, C. Gemel, T. Steinke, F. Schröder, R.A. Fischer, *Dalton Trans.* **2005**, 1, 44

26. A. Moreno, P.S. Pregosin, G. Laurenczy, A.D. Phillips, P.J. Dyson, *Organometallics* **2009**, 28, 6432 and references therein

CHAPTER THREE

RE-VISITATION AND CLARIFICATION OF THE REAL NATURE OF AN ALLEGED TRIMERIC MAGNESIUM CO_2 COMPLEX

NOTES ON MAGNESIUM-CO_2 CLUSTERS

Modern scientific literature is enriched with numerous studies detailing the activations and fixations of carbon dioxide.[1] which have opened new avenues and perspectives for the chemistry of this ever-challenging molecule.[1] Today, the field of transition metal mediated CO_2 chemistry is regarded as a promising research endeavor constantly pushing to discover new catalytic utilizations of carbon dioxide. Main group elements play an equally important role in the chemistry of CO_2 especially considering their role in natural systems.[2]

The Chang group has synthesized a variety of interesting main-group amide complexes, utilizing mostly magnesium and aluminum, that have the ability to insert/fixate CO_2 in various bonding modes to either mononuclear and/or dinuclear magnesium complexes.[2,3] One of the first of such complexes features an unusual tetrameric complex $[Me_2Al(\mu\text{-}^iPr_2N)_2Mg(\mu\text{-}Me)]_4$ (**1**) containing tricoordinate magnesium atoms and a linear dimer $[Me_2Al(\mu\text{-}Et_2N)_2Mg(\mu\text{-}Me)]_2$ (**2**) containing tetracoordinate magnesium atoms. These species react with substituted acetylenes and eventually CO_2, to undergo metathesis and insertion reactions affording ethynyl-bridged aluminum-magnesium complexes and subsequent CO_2 insertion compounds **3-14** (***Scheme 1***).[2] Complexes **3** and **4** readily react with CO_2 resulting in quantitative amounts of white crystalline $\{[Me_2Al(\mu\text{-}^iPr_2N)_2Mg[u\text{-}OOC(C{\equiv}CR)]\}_2$ (R = C_6H_5 (**9**); C_6H_4-*p*-CH_3 (**10**)) respectively. The resulting complexes show fair toluene solubility and the insertions of CO_2 are believed to take place at the magnesium-carbon bond of the ethynyl bridges rather than at the aluminum-nitrogen bond based on elemental analysis data.

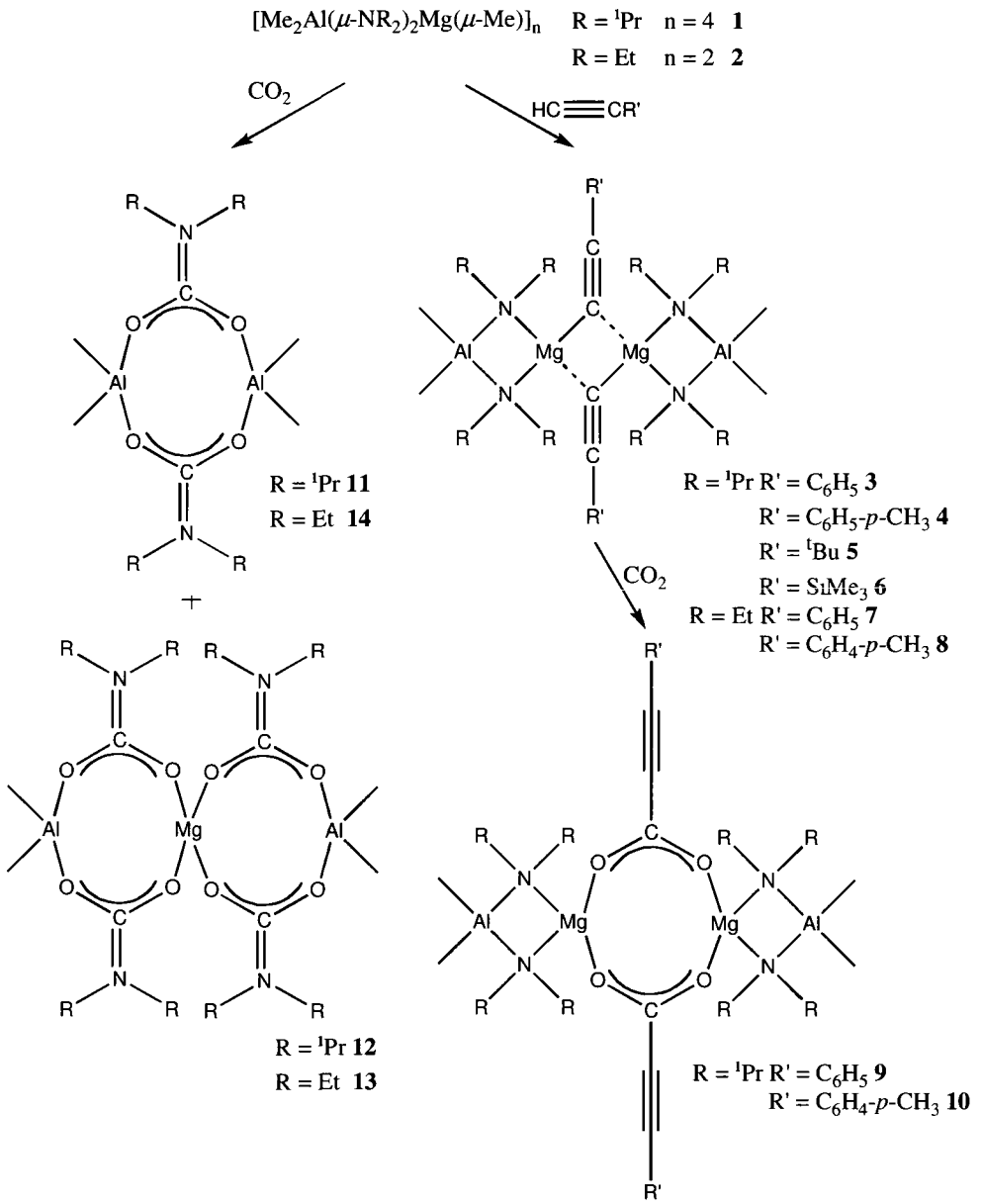

Scheme 1: Syntheses of acetylene and CO_2 insertion and metathesis compounds **3-14**

Further, compounds **1** and **2** also react with CO_2 directly resulting in various insertion products. Compound **1** yields a dialuminum carbamato complex **11** and an aluminum-magnesium mixed metal complex **12**. Similarly, the reaction of compound **B** gives the dialuminum-CO_2 insertion product **13,** which, upon sublimation results in compound **14**.

These early carbamato complexes of dialuminum and aluminum-magnesium mixed metal systems were some of the initial observations made by Chang *et. al.* regarding carbon dioxide fixation on main group metal systems.[2]

These observations were followed by a detailed study on the effect of varying steric environments on aluminum-magneisum mixed metal systems at their subsequent affect on CO_2 fixation.[3b] The heightened sensitivity of organomagneisum compounds to air and water, at times, make it difficult to obtain single crystals. Efforts by Chang *et. al.* to obtain suitable crystals for X-ray analysis lead them to discover that less bulky Y groups in MgY_2 (Y = iPr, C≡CPh, NMe_2) react with CO_2 to yield linear magnesium carboxylato and carbamato trimers while bulky Y groups (Y = NEt_2, N^iPr, NPh_2) yield cage carbamato magnesium compounds **15-25** (***Scheme 2***).[3b] A solvent effect was also observed, particularly a dimer of $[Mg_2(O_2CNPh_2)_4(HMPA)_2]$ was obtained from a hexamer of the caged compound $[Mg_6(O_2CHPh_2)_{12}]$ after the addition of HMPA/THF.

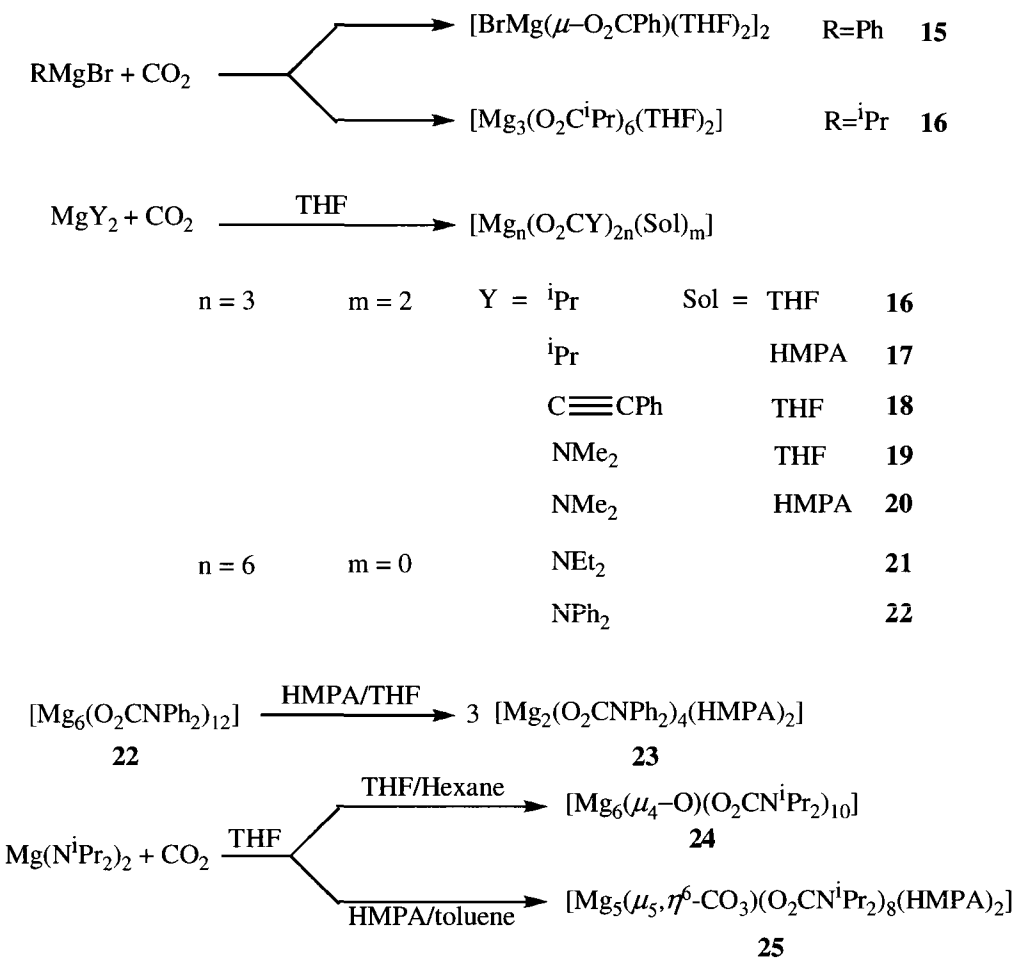

Scheme 2: Reaction scheme detailing formation of various Mg-CO_2 insertion products

The products obtained from the various insertions of carbon dioxide are divided into three categories: (1) linear, multinuclear carboxylato and carbamato magnesium compounds, such as **15-20** and **23**; (2) carbamato magnesium cage compounds, such as **21** and **22**; and (3) μ_4-O or μ_5-O carbamato magnesium cage compounds, such as **24** or **25.** Structural analysis, via X-ray, of compounds **15**, **17** and **20-25** demonstrated the existence of various bonding modes between the carboxylato and carbamato groups and magnesium, including (c) (μ_2,η^2), (d) (μ_2,η^3) (e) (μ_3,η^3) and (g) (μ_4,η^4) as shown in ***Figure 1***.

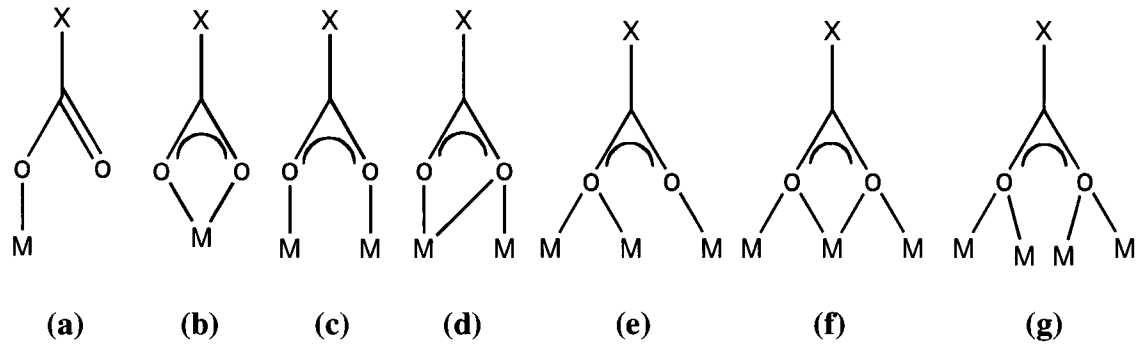

Figure 1: Possible bonding types of carboxylato (X: C), carbamato (X: N), and carbonato (X: O) ligands: (a) μ_1,η^1; (b) μ_1,η^2; (c) μ_2,η^2; (d) μ_2,η^3; (e) μ_3,η^3; (f) μ_3,η^4; (g) μ_4,η^4

Compound **15** (***Figure 2***) features the type (c) bonding mode where two magnesium atoms are linked to two bridging $PhCO_2$ in a coplanar eight-membered ring. With bromine atoms and two THF oxygen atoms coordinated to each magnesium centre, a trigonal bipyramidal spatial orientation results. The Mg-O bond lengths (1.233(7) Å and 1.255(7) Å) fall between those of a single covalent C-O bond (1.43Å) and a covalent double bond (1.20Å) indicating partial double bond character.[3b]

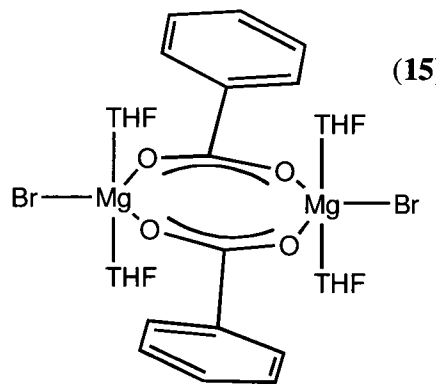

(15)

Figure 2: Structure of **15** $[BrMg(\mu\text{-}O_2CPh)(THF)]_2$ based on X-ray data

The same double bond character is noted in the caged carbamato compounds $[Mg_6(O_2CNEt_2)_{12}]$ (**21**) and $[Mg_6(O_2CNPh_2)_{12}]$ (**22**). Both compounds **21** and **22** contain a Mg_6 core whose skeletons can be described, respectively, as a twisted boat cyclohexane and a chair form cyclohexane. The bonding modes in these compounds are comprised of a combination of type (c), (e) and (g) in compound **21** and type (c) and (e) in **22**, with C-O bond lengths ranging between 1.234(5) and 1.289(4) Å in both compounds. Sterics play an important role in the formation of these caged compounds but solvent effects specifically in complex **22,** are another factor, which determine the structural outcome of these Mg-CO_2 clusters. Originally crystallized from a hexane solution, compound **22** transforms from a hexamer to a dimer, $[Mg_2(O_2CNPh_2)_4(HMPA)_2]$, when recyrstallized from a HMPA/THF solution.[3b] This happens almost instantaneously upon addition of the HMPA/THF solution but is not the first time this type of effect has been observed in polymeric metal systems. Quite often, deaggregation of polymeric zinc and magnesium compounds has been observed in the presence of strong donor solvents.[4]

The work by Chang *et. al.* on the insertions of CO_2 into magnesium–alkyls and amides is of great interest since the transformation of CO_2 into amides, which has been comprehensively reviewed,[11] is yet another page in the quest for the conversion of an abundant compound into a more valuable organic product.[5] The previously discussed paper of Chang *et. al.* outlines possible bonding modes of carbamates to either mononuclear, dinuclear and caged magnesium complexes. Among all the compounds reported in that study the bonding modes of type (a), (c) and (d) were relatively common and Chang *et. al.* also noted that type (b) (μ_1,η^2) bonding was not and has not yet been observed. The absence of this chelating mode is attribute to the fact that the electron

density donated by two oxygen atoms to magnesium will be too great and thus, the already strained four-member ring is not likely to form. Nonetheless, Chang *et. al.* also noted that this form of bonding is possible in less electron donating systems, particularly when the oxygens are replaced by sulfur or –NR species. Ideally, within Mg-CO_2 systems, the oxygen atoms will tend to adopt bridged bonding modes to multiple Mg atoms resulting in reduced electron density and strain at one specific magnesium centre. It is only recently though, that Kemp *et. al.* discovered that the formal insertion of CO_2 into $Mg_2(NCy_2)_4$ in THF/HMPA forms an unsymmetrical dinuclear compound $[Mg_2(O_2CNCy_2)_4(HMPA)]$ (**26**) which demonstrates, among others, the heretofore unknown chelating type (b).[5]

Compound **26** was formed upon bubbling gaseous CO_2 into a mixed THF/HMPA solution of $Mg_2(NCy_2)_4$ for 30 minutes. The crystals obtained from a hexane solution revealed a dinuclear structure in which the two magnesium atoms are connected by four bridging carbamato ligands (***Figure 3)***.

(26)

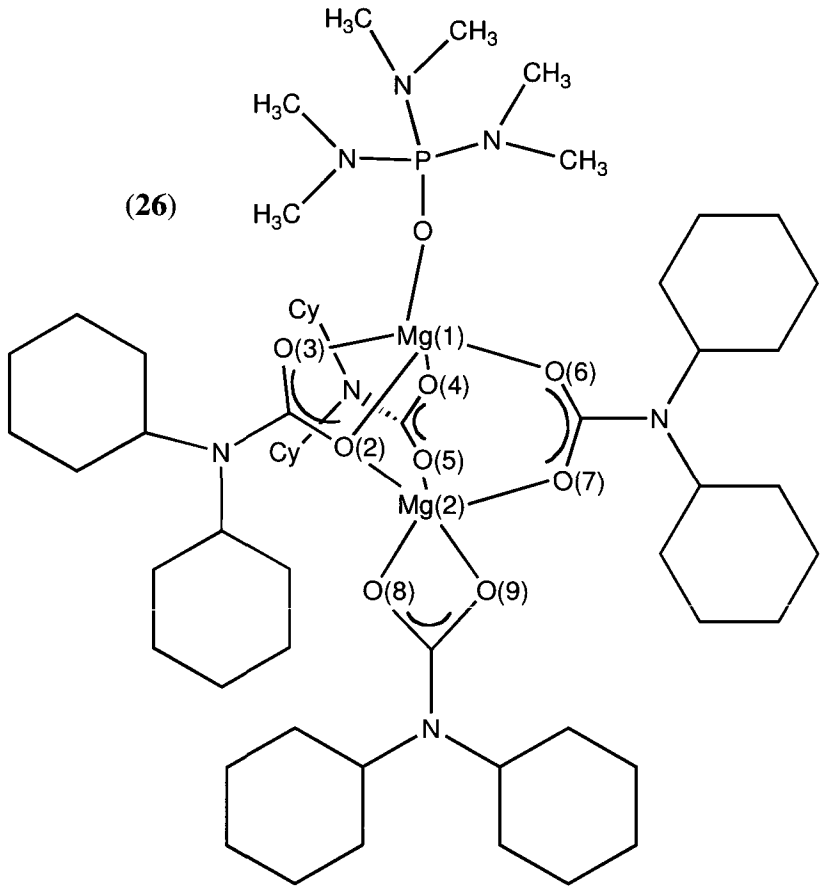

Figure 3: Structure of $[Mg_2(O_2CNCy_2)_4(HMPA)]$ demonstrating the type (b) μ_1,η^2 bonding mode

The interesting property of this structure is that the four carbamato ligands bind the magnesium centers via three different bonding modes: two of the carbamato groups bind in the μ_2,η^2 fashion, one in the μ_2,η^3 fashion and one in the previously unknown bonding mode of μ_1,η^2. Within this ligand the Mg(2)-O(8) and Mg(2)-O(9) bond lengths are 2.041 and 2.108 Å respectively and the O(8)-Mg(2)-O(9) bond angle of 64.18° is fairly similar to the N-Mg-N bond angles of 62.3-65.6° reported in terminal bidentate Mg-carbodiimides, but slightly less than those seen in sulfur analogues which use carbon disulfide as ligands.[5]

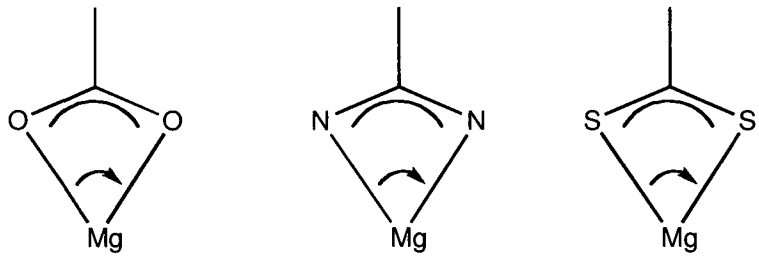

Bond Angle Range (°)	64.18 (in **26**)	62.3-65.6	66.83-72.34

Figure 4: Bond angle ranges in magnesium chelates

While the reason for this particular bond formation is not known for certain, it is hypothesized that the lack of coordinating solvent to Mg(2) versus Mg(1) in the solid state must play a role. As previously mentioned, Chang *et. al.* theorized that the electron density on the oxygen atoms is too great in order to form in the highly strained terminal four-membered ring. It appears that the absence of any coordinating solvent ligated to Mg(2) in the solid state allows the atom to be more receptive to the greater electron density donated by the oxygen atoms. Compound **26** completes the structural motifs believed possible for CO_2 bonding to mono- and dinuclear Mg carbamato complexes and at the same time reveals the importance of understanding and controlling the bonding of CO_2 to metal centers in order to facilitate possible future conversions.[5]

There are numerous factors that determine the wide range of bonding modes in the coordination of CO_2 to metal centers.[1] Identifying these governing factors is critical to controlling electron transfer and thus the reactivity of CO_2 with respective metal centers.[6–8] Thus it is seems valid to state that *d*-electrons are of critical importance in these complexes since CO_2 coordination has never been observed in d^0 or main-group metal systems until recently. New findings[9] by Cheng *et. al.* describing robust end-on

coordination of CO_2 to magnesium cations accompanied by the formation of an unprecedented Mg/Al-containing cluster [{$R_2Al(\mu$-$NSiMe_3)(\mu$-$OSiMe_3)Mg(THF)_2(\mu$-$O_2C)\}_3$]·2 THF (R = Me (**A**), Et (**B**)) (***Figure 5***) were sensational to say the least.

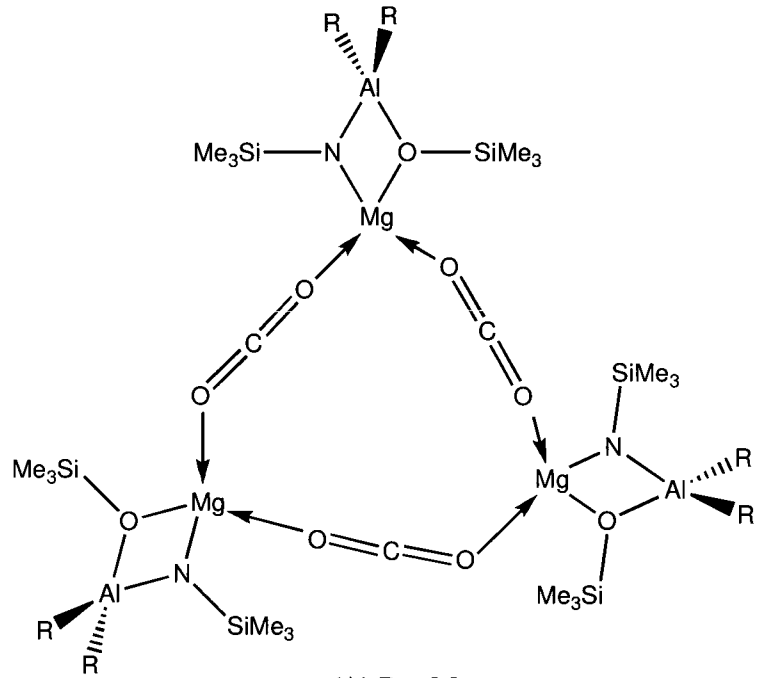

(**A**) R = Me
(**B**) R = Et

Figure 5: Schematic representation of compound **A** and **B**. Coordinated THF molecules omitted for clarity.

By taking into consideration the fact that the oxygen atoms of CO_2 do not possess sufficient basicity to form stable adducts with Lewis acids, this claim may certainly be regarded as a major breakthrough. Furthermore, amongst the numerous bonding modes of CO_2 that have been practically demonstrated there have been only two cases of a genuine end-on-bound CO_2 complex.[10a,b] The first involves a strongly reducing trivalent uranium center, for which it seems likely that partial electron transfer plays a role. The second involves an inorganic polyoxoanion consisting of Mo and Co metal centers linked by

linearly bound CO_2. Nevertheless, even in the uranium system CO_2 is only weakly bound to the metal centre. As a rule with no exception, until very recently, only low and medium valent metal centres have been used for CO_2 coordination. Thus compounds **A** and **B** generated by Cheng *et. al.* would represent the first case of CO_2 robust coordination to a non-transition metal center in an unprecedented bridging end-on fashion. It should also be noted that irreversible fixation of the CO_2 molecules occurs in THF, the oxygen atom of which is normally regarded as a far better donor than the oxygen atoms of CO_2.

These observations made us doubtful about the original authors' interpretation and, aiming at probing alternative possibilities, we have now re-evaluated the reported data. In particular, the experimental data provided by Cheng *et. al.* has been revisited in order to re-examine the apparent co-ordination of CO_2 in this tri-meric magnesium cluster compound. Herein I report conclusive proof that the magnesium-CO_2 system should be re-interpreted as a magnesium-CNO cluster.

RESULTS AND DISCUSSION

The formation of complexes **A** and **B** was originally rationalized by assuming the attack of CO_2 at only one silazanate group[5]. There was no clear explanation as to why the second silazanate group did not follow the same fate in the presence of excess CO_2. No conclusive evidence was provided for the identification of the bridging imido group generated by the attack of Me_3Al on the $[Mg(OSiMe_3)\{N\text{-}(SiMe_3)_2\}]$ intermediate (***Scheme 3***).

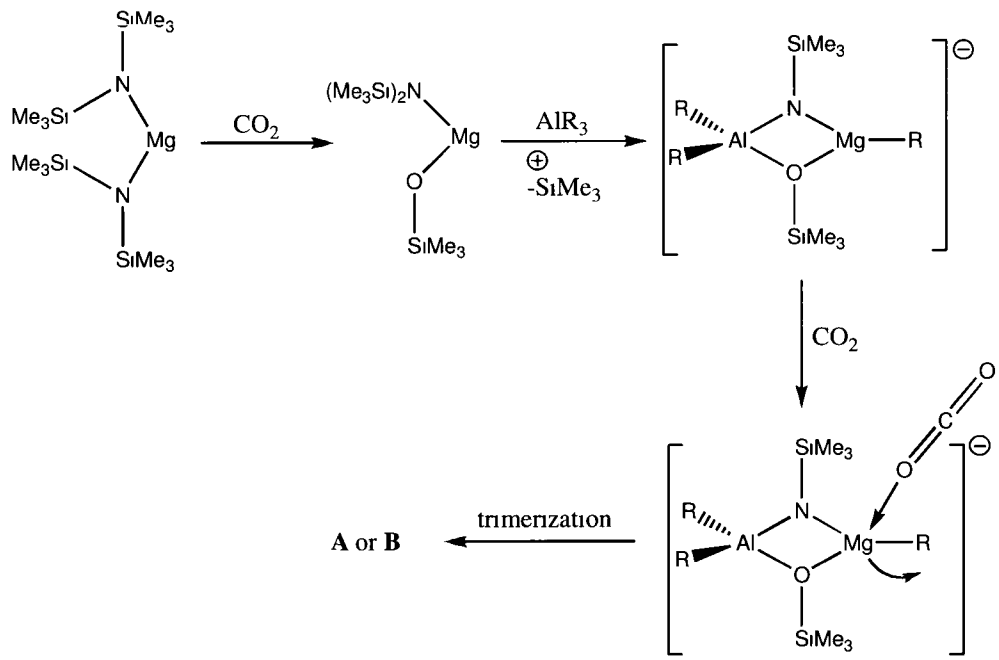

Scheme 3: Proposed reaction pathway for the formation of **A** and **B**

The presence of disorder between the imido and silanolate group, with equal occupancy, was claimed to account for the crystallographic equivalency of the two donor atoms bridging the Al and Mg centers. This interpretation was the only possibility that would allow the charges to be balanced within the complex thus concluding that the triatomic

units bridging the three Mg atoms had to be CO_2. The ^1H NMR spectra also unexplainably showed only one resonance for the silanolate and silylimido groups together.

To further probe Chang's proposed structure we performed DFT calculations. Geometry optimization (***Figure 6***) of the full complex **A** led to fragmentation of the apparent complex and release of CO_2, which thus appears not to be strongly bound at all. This result only substantiated suspicions behind the initial assignment of the bridging molecular units as CO_2.

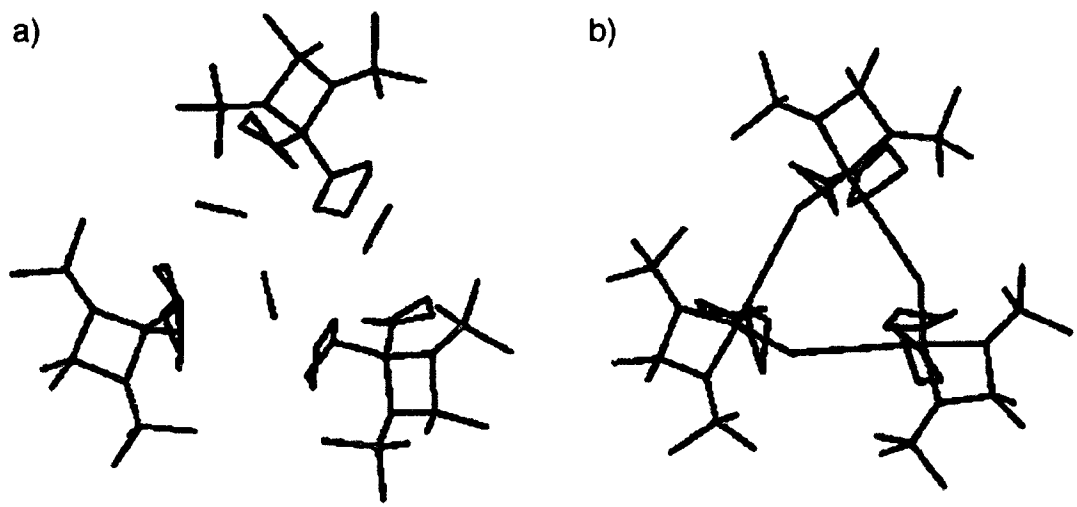

Figure 6: a) Partially optimized structure of **A**; CO_2 units are dissociating. b) Optimized structure of **A** with N and O atoms exchanged.

The preparation of complex **A** by Chang *et al.* outlines the addition of one equivalent of $AlMe_3$ to a solution of $Mg[N(SiMe_3)]_2$ in THF under an atmosphere of CO_2. The experimental procedure was followed closely but in this re-investigation the magnesium silazanate precursor $(NSiMe_3)_2Mg_2(\mu\text{-}NSiMe_3)_2$ (**1**) was synthesized by combining di-butyl magnesium with two equivalents of hexamethyldisilazane in hexane

at room temperature and stirring vigorously overnight (***Scheme 4***).

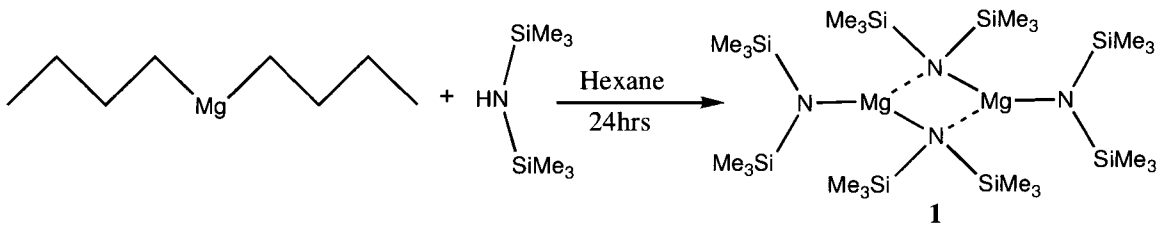

Scheme 4: Reaction pathway for the formation of complex **1**

Colourless white crystals, in good yield, were obtained from a concentrated hexane solution over a period of two days, isolated and vacuum dried prior to proceeding. Complex **1** is a bimetallic magnesium(II) d^0 molecule with bridging silylimido moieties. The structure of **1** was elucidated by X-ray diffraction (***Figure 7***) and confirmed again by ^{1}H NMR characterization.

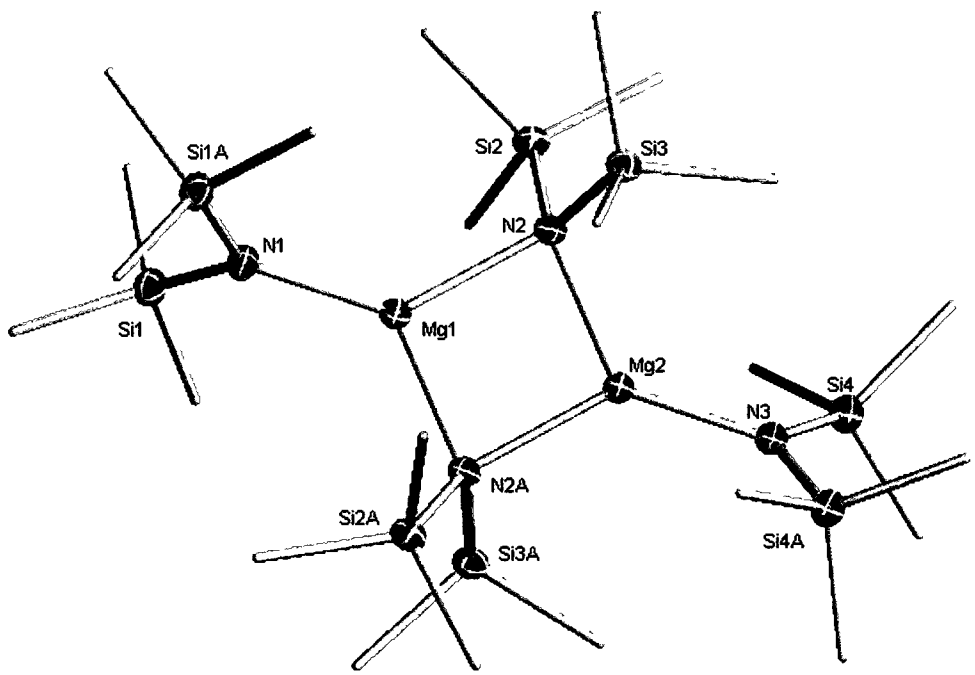

Figure 7: Thermal ellipsoid plot of $(NSiMe_3)_2Mg_2(\mu\text{-}NSiMe_3)_2$ showing selected atom labeling. Thermal ellipsoids are drawn at the 50% probability level.

Complex **1** was then dissolved completely in a THF solution to which $AlMe_3$ was added in a dropwise manner. The resulting solution was cooled in an ice bath for two hours under an atmosphere of carbon dioxide. The trimeric complex **2** was successfully re-synthesized as air-sensitive, colorless crystals in relatively low yield. The crystal structure confirmed the formula $[\{Me_2Al\text{-}(\mu\text{-}ESiMe_3)_2Mg(THF)_2(\mu\text{-}E_2C)\}_3]\cdot 1.5$ THF (E = O, N, or a combination of both). The lattice molecule of THF present in the structure gave better refinement when refined with partial occupancy (***Figure 8***).

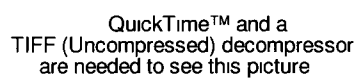

Figure 8: Thermal ellipsoid plot of complex **2** $[\{Me_2Al\text{-}(\mu\text{-}ESiMe_3)_2Mg(THF)_2(\mu\text{-}E_2C)\}_3]\cdot 1.5$ THF (E = N or O) where ellipsoids are drawn at 50% probability

Upon closer inspection of the crystal structure there was no indication of the presence of any disorder involving the two atoms bridging the Mg and Al centers as described by Chang *et. al.* The two atoms bridging the Mg and Al centres could be best refined as the oxygen atoms of silanolate groups. Further analysis of the X-ray structure showed a 50:50 disorder in the three-atom XCY units bridging the Mg atoms[8] (***Figure 9***).

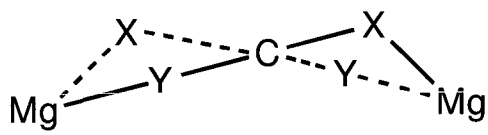

Figure 9: Disorder in bridging XCY units.

Each arrangement of the XCY unit has a bent Mg-X-C geometry and a nearly linear Mg-Y-C geometry while the carbon atoms of the two arrangements coincide. The varying angles around atoms X and Y are strong indicators that X and Y represent different atoms. A symmetrical CO_2 molecule would not be expected to exhibit differing bond angles at both its oxygen atoms. Making the assumption that all the atoms bridging the Mg and Al centers are oxygen atoms, electro-neutrality requires the XCY units to be NCO moieties. The data obtained from the X-ray structure does not allow confident N and O assignments as both the X and Y atoms refine equally well as either N or O, or even as a mixture of both atoms. In this re-interpretation, the atoms were refined with the X and Y atoms as oxygen and nitrogen respectively. The negative charge on the bridging NCO unit could explain the robust coordination to the Mg centers observed even in the presence of a Lewis base such as THF.

DFT geometry optimization of the N/O-switched molecule and simplified model compounds resulted in geometries very close to the observed geometries of complex **1a** (***Figure 6b***). Particularly, the peculiar bent coordination at one end only of apparent CO_2 is now fairly precisely reproduced. These calculations also helped to explain the preferential formation of a trimeric structure. The NCO unit prefers a nearly linear geometry at the N atom and a bent geometry at the O atom in a hypothetical monomeric compound $[Me_2Al(OSiMe_3)_2Mg(THF)_2(NCO)]$ (Mg-N-C 163° ; $[Me_2Al(OSiMe_3)_2Mg(THF)_2(OCN)]$: Mg-O-C 128°). In another hypothetical dimeric structure, a bent angle at the N atom cannot be avoided, although it remains less bent than the O atom ($[\{Me_2Al(OSiMe_3)_2Mg(THF)_2(\mu\text{-}NCO)\}_2]$: Mg-N-C 150°, Mg-O-C 123°). Trimer formation relieves the angle strain by allowing linear coordination at the N atom, as seen in both the X-ray structure and the calculated geometry (Mg-N-C 168°, Mg-O-C 142°).

The ^1H NMR spectra in d_8THF displays only one sharp proton resonance for the O-$SiMe_3$ group and one for the Al-CH_3 groups at δ = 0.06 and 0.97ppm respectively (***Figure 10***).

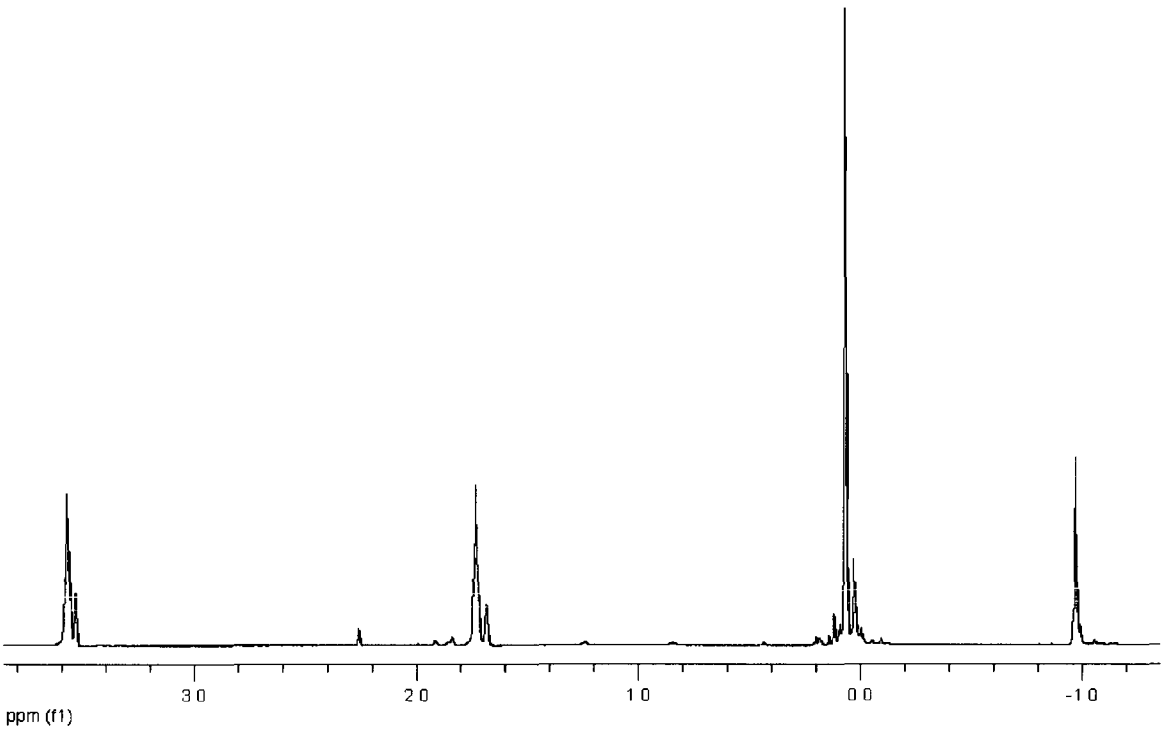

Figure 10: ^{1}H NMR of **2** in d^{8} THF

Although the bound Me_3Si groups at either N or O could, in principle, produce identical chemical shifts in the H^{1}-NMR spectra, this coincidence is much less likely in the ^{13}C NMR spectra, which also showed only one resonance each for the O-$SiMe_3$ and $AlCH_3$ groups at δ = 3.21 and 5.22ppm, respectively (***Figure 11a***).

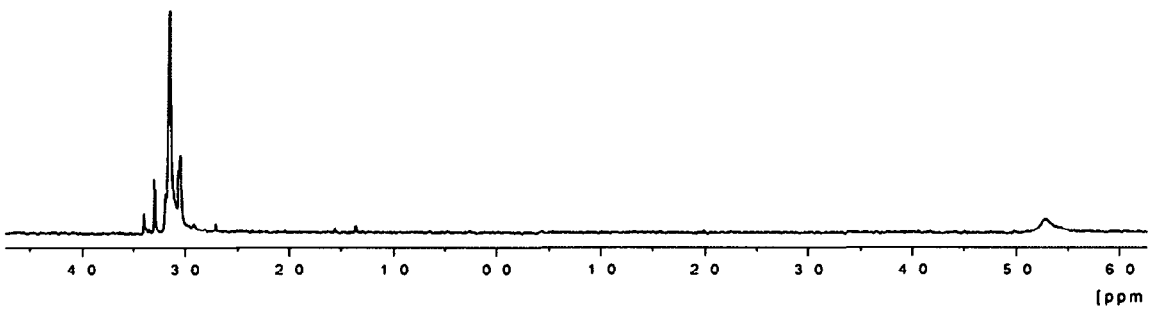

Figure 11a: ^{13}C NMR of **2**

The ^{29}Si NMR spectrum, in d_8 toluene as well, showed only one resonance at $\delta = 14.13$ ppm in the temperature range 355–260K rather than the two resonances which would be expected if both silanolate and silylimido groups were to be present in the complex (***Figure 11b***). On the other hand, two nonequivalent O-$SiMe_3$ groups could be expected, in theory, for a *bis*(silanolate)-bridged complex with the group being *cis* or *trans* to the nitrogen of the NCO bridge. Indeed, cooling of a d_8 THF solution resulted in splitting of the silanolate resonances in the ^1H NMR spectrum, thus giving rise to two singlets at 203K (***Figure 11c***). The variable-temperature ^{29}Si-NMR, in the same solvent, shows a far more complex solvent-dependent fluxional behavior compared to the d^8 toluene solution, for which no straightforward interpretation is possible. Considering that the structure is formed by three different anions O-$SiMe_3$, -NCO and -Me there may be scrambling with different ratios over the two cations which form mono- and polynuclear structures, thus a very complex fluxional behavior can be anticipated. Finally, the ^{14}N NMR spectrum gave a rather broad resonance at $\delta = 304.67$ ppm in d_8 THF (the resonance of silazanate groups occurs in the region around $\delta = 338$ ppm) which is within the expected region for an NCO group (***Figure 11d***).

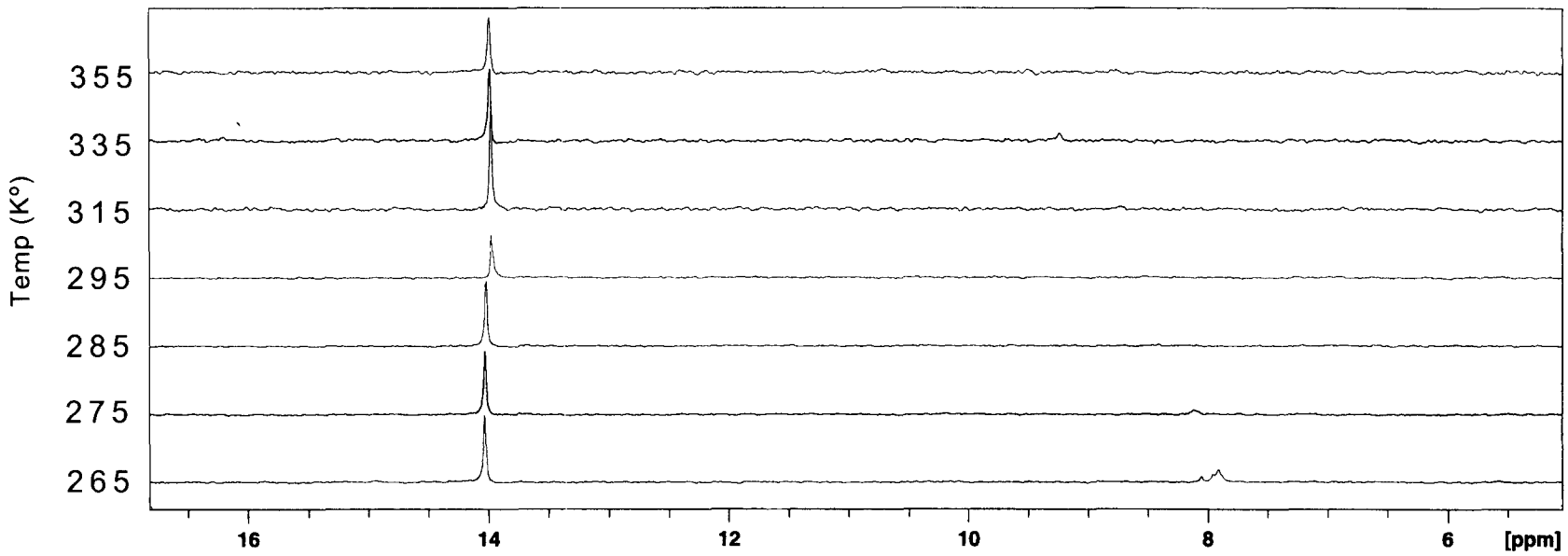

Figure 11b: Variable temperature ^{29}Si NMR of **2**

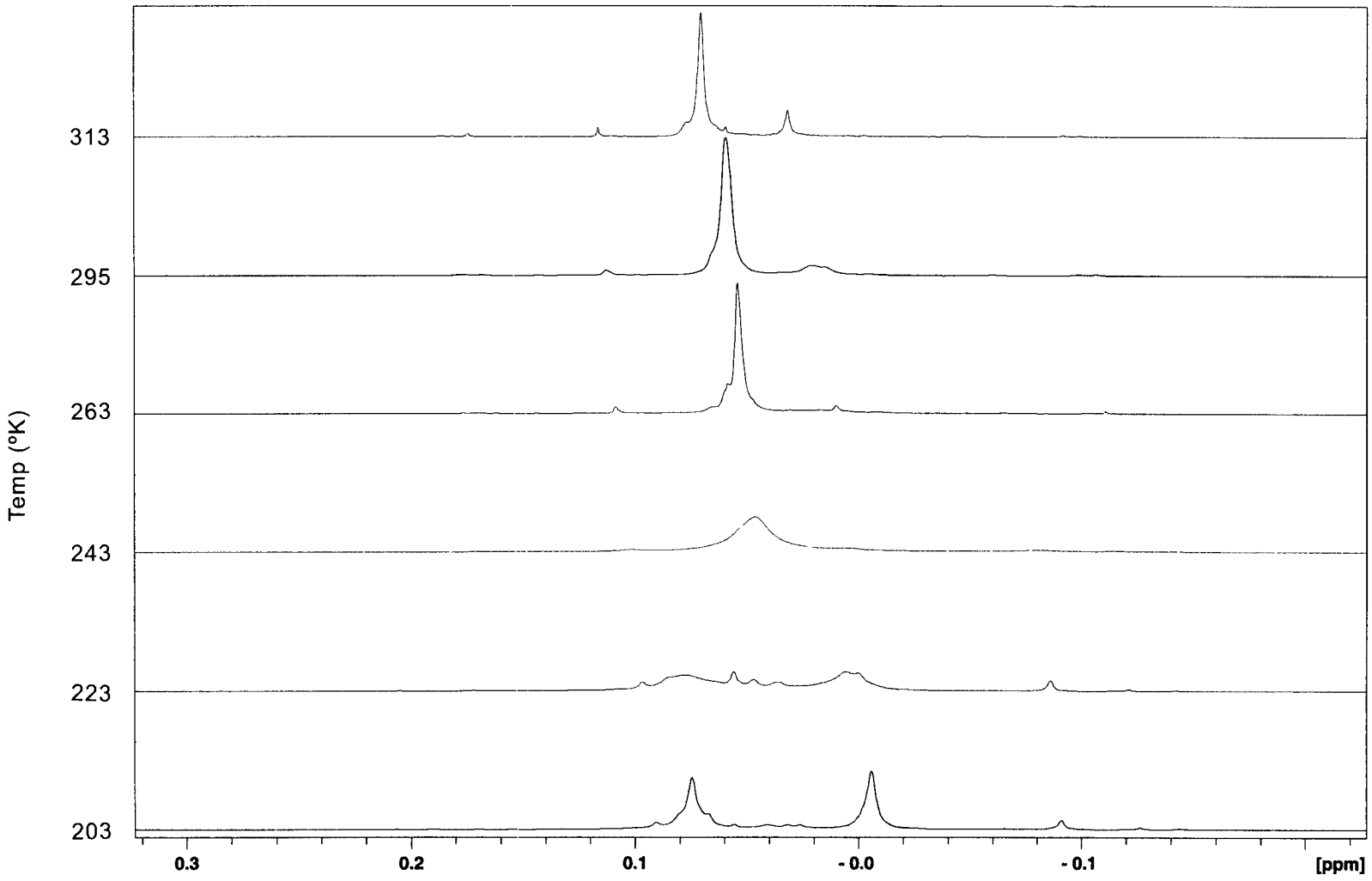

Figure 11c: Variable temperature ^{1}H NMR of **2** in d_8 THF

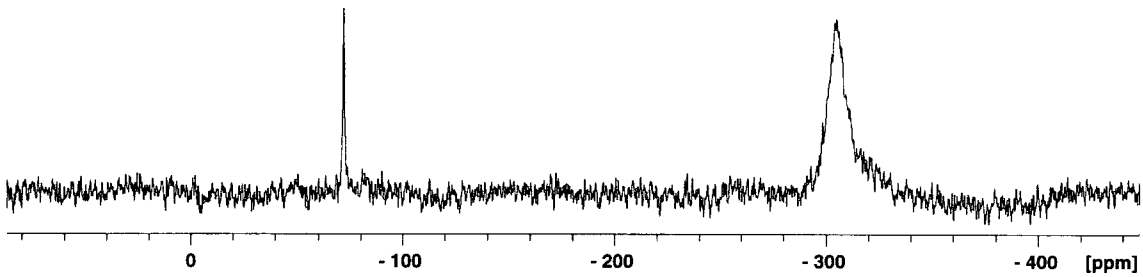

Figure 11d: ^{14}N NMR of **2** in d_8 THF

In addition to the NMR evidence, a chemical degradation of **2** with a diluted solution of aqueous KOH brought the solution to pH 8 and subsequently caused the precipitation of $Al(OH)_3$ and $Mg(OH)_2$. Centrifugation of $Al(OH)_3$ and $Mg(OH)_2$ followed by neutralization with HNO_3 and treatment with $AgNO_3$, afforded a colorless precipitate of Ag(NCO), which showed the characteristic intense resonance at 2176 cm^{-1} in the IR spectrum. If the bridging molecules had been CO_2 one would not expect the formation of an Ag(NCO) complex as observed.

A possible alternative rationalization for the formation of $[\{Me_2Al(\mu\text{-}OSiMe_3)_2Mg(THF)_2(\mu\text{-}OCN)\}_3]\cdot 1.5(THF)$ may consist of the reaction of $[\{[(Me_3Si)_2N]Mg[\mu\text{-}N(SiMe_3)_2]\}_2]$ with CO_2 to afford Me_3SiNCO (***Scheme 5***).

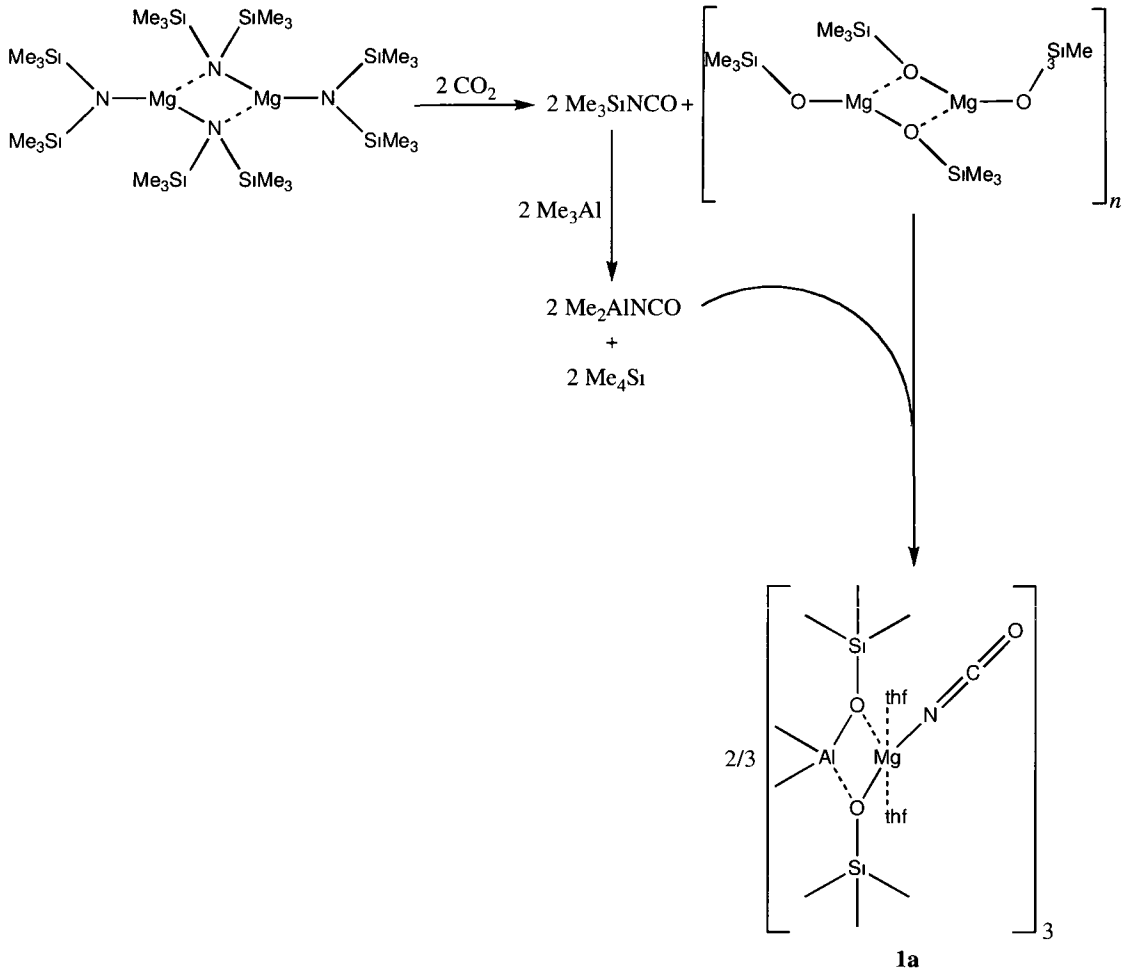

Scheme 5: The proposed formation of **2** with NCO groups.

In turn, Me_3SiNCO reacts with Me_3Al to form NCO- anions that are incorporated into the Mg-Al cluster to form the final trinuclear cluster. Furthermore, the formation of Me_3SiNCO was observed in a GC–MS of the solution that was obtained from exposure of a solution of $[\{[(Me_3Si)_2N]Mg[\mu\text{-}N(SiMe_3)_2]\}_2]$ to CO_2. As well, the reaction of Me_3Al with Me_3SiNCO in the stoichiometric ratio of 1:1, completely consumed the two starting materials to afford a complex mixture from which, besides Me_4Si, no component could be conclusively identified. Nonetheless, the crude reaction mixture that was obtained upon solvent evaporation produced a broad resonance in the ^{14}N NMR spectrum at δ =

248ppm and a series of four IR absorptions (2255, 2202, 2143, 2065 cm^{-1}), which can only be attributed to Al coordinated NCO- anions.

In conclusion, the observations above suggest that indeed the presence of d-electrons is a large contributing factor to true co-ordination and fixation of CO_2. Thus, rather than a case of irreversible fixation of CO_2 at magnesium cations, complex **1a** is more reasonably formulated as the isocyanate derivative $[\{Me_2Al(\mu\text{-}OSiMe_3)_2Mg(THF)_2(\mu\text{-}OCN)\}]\cdot 1.5$ THF.

EXPERIMENTAL SECTION

General Experimental Details

All operations were performed either under a nitrogen atmosphere using standard Schlenk techniques or in a purified nitrogen-filled dry-box equipped with a vacuum-line manifold to supply CO_2. The di-*n*-butyl magnesium solution $[CH_3(CH_2)_3]_2$ (1.0 M in heptane) and trimethylaluminum $AlMe_3$ (2.0 M in toluene) were purchased from Aldrich and used as received. Hexamethyldisilazane $(CH_3)_3SiNHSi(CH_3)_3$ (for GC ≥99%) was obtained from Fluka and used as received. Chemical degradation experiments were carried out in air on samples weighed inside a drybox. Infrared spectra were recorded on a Mattson 9000 and Nicolet 750-Magna FT-IR instrument from Nujol mulls prepared in a dry box. NMR spectra were recorded with a Varian AMX-500 MHz spectrometer by using NMR tubes that were prepared inside a drybox and flame-sealed. Data for X-ray crystal structure determinations were obtained with a Bruker diffractometer equipped with a Smart CCD area detector.

Preparation of $\{[(Me_3Si)_2N]Mg[\mu\text{-}N(SiMe_3)_2]\}_2$ (1)

Hexamethyldisilazane (≥ 99.0%, 16.6 mL, 79.4 mmol) was added dropwise to solution of di-*n*-butyl magnesium (1.0 M in heptane, 36.1 mL, 185.7 mmol) which resulted in an immediate exothermic reaction accompanied by vigorous gas production. The reaction mixture was set to stir and reflux overnight at 130°C. The resulting solution was cooled and concentrated in vacuo (25 mL) until slight precipitation of the product occurred. The solution was then heated gently allowing any precipitate to re-dissolve. The reaction vessel containing to solution was allowed to stand for 24 hours resulting in the formation of colourless needles. The crystallization procedure was repeated three times yielding **1** in a moderate yield (7.32g, 10.6mmol, 53%). H^1-NMR (500 MHz, C_6D_6, 23°C): δ= 0.39 (d, 36 H, -$(SiMe_3)_8$)

Preparation of $[\{Me_2Al(\mu\text{-}OSiMe_3)_2Mg(THF)_2(\mu\text{-}OCN)\}]\cdot 1.5$ THF (2)

A solution of $AlMe_3$ (2.0 m in toluene, 2.2 mL, 4.4 mmol) was added dropwise to a solution of $\{[(Me_3Si)_2N]Mg[\mu\text{-}N(SiMe_3)_2]\}_2$ (1.5 g, 2.17 mmol) in THF (20 mL). The resulting solution was cooled in an ice bath and stirred for 2 h in an atmosphere of carbon dioxide. The resultant solution was concentrated to a smaller volume (10 mL) and cooled in a freezer. Colorless crystals of **2** separated upon standing five days (yield: 21 %). H^1-NMR (500 MHz, [d_8]THF, 23°C): δ= -0.97 (s, 18 H, Al-CH_3), 0.06 (s, 54 H, $OSiMe_3$), 1.78 (m, 30 H, THF), 3.59 ppm (m, 30 H, THF) ; ^{13}C NMR (125.72 MHz, [d_8]THF, 23°C): δ= -5.22 (Al-CH_3), 3.21 ($OSiMe_3$), 67.65

(THF), 25.21 (THF), 120.98 ppm (NCO) ; ^{29}Si NMR (99.32 MHz, [D_8]THF, 263 K): δ = 6.96 ppm ; ^{29}Si NMR (99.32 MHz, [d_8]toluene, 23°C): δ = 14.13 ppm ; ^{14}N NMR (36.12 MHz, [d_8]THF, 23°C): δ = -304.67 ppm. DFT: Density functional calculations were performed with the TUR- BOMOLE program (R. Ahlrichs, M. Bär, M. Häser, H. Horn, C. Kömel, *Chem. Phys. Lett.* **1989**, 162, 165 ; O, Treutler, R. Ahlrichs, *J. Chem. Phys.* **1995**, 102, 346 ; R. Ahlrichs, et al., Turbomole Version 5, January **2002** ; Theoretical Chemistry Group, University of Karlsruhe) in combination with the OPTIMIZE routine of Baker (J. Baker, *J. Comput. Chem.* **1986**, 7, 385 ; PQS Version 2.4, **2001**, Parallel Quantum Solutions, Fayetteville, Arkansas, USA ; the Baker optimizer is available separately from PQS upon request). All relevant structures were fully optimized at the unrestricted RI-bp86 (K. Eichkorn, F. Weigend, O. Treutler, R. Ahlrichs, *Theor. Chem. Acc.* **1997**, 97, 119 ; A. D. Becke, *Phys. Rev. A* **1988**, 38, 3089 ; J. P. Perdew, *Phys. Rev. B* **1986**, 33, 8822) and b3-lyp levels (C. Lee, W. Yang, R. G. Parr, *Phys. Rev. B* **1988**, 37, 785 ; A. D. Becke, J. *Chem. Phys.* **1993**, 98, 1372 ; A. D. Becke, *J. Chem. Phys.* **1993**, 98, 5648 ; note that the Turbomole functional "b3-lyp" is not identical to the Gaussian "B3LYP" functional) by employing the standard SV(P) basis sets (A. Schäfer, H. Horn, R. Alrichs, *J. Chem. Phys.* **1992**, 97, 2571).

Table 1. Crystal Data and Structure Analysis Results			
	1	**2***	**Chang Complex**
Formula	$C_{34}H_{72}Mg_2N_4Si_8$	$C_{57}H_{132}Al_3Mg_3N_3O_{16.5}Si_6$	$C_{59}H_{136}Al_3Mg_3N_3O_{17}Si_6$
M_w	690.20	1446.07	1482.12
Crystal system	Orthorhombic	Orthorhombic	Orthorhombic
Space group	*Pbcn*	*Pbcn*	*Pbcn*
a (Å)	18.040(8)	12.526(4)	12.4718(6)
b (Å)	14.888(7)	25.615(6)	25.4146(11)
c (Å)	18.038(8)	28.167(6)	28.0272(12)
α (deg)	90	90	90
β (deg)	90	90	90
γ(deg)	90	90	90
V (Å^3)	4270(3)	9037(5)	8883.7(7)
Z	4	4	4
Radiation (Kα, Å)	0.71073	0.71073	0.71073
T (K)	198	213	150
D_{calcd} (g cm^{-3})	1.074	1.063	1.108
μ_{calcd} (mm^{-1})	1.607	0.194	0.199
F_{000}	1520	3144	1384
R, R_w[2 a]	0.0439, 0.1129	0.0671, 0.1581	0.1225, 0.2401
GoF	1.039	1.099	1.061

[a] $R = \Sigma||F_0| - |F_c||/\Sigma|F|$, $R_w = [\Sigma(|F_0| - |F_c|)^2/\Sigma wF_0^2\}^{1/2}$

*CCDC-606505 contains supplementary crystallographic data

REFERENCES

1. a) J. C. Calabrese, T. Herskovitz, J. B. Kinney, *J. Am. Chem. Soc.* **1983**, 105, 5914 ; b) D. H. Gibson, *Chem. Rev.* **1996**, 96, 2063 ; c) A. Behr, *Angew. Chem.* **1988**, 100, 681; *Angew. Chem. Int. Ed. Engl.* **1988**, 27, 661; d) X. Yin, J. R. Moss, *Coord. Chem. Rev.* **1999**, 181, 27; e) D. Walther, M. Ruben, S. Rau, *Coord. Chem. Rev.* **1999**, 182, 67; f) Y. Tang, L. N. Zakharov, A. L. Rheingold, R. A. Kemp, *Organometallics* **2004**, 23, 4788; g) C.-C. Chang, B. Srinivas, M.-L. Wu, W.-H. Chiang, M. Y. Chiang, C.-S. Hsiung, *Organometallics* **1995**, 14, 5150, h) D.B Dell'Amico, F. Calderazzo, L. Labella, F. Marchetti, G. Pampaloni, *Chem. Rev.* **2003**, 103, 3857; i) R. Zevenhoven, S. Eloneva, S. Teir, *Catal. Today* **2006**, 115, 73; j) K.M. Kerry Yu, C.M.Y. Yeung, S.C. Tsang, *J. Am. Chem. Soc.* **2007**, 129, 6360; k) P. Braunstein, D. Matt, D. Nobel, *Chem. Rev.* **1988**, 88, 747; l) P.G. Jessop, T. Ikariya, R. Noyori, *Chem. Rev.* **1995**, 95, 259; m) P. G. Jessop, F. Joó, C-C. Tai, *Coord. Chem. Rev.* **2004**, 248, 2425; n) W. Leitner, *Coord. Chem. Rev.* **1996**, 153, 257; o) X. Yin, J.R. Moss, *Coord. Chem. Rev.* **1999**, 181, 27. p) T. Sakakura, J-C. Choi, H. Yasuda, *Chem. Rev.* **2007**, 107, 2365

2. C.-C. Chang, B. Srinivas, M-L. Wu, W-H. Chiang, M.Y. Chiang, C-S. Hsiung, *Organometallics* **1995**, 14, 5150

3. a) C.-C. Chang, M.S. Ameerunisha, *Coord. Chem. Rev.* **1999**, 189, 199; b) K.-C. Yang, C.-C. Chang, C.-S. Yeh, G.-H. Lee, S.-M. Peng, *Organometallics* **2001**, 20, 126; c) K.-C. Yang, C.-C. Chang, C.-S. Yeh, G.-H. Lee, Y. Wang, *Organometallics* **2002**, 21, 1296

4. W. Clegg, F.J. Craig, K.W. Henderson, A.R. Kennedy, R.E. Mulvey, R.A. O'Neil, D. Reed, *Inorg. Chem.* **1997**, 36, 6328

5. Y. Tang, L.N. Zakharov, A.L. Rheingold. R.A. Kemp, *Organometallics* **2004**, 23, 4788

6. a) D. Min, S. W. Lee, *Inorg. Chem. Commun.* **2002**, 5, 978 ; b) L. J. Farrugia, S. Lopinski, P. A. Lovatt, R. D. Peacock, *Inorg. Chem.* **2001**, 40, 558 ; c) W. J. Evans, C. A. Seibel, J. W. Ziller, *Inorg. Chem.* **1998**, 37, 770.

7. a) T. Tsuda, S.-I. Sanada, T. Saegusa, *J. Organomet. Chem.* **1976**, 116, C10 ; b) G. Fachinetti, C. Floriani, A. Chiesi-Villa, C. Guastini, *J. Am. Chem. Soc.* **1979**, 101, 1767; c) L. J. Procopio, P. J. Carroll, D. H. Berry, *Organometallics* **1993**, 12, 3087; d) I. Castro-Rodriguez, K. Meyer, *J. Am. Chem. Soc.* **2005**, 127, 11 242 ; e) D. S. Laitar, P. M J. *Am. Chem. Soc.* **2005**, 127, 17 196.

8. a) S. Gambarotta, M. Pasquali, C. Floriani, A. Chiesi-Villa, C. Guastini, *Inorg. Chem.* **1981**, 20, 1173 ; b) S. Gambarotta, F. Arena, C. Floriani, A. Gaetani-Manfredotti, *J. Chem. Soc. Chem. Commun.* **1982**, 835 ; c) S. Gambarotta, F. Arena, C. Floriani, P. F. Zanazzi, *J. Am. Chem. Soc.* **1982**, 104, 5083.

9. C.-C. Chang, M.-C. Liao, T.-H. Chang, S.-M. Peng, G.-H. Lee, *Angew. Chem.* **2005**, 117, 7584 ; *Angew. Chem. Int. Ed.* **2005**, 44, 7418;

10. a) I. Castro-Rodriguez, H. Nakai, L. N. Zakharov, A. L. Rheingold, K. Meyer, *Science* **2004**, 305, 1757; b) G. Gao, F. Li, L. Xu, X. Liu, Y. Yang, *J. Am. Chem. Soc.* **2008**, 130, 10838

CONCLUDING REMARKS

The chemistry of ruthenium β-diketiminates is in its infancy. With only one publication in the literature, the results outlined within this work provide new results detailing the behaviour of this ligand-metal combination and these preliminary results point towards a potentially vast new area of β-diketiminate chemistry. The formation of [η^5-cymene($^{i\text{Pr}}$ArNCMe)$_2$C]Ru[($^{i\text{Pr}}$ArNCMe)$_2$CH] (**1**) and [($^{i\text{Pr}}$ArNCMe)$_2$CH]Ru[η^5-1-methyl-4-(propan-2-ylidene)cyclohexa-2,5-dien-1-yl] (**2**), as outlined in chapter two, not only demonstrate the unique nucleophilic character of the β-diketiminate ligand but also the non-innocence of the π-bound cymene ring. Both the unprecedented action of the nucleophilic β-diketiminate and the involvement of the cymene ring are thought to be related to the steric environment created around the ruthenium centre. Based on these conclusions, the logical expansion of this work lies in varying the steric and electronic properties of the β-diketiminate ligand. This should affect the susceptibility of the π-bound arene to nucleophilic attack, and ultimately expand the collection and possible applications of these ruthenium β-diketiminate complexes towards small molecule activation (CO_2). Dyson *et. al.* have already demonstrated the affinity of a similar system towards small molecule activation, but on a ruthenium(II) centre, which displays reactivity familiar to other metal β-diketiminate systems with similar small molecules. Exploring the reactivity of this system in the ruthenium(I) oxidation state will undoubtedly be much more interesting and contribute to the sparse field of ruthenium(I) chemistry. Although one of the goals of this project was to stabilize a low-valent ruthenium centre, this ultimate goal is still within grasp but future work will require a

systematic experimentation with varying β-diketiminate ligands in order to discover the appropriate electronic and steric constraints that will allow this remarkable ligand to certainly stabilize a ruthenium(I) centre.

While we were working at preparing highly reactive Ru system for CO_2 activation, the ground shaking claim of Chang *et. al.* detailing the robust end-on coordination of CO_2 within a trimeric magnesium cluster appeared in the literature. We felt compelled to test the reliability of the data. A thorough re-visitation of this report confirmed the true nature of the complex as $[\{Me_2Al(\mu\text{-}OSiMe_3)_2Mg(THF)_2(\boldsymbol{\mu\text{-}OCN})\}_3]$ and not $[\{R_2Al(\mu\text{-}NSiMe_3)(\mu\text{-}OSiMe_3)Mg(THF)_2(\boldsymbol{\mu\text{-}O_2C})\}_3]$. By not relying solely on the X-ray structure but complimenting the X-ray data with a detailed NMR study, all observations indicated that, rather than a sensational case of irreversible fixation of CO_2 at magnesium cations, the complex more reasonably contains linearly bound isocyanate molecules. This misinterpretation is an excellent reminder of the importance in testing and verifying hypotheses and results carefully and critically before publication. More significantly though, it shows the constant pursuit for new and more remarkable complexes of CO_2 can only be achieved with transition metals.

The ability of this molecule to capture every scientist's imagination has never been more powerful, given the current climatic conditions. Future work in this field, without a doubt, will be centered on catalytic transition metal or biological conversion systems. Although catalytic conversions of CO_2 in organometallic chemistry remain a hot topic, a system that can convert the molecule under mild conditions into useful C_1 feedstock is the ultimate goal. This process will require a unique metal, which is stable in a variety of solvents, under various atmospheric conditions and not to mention

catalytically robust. One cannot help but thinking of ruthenium as a potential choice, given all of its unique properties, proven stability and catalytic nature. Regardless of the metal choice, it is an easy prediction that this Holy Grail within transition metal chemistry will experience in the near future a steady growth of findings and advances.